Surface modification for enhanced cell adhesion under high shear stress conditions

Siddique, Asma

(2020)

Surface modification for enhanced cell adhesion under high shear stress conditions

TECHNISCHE UNIVERSITÄT DARMSTADT

Asma Siddique
Faisalabad, Pakistan

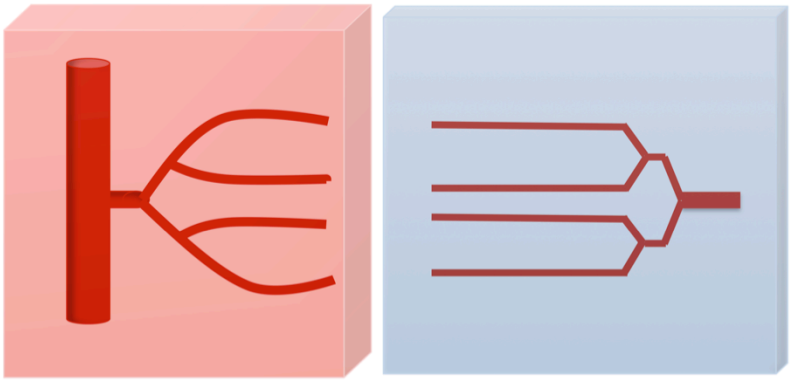

Physics of Surfaces
Fachbereich Material- und Geowissenschaften
Technische Universität Darmstadt

Surface modification for enhanced cell adhesion under high shear stress conditions

A thesis approved in fulfillment of the requirements for the degree of Doctor rerum naturalium (Dr. rer. nat.)

Asma Siddique
Faisalabad, Pakistan

Referee: Prof. Dr. Robert Stark
Co-referee: Prof. Dr. Markus Biesalski

Date of submission: 24.09.2019
Date of examination: 05.12.2019

Fachbereich Material- und Geowissenschaften
Technische Universität Darmstadt

Declaration

The work described in this thesis was carried out in the group of Physics of Surfaces, Department of Materials Science, Technische Universität Darmstadt. I hereby declare that the work in this thesis is the author's original work and no part of the thesis has been submitted for a degree at any other university or institute. Prior to the submission of this thesis, some work has been published as described in the relevant chapters herein.

Erklärung

Hiermit erkläre ich an Eides statt, dass ich die vorliegende Dissertation selbstständig und nur mit den angegebenen Quellen und Hilfsmitteln angefertigt habe. Von mir wurde weder an der Technischen Universität Darmstadt noch an einer anderen Hochschule ein Promotionsversuch unternommen.

Asma Siddique

Darmstadt,

Contents

List of Tables

List of Figures

List of Abberviations

AFM	Atomic Force Microscopy
AHPCS	Allylhydridopolycarbosilane
APTES	(3–aminopropyl)triethoxy silane
APTMS	3–(aminopropyl)trimethoxysilane
ATRP	Atom Transfer Radical Polymerization
BSA	Bovine Serum Albumen
CA	Contact angle
CCl_4	Carbon tetrachloride
CO_2	Carbon dioxide
Coll	Collagen
Coll–1	Collagen type 1
coll–5	Collagen at pH 5
coll–7	Collagen at pH 7
coll–9	Collagen at pH 9
DDM	n–dodecyle–β–D–maltoside
DMEM	Dulbecco Modified Eagle Medium
ECM	Extra cellular matrix
ECs	Endothelial cells
EDTA	Ethylendiamintetraacetic acid
FAK	Focal adhesion kinase
GA	Glutaraldehyde
GOX	Glucose peroxidase
GPa	Gaga Pascal
GPTCS	3–chloropropyltrichlorosilane
GPTMS	3–glycidoxypropyltrimethoxysilane

HFBI	Hydrophobin
HRP	Horseradisch peroxidase
HUVECs	Human umbilical vein endothelial cells
IEP	Isoelectric point
IFF	Interstitial fluid flow
IgG	Immunglobulin G
IGM	Immunglobulin G
KPa	Kilo Pascal
LBL	layer–by–layer
LOC	Lab on chip
LRP	Living radical polymerization
LSGS	Low serum growth supplement
MPA	Mega Pascal
MSCs	Mesenchymal stem cells
NA	Numerical Aperture
$NaBH_4$	Sodium Borohydride
$NaCNBH_3$	Sodium Cyanoborohydride
O_2	Oxygen
PAA	Poly(acrylic acid)
PAH	Poly–(allyamine hydrochloride)
PBS	Phosphate-buffered saline
PC	Polycarbonate
PDDA	Poly–(diallyldimethylammonium chloride)
PDMS	Polydimethylsiloxan
PEG	Polyethylene glycol

PEI	Polyethyleneamine
PEM	Polyelectrolytes multilayer
PET	Poly(ethylene terephthalate)
PGs	Proteoglycans
PLL	Poly–L–lysine
PLL-PEG	Poly–L–lysine–g–polyethylene
PMMA	Poly(methyl methacrylate)
PS	Polystyrene
PVA	poly(vinyl alcohol)
PVA	Poly(vinyl alcohol)
PVC	Poly(vinyl chloride)
rms	Root mean square
SAMs	Self–assembled monolayers
$SiCl_4$	Silicon tetrachloride
vWF	von Willebrand factor
μTAS	Miniaturized Total chemical Analysis System
Wa	Watt

Abstract

The vascular system, one of the bases of life mechanisms, connects tissues and organs by means of blood vessels, supplies nutrient–containing blood throughout the body and removes waste products. Any functional abnormalities in vascular system can cause critical diseases such as tumor, angiogenesis and cancer. Cardiovascular diseases are the leading cause of death globally. Therefore, the vascular science is a field with strong translational focus to develop insight in vascular physiology and disease treatments. Many of the vascular functions, hemodynamic forces, cellular interactions and related diseases are strictly associated to the physical geometry of vasculature. Moreover the endothelial lining of blood vessels is subjected to a continuous hemodynamic shear stress, which is also essential to regulate cell morphology and functions. Replication of cardiovascular system *in vitro* requires a dynamic 3D microenvironment to modulate the fundamentals of vasculature and diseases models.

Meanwhile, the introduction of microfluidics in vascular research enables us to study disease models in particular dimensions and at well-defined shear stress.

Polydimethylsiloxane (PDMS) based microfluidic systems, lined with endothelial cells, provide a versatile platform to study the mechanoresponse of cells *in vitro*. Extracellular matrix proteins are used to coat PDMS surface prior to cell growth to provide cell a natural environment. However, the long-term cell studies are limited due to instability of coated proteins inside PDMS microchannels under physiological shear stress conditions. To increase the stability under flow conditions, various protein-substrate linkages were developed for stable cell growth. PDMS surface was functionalized by using four different methods (i) O_2 plasma (ii) (3-Aminopropyl)triethoxysilane (APTES) (iii) APTES-Gluteraldehyde and (iv) protonated APTES, in order to develop a stable bond with collagen–an ECM protein. Moreover, collagen at three different pH values (pH 5, 7 and 9), which attributed to certain charge distribution on molecules, was used to further enhance its bond strength with variety of functionalized surfaces. Different microfluidic device designs were used to evaluate coating efficiency and cell growth under continues shear stress (10-300 dyn/cm^2), which is even higher than physiological shear stress. The comparison of all surface modification methods showed that, the electrostatic interaction between APTES mediated surfaces and collagen molecules at higher pH values found to be very stable for subsequent cell growth at high shear stress.

Therefore, the surface modification technique based on APTES can also be applied to other ECM proteins, enabling long term in vitro cell studies in PDMS micro-channels to replicate blood vessels and related disease models.

Zusammenfassung

Das Gefäßsystem, eine wichtige Basis für die Lebensfunktion, verbindet Gewebe und Organe durch Blutgefäße, versorgt den Köper mit nährstoffreichem Blut und entsorgt Abfallprodukte. Jegliche Fehlfunktion des Gefäßsystems kann schwerwiegende Krankheiten verursachen, wie z. B. Tumorgenese, Angiogenese oder Krebs. Kardiovaskuläre Krankheiten sind die weltweit häufigsten Todesursachen. Aus diesem Grund ist die Gefäßwissenschaft ein Gebiet mit starkem translationalen Fokus auf die vaskuläre Physiologie und Krankheitsbehandlung. Viele Gefäßfunktionen, hämodynamische Kräfte, zelluläre Wechselwirkungen und assoziierte Krankheiten können direkt mit der physikalischen Geometrie der Gefäße in Zusammenhang gebracht werden. Darüber hinaus sind Endothelzellen in den Blutgefäßen einer permanenten hämodynamischen Scherspannung ausgesetzt, die auch für die Zellmorphologie und -funktion verantwortlich ist. Um das Gefäßsystem für Krankheitsmodelle in vitro zu mimen wird eine dynamische dreidimensionale Mikroumgebung benötigt.

Die Entwicklung von mikrofluidischen Systemen für die Gefäßforschung ermöglichte die Untersuchung von Krankheitsmodellen in drei Dimensionen und bei exakt definierten Scherspannung. Die auf Polydimethylsiloxan (PDMS) basierenden mikrofluidischen Systeme, deren Kanäle mit Endothelzellen beschichtet sind, bieten eine vielseitige Plattform, um die mechanoresponsiven Eigenschaften von Zellen in vitro zu untersuchen. Um den Zellen eine natürliche Umgebung zu schaffen, werden Moleküle der extrazellulären Matrix (EZM) als Beschichtung der PDMS-Oberflächen verwendet. Langzeituntersuchen sind jedoch durch die Instabilität der Proteinbeschichtung in den PDMS-Mikrokanälen bei Verwendung physiologischer Bedingungen in Bezug auf die Scherspannung beschränkt. Um die Stabilität bei Scherbedingungen zu verbessern, wurden diverse Protein-Substrat-Verbindungen für ein stabiles Zellwachstum entwickelt. In dieser Arbeit wurden PDMS-Oberflächen mit vier verschiedenen Methoden funktionalisiert: (i) Sauerstoffplasma (ii) (3-Aminopropyl)triethoxysilan (APTES) (iii) APTES-Gluteraldehyd und (iv) protoniertes APTES um eine stabile Verbindung mit dem Kollagen, ein Protein der extrazellulären Matrix, zu generieren. Darüber hinaus wurde Kollagen bei drei unterschiedlichen pH-Werten (pH 5, 7, und 9) verwendet, die zu bestimmten Ladungsverteilungen der Moleküle führen, um die Bindungsstärke mit den verschieden funktionalisierten Oberflächen weiter zu erhöhen. Des Weiteren wurden unterschiedliche geometrische Ausführungen der mikrofluidischen Systeme entwickelt, um die Beschichtungseffizienz und das Zellwachstum bei kontinuierlicher Scherspannung (10-300 dyn/cm^2, höher als die physiologische Scherspannung) zu bewerten. Der Vergleich der verwendeten Oberflächenmodifikationen ergab, dass die elektrostatischen Wechselwirkungen zwischen APTES-beschichteten Oberflächen und den Kollagen-Molekülen bei hohem pH-Wert zu stabilen Bedingungen für das anschließende Zellwachstum bei hoher Scherspannung führen. Diese Methode der Oberflächenmodifikation basierend auf APTES kann auch auf andere EZM-Proteine angewendet werden, was Langzeit-*in-vitro*-Zellstudien in PDMS-Mikrokanälen ermöglicht, um Blutkanäle und zugehörige Krankheitsmodelle zu replizieren.

Chapter 1. Introduction

1.1. Background

Cardiovascular diseases (CVDs), disorders of heart and blood vessels, are the number one cause of deaths worldwide. CVDs take the lives of 17.9 million people every year, 31% of global deaths [1]. Including common entities, such as hypertension and diabetes, blood vessel pathology is a major reason of heart attack and stroke. Large numbers of patients suffer vascular diseases, resulting in a clear clinical need for functional arterial replacements [2, 3].

Diseases like vascular blocking and thrombosis oftenly caused by pathological biophysical interactions among blood cells, endothelial cells, and blood soluble factors (e.g., cytokines, coagulation factors, etc.).

The vascular system, one of the bases of life mechanisms, supplies nutrient–containing blood throughout the body and removes waste products. Tissues and organs are connected to each other by means of blood vessels. Any functional abnormalities either acute or chronic pathological states of the vascular system can cause diseases related to blood vessels as well as other critical diseases such as tumor, angiogenesis and cancer [4]. Moreover the variations in the biophysical properties, such as cell adhesion, cell aggregation, and cell deform abilities contribute to a disease states, ultimately leading to disturbance of micro vascular flow in vital organs [5, 6].

Therefore, the response of blood vessel building blocks (endothelial cells or smooth muscle cells) to relevant biological, chemical, or physical stimuli is needed to explore in detail. Conventionally, the experimental setup was based on classical cell culturing techniques in petri plates by subjecting the cells to the various stimuli and analyzing the results by biological or biochemical techniques. However, the results obtained in static *in vitro* experiments seems far away from dynamic *in vivo* conditions, where vascular endothelial cells are constantly subjected to shear stress caused by the blood flow and smooth muscle cells are stretched because of the blood vessel cardiac cycle [7, 8].

Blood vascular system consists of three–dimensional environment comprising an elastic extracellular matrix, fibroblasts cells, and smooth muscle cells also thoroughly lined with endothelial cells. Moreover the flowing blood composed of platelets, red blood cells and leukocytes, generates certain shear stress to endothelial lining. Both, the three–dimensional environment and the dynamic mechanical changes with each cardiac cycle are very important factors in proper vascular functioning [9-11].

Thus, there has been great interest in the study of blood vessels and related diseases either by using animal models or in vitro three–dimensional experimental platforms.

Although animal models have vastly enhanced our understanding about these diseases, however, the results from animal experiments are neither always validate to humans nor free from ethical concerns. On the other hand, in vitro systems have the

potential to offer valuable quantitative insights into vascular studies but these common static platforms have difficulty in clarifying some of the essential mechanisms related to human vascular diseases due to dimensional differences and the absence of the physiological level of fluid flow. Efforts have been placed on developing the vascular system in vitro and to design the laboratory setups that allow a precise control on relevant parameters [4, 12].

Recently, the field of microfluidics has gained much interest among scientists as it addresses all the shortcomings of in vitro studies and has ability to recapitulate complex environments found in vivo. Microfluidic technology offers physiologically realistic and simple setups that allows for scaling up and parallelization of experimental setup, leading to better understandings about cell and tissue physiology in 3D environment. Moreover, a precise control of the flow rate allows one to apply certain defined shear stress to the cells [8, 13]. Various synthetic and biologically derived polymers are used for *in vitro* cell culturing but Polydimethylsiloxan (PDMS) and glass based system is the most widely used system in bio microfluidics due to its biocompatibility, optical transparency, gas permeability and above all its cost effectiveness.

A number of microfluidic assays have been developed for cell shear studies in PDMS-based microfluidic devices. For example, the endothelial cells (the inner lining of blood vessels) are directly exposed to physiological shear stress in the organism. To model the high-stress conditions *in vitro,* it is important to provide in-vivo-like attachment of the cells to the substrate because the cell-substrate interaction determines the stability of the focal adhesion complex on the surface [14]. However, the hydrophobicity and the hydrophobic recovery of PDMS is still a challenge for long-term cell studies under dynamic conditions. A variety of surface modification techniques are available for PDMS to improve its bio-contact properties. In particular, extra cellular matrix (ECM) proteins such as collagen or fibronectin are usually used to coat the PDMS surface to provide a natural moiety for the attachment and survival of the cells [15, 16].

Nevertheless, it is still a challenge to produce thin homogeneous layer of proteins throughout the micro-channel and to ensure the stability of the coating under flow conditions for long-term cell studies.

The particular objective of this thesis is to develop simple and steadfast protein immobilization methods for stable endothelial growth inside PDMS-based microfluidic devices at high shear stress. The magnitude of shear stress in our arteries ranges from 0.7 dyne/cm^2 to 130 dyne/cm^2. However already developed systems are restricted to experimental time limits due to instability of cell-surface bond at high flow rate flow, especially in narrow channels and continues studies are only possible when experiments are performed at very low flow rate. Therefore it is highly needed to develop a dynamically stable microfluidic experimental setup, which enables continuous cell studies at physiological conditions.

In this thesis, not only new protein coating methods are developed but these methods are also compared with classical coating procedures in terms of stability of protein–substrate bond under flow. Surface chemistries for all coating procedure are explored for biocompatibility by evaluating the cell viability. Moreover, various configuration and dimensions of microfluidic systems were used to evaluate the

efficiency of coating methodology in narrow channels for enhanced cell growth and proliferation.

1.2. Introduction to microfluidics

Microfluidics is a technology, which deals with controlling and manipulating fluid flows in small volumes (mL, nL, pL) in precisely defined geometries and facilitates the analysis of single cell level, to a large cell populations in simple channels as wells as in fully integrated and automated chips, Lab on chips (LOC). LOCs are the microsystems, which are capable of incorporating entire biological or chemical laboratories in a single chip [17, 18]. Different polymer substrates are used to fabricate of small channels, which can be connected to a liquid flow system (pump) for this purpose of fluid flow. The geometry of the flow channels can be precisely controlled by using microfluidic designing and fabrication techniques [13].

The concept of miniaturization of analytical setups was first introduced by Richard P. Feynman [19] in his talk "There's Plenty of Room at the Bottom" to American Physical Society Terry *et al.,* [20] fabricated the first miniature gas chromatography device on a silicon wafer The concept of Miniaturized Total chemical Analysis System (μTAS) was formulated in 1990 by Andreas Manz and colleagues, which was the actual start towards the field of microfluidics [21]. Figure 1 represents a simplest microfluidic device design, which can be expanded to complex architecture.

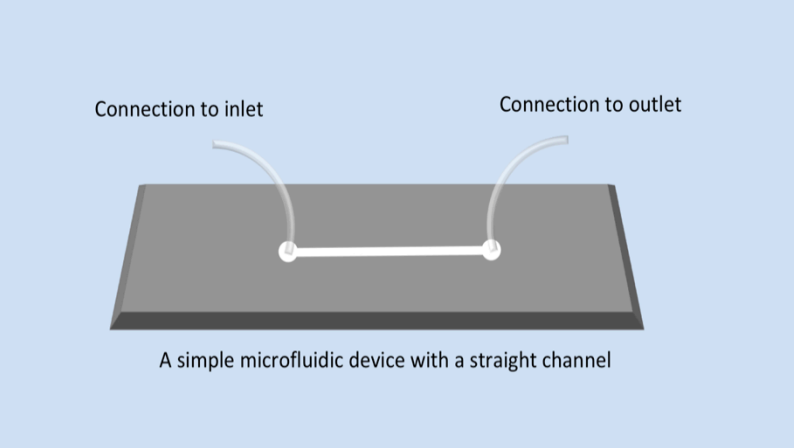

Figure 1: A simplest microfluidic device design.

1.2.1. Advantages:

Microfluidics based setups have been developed for a large range of applications in almost all scientific disciplines especially chemistry, biochemistry and biophysics. As the surface–to–volume ratio is inversely proportional to the length of the fluid, when system is reduced from macro to micro scale, surface–to–volume ratio increases significantly. Therefore, the probability of molecules to react with each other increases within a limited area leading to more efficient reactions. Furthermore the diffusion rate also increases at micro scale resulting in faster mixing of solute into a solvent so many reactions in limited number of time can be possible. Traditional reactions in the lab are performed in different steps with multiple instruments but microfluidic offers a setup with multiple reactions on one chip, which reduces the cost of experiments.

Their ability to manipulate small amounts of fluids leads to the possibility of performing analysis with a minor quantity of samples, thus making most bio–analysis very feasible and inexpensive, especially where the available volume of sample is limited or expansive. Microfluidics devices allow a high level of automation in the measurement in case of point–of–care diagnostics. In short, microfluidics offers a simple to use portable device, which can be easily fabricate and operate and can be easily dispose off [22-25].

Microfluidics channels dimensions offer the laminar flow of liquids. As in microfluidic systems, the interplay among forces and their importance is totally different as compared to macro scales for example the forces that act on the volume of fluid like gravity becomes less important as compared to the viscosity of the liquid [25, 26].

Flow condition in a micro channel can be defined by Reynolds number (Re).

$$\boldsymbol{Re} = \frac{\boldsymbol{\upsilon L}}{\boldsymbol{\nu}} \tag{1}$$

Where υ is flow velocity, L is length scale of flow and ν viscosity of liquid. For a fluid flow in pipe, when Re is smaller than 1500, the flow is laminar. When Re is greater than 2300, the flow is turbulent. For microfluidics, the value of Re is usually very low and flow is generally laminar [24, 27].

1.2.2. Microfluidic cell culture:

Classical cell culturing techniques may offer a wide room to establish different cell culturing protocols and have ability to scale up an experiment but mainly offers only an end pint analysis. The cells are used to grow on a typical rigid surface with fixed device architecture where the perfusions and gradients are difficult to achieve. Where as in microfluidic cell culture, flexibility of device designs propos more flexible, controlled real time and sometimes automated on chip analysis by using less number of cells and small amount of reagents [18].

Microfluidics offer a number of advantages over traditional cell culture

1- Flexibility of device design

Microfluidic device design can be tailored according to the need of individual cell type and experiment. So that, the complexity of physiological architecture of human organs can be achieved up to certain level. For example Ramadan *et al*., [28] developed an *in vitro* model to study the absorption of nutrients in human gastrointestinal tract by using microfluidic set up. Efforts have been also made to mimic the organ specific architect and functionality of lungs, Vasculature and brain by using microfluidic technology [29-31]

2- Reduced consumption of reagents.

Microfluidic cell culture reduced the consumption of reagents and chemicals, which is helpful to perform experiments with expansive reagents. Decreased amount of reagents and consumables also reduces the risk of contamination.

A typical macroscopic culture contains 10^4–10^7 cells and the measurements represent the average of a large group of the cells. While in microfluidic experiments, measurements with a small population of the cells or even with the single cell are possible. Macroscopic methods used to study cell migration includes Boyden chamber and scratch assay [32]. These methods are relatively easy to setup but they are time consuming, large number of cells are required, chemical gradient cannot be establish and single cell resolution cannot be achieved. Instead, microfluidic cell culture offers a better understanding about thermodynamic, kinetic and mechanical characteristics of cell locomotion on single cell level. Huang *et al*., [33] developed a microfluidic cell culture device with small compartments. They characterized cellular morphology and its locomotion mechanism during brain tumor stem cell migration by resolving the behavior of individual cells. Long term observation of response of normal and disordered single cell towards various drugs demonstrated the potential of microfluidic assays. Various designs of microwells and hydrodynamic systems can be used to trap single cells. Moreover, controlled pairing and fusion of cells would otherwise be impractical [34-36]. Various groups have also studied the gene expression of single cell with the help of microfluidic experimental setup [37-39].

3- Real time data acquisition

Incorporation of analytical biosensors into a cell culture platform is another advantage belongs to microfluidic cell culture technique. In conventional biosensors resulted data is based on cell population and gives the collective response of cells against any stimuli. Contrary, chip–based biosensors offer on site, single cell sensing system to record cell response to stimuli without mixing the information of cell–cell contact [40]. Moreover, in metabolic studies/analysis, traditional cell culture protocols require a multistep experimental setup starting from sample preparation (cell lysis) to sample extraction and appropriately diluted analyte preparation. Sample measurements require high–resolution separation techniques and sensitive detection. Microfluidic systems have potential to combine above–mentioned analytical chemistry with a single cell on a single chip, thus increasing reproducibility [41]. Microfluidic cell culture devices are used after direct coupling with mass spectrometer, electrochemical sensors and other analytical tools in order to get a real time quantitative data [42, 43].

4- High throughput capabilities with high experimental control.

Traditionally, high–throughput drug assays are carried out in microtiter well plates, where the drug solutions are added to the target cells or molecules in the entire well plate. Then the plates are incubated for days before all the wells are read out in parallel. One microfluidic approach handles similar volumes by using chambers for compartmentalization instead of well plate [44]. Another approach is based on droplet microfluidics, offering higher sensitivities by using water–in–oil emulsion droplets to compartmentalize reactants into picolitre volumes. These droplets increase throughput by reducing the volume and increasing the rate at which assays can be performed. Finally these droplets are detected on chips on the bases of variety of readouts. High throughput screening workstations are normally capable of screening tens of thousands of compounds in a day [45, 46].

1.2.3. Microfluidics in Vascular research:

The blood vascular system, being in contact with almost all tissues organs is found throughout the body. It also serves as the connection among various tissues and organs and is considered as basis of life mechanisms [47, 48]. Blood vessels transport nutrients, immune cells oxygen and other molecules to, and waste products away from all tissues in our body. The branches of vascular network well organized themselves spatially in order to provide sufficient nutrients to the cells of all organs and supporting tissues [49, 50]. The inner lining of blood vessels is composed of a monolayer of endothelial cells (ECs) that forms a semipermeable barrier "endothelium", which is responsible for the transfer of molecules [51]. Moreover, under continues flow of blood, the endothelial cells face various levels of shear stress in different parts of body, which is essential to regulate many of endothelial functions. In one of the study, Wang et al., [52] reported shear stress dependent cytoskeleton remoulding, activation of von Willebrand factor (vWF), and re–organisation of angiogenesis factors such as tetra peptide acetyl–Ser–Asp–Lys–Pro (AcSDKP) of endothelial cells by using multishear microfluidic device.

Microvasculature, due to a continues interaction of endothelium and blood cells, majorly contribute to functional abnormalities of the blood vessel themselves and also to variety of disorders including sickle cell disease, malaria, microangiopathy, cancer metastasis and stroke [12, 53-55]. Therefore, the study of blood vessels and related diseases has become one of the most significant areas of research. There had been a long–standing interest to study vessel diseases by using animal models and two–dimensional static experimental platforms. However the results from animal models are not applicable to humans, nor free from ethical concerns [56]. On the other hand, common static platforms face difficulty to explain some fundamental disease mechanisms due to dimensional differences and lack of fluid flow. As it is already known that many of the vascular functions, hemodynamic forces, cellular interactions and related diseases are strictly related to of physical geometry of vasculature [57, 58].

Ideally, Microfluidics offer a platform to investigate these vascular events *in vitro* and eliminates all the shortcomings and difficulties related to two dimensional or *in vivo* systems and simulation models (figure 2).

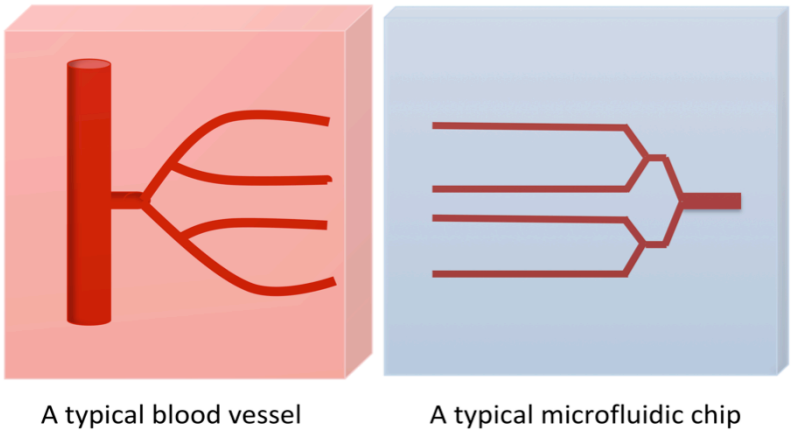

Figure 2: A representation of vascular on chip model.

Consequently, microfluidic devices have been exploited micro vascular research, due to their ability to impose laminar flow on monolayers of vascular ECs [59, 60]. Huh et al., [61] used a microdevice to develop a microengineered disease model of pulmonary edema in human lungs. This device was used to reproduce drug (interleukin–2) toxicity–induced pulmonary edema observed in human cancer patients. This on–chip disease model revealed that mechanical forces associated with physiological breathing motions play a crucial role in the development of increased vascular leakage that leads to pulmonary edema. These studies also led to identification of potential new therapeutics, which might prevent this life–threatening toxicity of drugs in the future. Tsai et al., [12] designed an in vitro "endothelialized" microfluidic microvasculature. Under controlled flow conditions, the model enabled quantitative investigation of biophysical alterations in hematologic disease collectively lead to microvascular occlusion and thrombosis. The model also explained that the shear stress influences microvascular thrombosis and the efficacy of the drug eptifibatide.

Thus briefly, the emergence of microfluidics technology in vascular research enhances our understanding about microcirculatory dynamics, shear response of the cells and vascular diseases.

1.3. Fabrication of microfluidic devices:

A special emphasis is to use most practical and the recently developed methods for microfluidic device fabrication, which includes, laminate, molding, 3D printing, and high–resolution nanofabrication techniques [62]. A variety of materials have been used to produce various microfluidic devices [63]. Silicon was the first material used for microfluidics [20]. Beside Silicon and glass [64], polymers have gained significant traction in microfluidics in the past 15 years commonly used polymers include Polydimethylsiloxan (PDMS) [65, 66], poly(methyl methacrylate) (PMMA) [67], polycarbonate (PC), poly(ethylene terephthalate) (PET), polyurethane, poly(vinyl chloride) (PVC), and polyester [68, 69].

1.4. PDMS-based microfluidic systems:

Before selecting a material for micro fabrication, its required function and application is highly considered. Materials interact directly with biological systems, human tissues, organs, cells and blood, categorized as 'biomaterials', are used for micro scale engineering for cellular systems [70].

A number of biocompatible polymers are contributing in bio microfluidics and vascular studies but PDMS is most widely used biocompatible polymer for this purpose. First of all, PDMS offers unique material properties in very low cost. Its biocompatibility has been already proved in many studies even for very sensitive primary cell lines [71-73]. Due to its optical transparency, high–resolution bright field as well as fluorescence imaging is possible without major obstacles. Many researchers have been already made it possible to detect, image and track single cells and molecules in PDMS microfluidic devices [71, 74, 75].

PDMS has a general elastic module of ≈ 0.6–3.7 MPa [76], which is much lower than the materials normally used for cell culturing such as glass (≈ 50 GPa) and polystyrene (≈ 3 GPa). Two–component based PDMS polymer kit offers an ideal platform for various types of cell studies. By using different blends of PDMS (bass to

cross linker ratio) it is possible to change the stiffness of PDMS over a wide range (5kPa–1.72MPa, [77] and 3.9 MPa–10 MPa [78]) which matches the stiffness of various human tissues such as brain (1.4–1.9kPa), cardiac muscle tissues (10–15kPa) and cartilage (0.5–0.9 MPa) [79]. It is already reported that the stem cells differentiation is also directed by matrix stiffness [80]. So taking advantage of PDMS and hydrogels, scientists have been studied stem cell differentiation on polymeric substrates after precisely controlling the matrix stiffens [81, 82].

For sustainable cell growth and proliferation, oxygen (O_2) and carbon dioxide (CO_2) are two major components. Besides cell viability, O_2 plays its role in cell morphology and differentiation. CO_2 stabilizes cell culture pH with media containing carbonate–based buffers. Therefore, it is necessary to maintain gas exchange level during cell culturing. O_2 and CO_2 permeability of PDMS is 3400 and 2200 $\mu m^2/s$ respectively, which is comparable to growth medium (2520 and 2400 $\mu m^2/s$ in water). Porous structure of PDMS offers gas permeability, which can be advantageous for oxygen and carbon dioxide transport in cellular studies [78, 83]. It ultimately means that if the thickness of PDMS over the cell is comparable to the layer of growth media in cell culture flask then the gaseous exchange will be approximately similar to the conventional cell culture in flask or petri plate. As PDMS is also permeable to water vapors (1700 $\mu m^2/s$ at 25 °C) [84] thus precise control on humidity is needed in case of microfluidic cell culture. Very High/small or an uncontrolled amount of evaporation can change the ionic concentration of media and can also vary the pH of the media [85]. High rate of evaporation can also cause the bubble formation in the device, which cause mechanical disturbance and become an ultimate cause of cell death. However, conducting experiment in a chamber with controlled temperature, humidity and gas exchange can offer a best solution for cell studies.

Thermal conductivity of PDMS (0.15W/mK) is significantly lower than water that helps to maintain culture at stable temperature [86]. Low electric conductivity of PDMS facilitates integration of electrodes into microfluidic devices. Wei et al., [87] used the PDMS microfluidic devices to measure electrical properties of single cells.

1.5. Surface properties of PDMS:

Despite of many advantages, hydrophobicity of PDMS with a water contact angle 109°–115° [78] is a major challenge that makes the use of PDMS difficult for many applications. Polystyrene, the most common cell substrate is also hydrophobic in nature [88]. To make polystyrene compatible for cell culturing, its surface is treated with plasma or corona discharge to make it hydrophilic and further with gamma radiation for sterilization purpose [89]. Polystyrene has been used for cell culturing since 1960s while PDMS has been used for cell culturing for less than two decades [88]. As described earlier that many of the studies have been done to investigate its biocompatibility, but the commercial process for improving its biocompatibility has not been established as polystyrene.

For example, PDMS suffers serious fouling problems from protein adsorption due to its hydrophobic–hydrophobic interaction, which limits the practical use of PDMS–based devices. Fouling initiated by nonspecific protein adsorption is a great challenge in biomedical applications, including biosensors, bioanalytical devices, and implants [90].

On the other hand, in case of protein/analyze adsorption, antifouling surface decrease the device performance. Furthermore a naturally growing cell is a part of a complex architecture establishing a direct contact with extracellular matrix proteins. This adhesion plays an integral role in cell communication and regulation, and is of fundamental importance in the development and maintenance of tissues. Therefore in order to develop cellular models *in vivo* it is important to provide cells and *in vitro* like environment. Truly hydrophobic and antifouling surfaces are not suitable for cell adhesion and growth studies. Thus various surface modification techniques had been develop for PDMS surface to make the devices suitable for biological studies. In this regard, anchoring PDMS surface with ECM proteins is the most preferred method to make surface suitable for cell studies [91, 92].

1.6. PDMS surface modification:

Therefore, depending upon the applications of PDMS surfaces and PDMS-based microfluidic devices; surface modification methods of PDMS can be discussed into two major categories

A: Anti–fouling Coatings of PDMS.
B: Protein immobilization techniques.

A: Anti–fouling Coatings of PDMS.

Surface modification method to produce nonbiofouling PDMS surfaces can be mainly divided into three categories.

1- Surface activation
2- Physical adsorption/ physisorption
3- Covalent modification

1.6.1. Surface activation:

Surface activation is done for cleaning and oxidization of PDMS surface to increase its hydrophilicity and it also facilitates the bonding of PDMS devices and microchips. The PDMS devices after peeling off from SU–8 contains open channels that can be closed after bonding PDMS channels with clean glass or another PDMS slab. For this purpose, surface of PDMS (containing channels) and glass/PDMS slab is etched with the help of gas (i.e. oxygen, nitrogen, compressed air etc.) plasma or corona discharge and joined together in way that etched surfaces face towards each other [93-95]. Gas plasma is a partially ionized gas with a certain number of free ions and electrons, which are not bound to any atom or molecule and in which radical species can grow. Plasma of a gas can react with substrate surface to generate functional groups on surface [96]. In case of PDMS bonding, these functional groups of both surfaces react together to form a bond that ultimately results in joining both surfaces (figure 3).

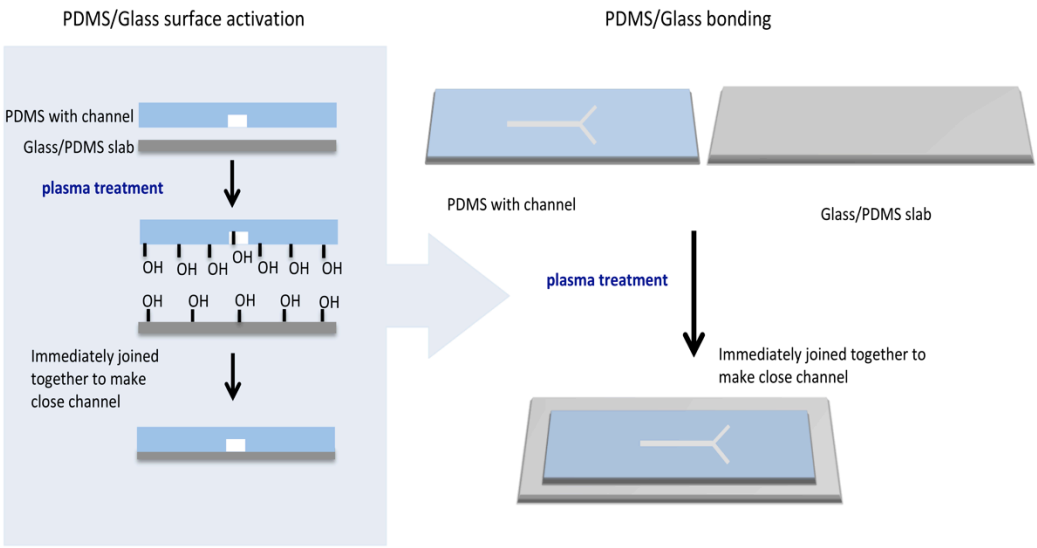

Figure 3: Surface activation of PDMS and/or glass surfaces and bonding for closed microfluidic channels.

Surface activation creates reactive silanol functional groups which can be subsequently used for further surface functionalizations. Oxygen plasma treatment [97, 98] corona discharges [99, 100] and UV/ozone [101, 102] are most commonly used methods for PDMS surface activation. Corona discharge and UV may cause deeper modification of PDMS surface but meanwhile induce cracking and weakness of surface and hydrophilic moieties are only formed in the presence of oxygen [101, 103]. Therefore Oxygen plasma treatment is most commonly used method for PDMS surface oxidation. After oxygen plasma treatment, surface hydrophobicity decreases and can be immediately and easily determine with the help of water contact angle [78].

Water contact angle is a measurement of the extant of hydrophobicity/hydrophilicity and surface energy of a material.

In an initial study, Fritz and Own [104] described the effect of plasma generated from various gases including argone, helium, nitrogen and oxygen. They showed that water contact angle on PDMS surface decreased upto 0–10° after treating with plasma of all gases. But the authors also noticed an increase in contact angle of all plasma treated surface after 24 h, which ultimately means the recovery of hydrophobicity of PDMS surfaces after some time of plasma exposure.

The major drawback of these simple surface activation techniques is the hydrophobic recovery of PDMS with the passage of time. Bodas and Malek [105] investigated that the migration of low molecular weight uncured PDMS oligomers towards surface is a reason of hydrophobic recovery of the surface. Eddington et al., [106] showed that removal of these low molecular weight species by thermal aging delays the hydrophobic recovery of oxygen plasma activated surfaces. A second plasma or a combined plasma treatment of various mixtures i.e., $SiCl_4$ or CCl_4 and proper storage can also enhance the time of hydrophobic recovery of PDMS surface [107, 108]. Storing PDMS samples, immediately after plasma treatment, under water and Luria–Bertani broth (LB broth), a common growth medium for bacteria, delayed

hydrophobic recovery considerably. PDMS samples stored in LB broth and water retained hydrophilic behavior for one week with contact angle maximum 20° to 30° respectively [109]. Lee and Yang [110] proposed that a long–lasting hydrophilic PDMS surface could be achieved by combining different methods. They used atmospheric pressure plasma followed by chemical vapor deposition on PDMS surface in order to get a long–term hydrophilic PDMS surface.

1.6.2. Physical adsorption/ physiosorption:

Physical adsorption is a process in which the electronic structure of the atom or molecule is barely perturbed upon adsorption on a surface but does not involves in a chemical bond formation. The fundamental interacting forces of physiosorption are caused by van der Waals forces and electrostatic interactions. Surface modification by physical adsorption is mostly used to prevent non–specific bonding of proteins in case of capillary electrophoresis. Numerous coating materials have been developed that could be physically adsorbed onto the microchannel surface via hydrophobic or electrostatic interactions. Examples of such materials include surfactants, amphiphilic copolymers and charged polymers such as polyelectrolytes, polysaccharides, and polypeptides [111].

Nonionic surfactants can be easily adsorbed on hydrophobic surfaces (figure 4a). Tween 20 [112] and n–dodecyle–β–D–maltoside (DDM) [113] are mostly used surfactants. Madadi and Casals–Terre [114] compared three different surfactants (Triton X–100, Brij 35 and Tween 20) at various concentrations to modify PDMS surface. They observed that all three surfactants decreased the contact angle of PDMS during 600s and Brij 35 was found to be most effective surfactacnt for the purpose.

Many of Polyethylene glycol (PEG) copolymers, also developed for biomaterials surface modifications, has been nicely reviewed by Tessmar and Göpferich [115].

Positively charged polyelectrolytes such as polyethyleneamine (PEI) [116], poly–L–lysine (PLL) [117] and chitosan [118] have been also used after grafting with PEG. Poly–L–lysine–g–polyethylene glycol (PLL–g–PEG) is a cationic copolymer, mostly used for surface functionalization due to its effective protein repellent properties, strongly adsorb on negatively charge surface. This copolymer is mostly used to coat O_2 plasma treated PDMS surface by developing a simple electrostatic interaction (figure 4b–i) [119, 120]. In advanced immunoassays, biochips and micro/nano biodetection devices are impacted by the non–specific adsorption of target molecules at the sample surface. Egea et al., [121] presented a simple and versatile low cost method for generating active surfaces composed of antibodies arrays surrounded by an efficient anti–fouling layer of PLL–g–dextran. Authors found this method very effective for reducing non–specific interactions responsible for a degraded signal/noise ratio.

Although physical adsorption is very simple method to attach molecules on surface but long–term stability is always difficult to achieve with this method. Another technique by utilizing layer–by–layer (LBL) self assembly of polyelectrolytes multilayer (PEM) was introduced by Decher [122] in 1997. In this method alternative layers of anionic and cationic polymers are electrostatically assembled on surface as represented in figure 4b–ii. These charged polymers are used to tune surface charges and control antifouling properties of surfaces. Polycationic

molecules such as Polybrene, polyethyleneimine, poly–(allyamine hydrochloride) (PAH), poly–(diallyldimethylammonium chloride) (PDDA), chitosan, and PLL can be alternatively adsorbed with polyanionic polymers such as, hyaluronic acid, dextran, and poly(acrylic acid) (PAA) to form the multilayer structure. The LBL self–assembly of polyelectrolytes on a charged surface offers another route of grafting PEG and other polymers onto substrates. Bovine serum albumin has also been used for PDMS surface modification with LBL technique [123].

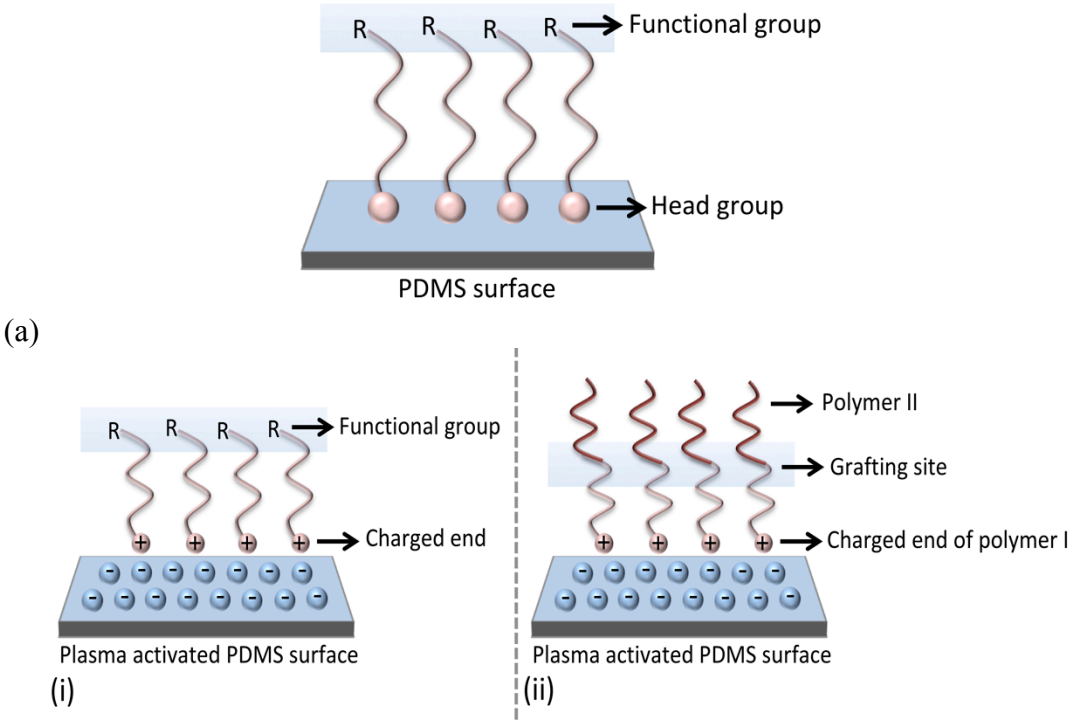

Figure 4: Schematic explanations of physiosorption on PDMS surface. (a) Adsorption of non–ionic polymers/ surfactants on hydrophobic surface, (b) electrostatic adsorption on plasma activated, negatively charged PDMS surface (b–i) direct adsorption, (b–ii) layer by layer deposition/ grafting.

Various proteins can also be conveniently adsorbed to various surfaces via intermolecular forces. The intermolecular forces, especially in case of proteins, are highly dependent on environmental condition such as pH, ionic strength, temperature, and surface condition. Therefore, immobilization of proteins in a reproducible manner can be difficult by using physisorption [124]. For PDMS, proteins are often adsorbed onto the bare surface owing to the hydrophobic nature of the substrate. In such systems, intermediate molecules are frequently used in order to attach to surface by covalent linkage and bond some hydrophobic or charged functional group on one end protein for physisorption [125].

1.6.3. Covalent modification:

Surface modification by via physisorption is very simple and quick way, however, these surfaces always suffer from thermal, mechanical, and solvolytic

instabilities due to their weak interactions of ligand to substrate. Covalent modifications could improve these inherent difficulties for more surface robustness. For this purpose, the most common method is establishment of self–assembled monolayers (SAMs) on surface. SAMs are prepared by spontaneous tethering of molecules with active chemical moieties onto reactive solid surfaces. Due to its ease of preparation, low cost, and versatility the field of SAMs has attracted vast research interests in many disciplines [126]. In a common practice, an oxidation/activation step on glass and PDMS surface (e.g. oxygen plasma, UV/ozone, or Piranha) is needed to generate surface silanol (Si–OH) groups before the SAM grafting [96]. Sui et al., [127] introduced an in situ approach for oxidation inside assembled PDMS microchannels with acidic H_2O_2 solution followed by a silanization process by injecting neat PEG–silane solution into the microchannel. This approach alleviated the use of specialized instruments for surface activation and post–assembly process after silanization. Furthermore, as illustrated in figure 5, SAMs also play a pivotal role as anchoring sites for further attachments of polymer chains and other groups or for initiation of surface anchoring [128].
Zhang et al. [129] modified O_2 plasma–pretreated PDMS microchannels with 3–glycidoxypropyltrimethoxysilane (GPTMS) and 3–chloropropyltrichlorosilane (CPTCS), which were further exposed to NH_2–PEG and alkyne–PEG solutions, respectively. Surface modification by this two–step grafting method decreased the contact angles to 70° for NH_2–PEG grafting and 64° for PEG for approximately 30 days. Chuah et al. [130] silanized PDMS surfaces with (3–aminopropyl)triethoxy silane (APTES) followed by glutaraldehyde (GA) crosslinking with APTES. The method was reported to modify PDMS surface properties such as reduction of hydrophobicity, increased protein immobilization, and variation of nanotopography.

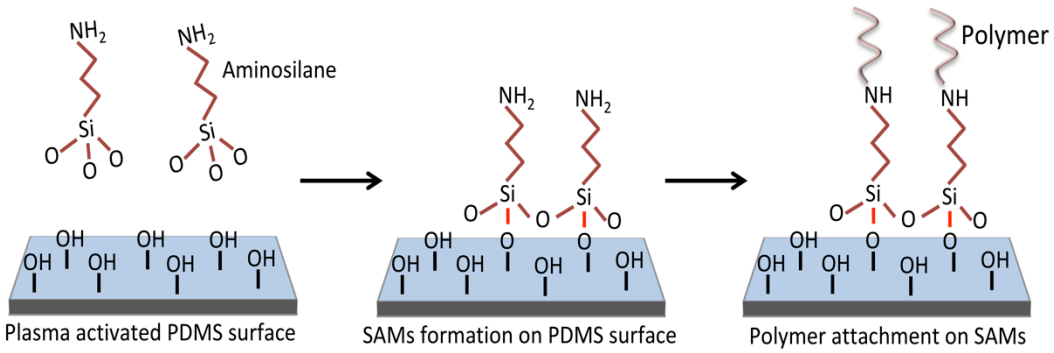

Figure 5: A general description of Aminosilane based SAMs on PDMS surface followed by a polymeric attachment.

Polymeric grafting is another widely used technique for modifying surface chemistry of PDMS. These covalent polymeric coatings are advantageous due to superior chemical and mechanical robustness with a high degree of flexibility to introduce a variety of functional group on substrate surface [131]. For example, a dens layer of alkaline–PEG was grafted on aldehyde–silane treated glass for DNA

oligonucleotide microarrays. After grafting, the terminal amino groups of the PEG layer were derivatized with the heterobifunctional cross–linker succinimidyl 4–[*p*–maleimidophenyl] butyrate to permit the immobilization of thiol–modified DNA oligonucleotides. Hybridization assays using DNA oligonucleotides and fluorescence imaging showed that PEG grafting improved the yield in hybridization. Additionally, the PEG layer reduced the nonspecific adsorption of DNA demonstrating that surfaces with a dense PEG layer represent suitable substrates for DNA oligonucleotide microarrays [132].

Wu et al., [133] has developed and characterized a fast and robust surface coating method on PDMS microchips. Where epoxy–modified polymers were directly adsorbed from aqueous solution onto plasma oxidized PDMS-based on H–bond interaction, and epoxies of polymer and silanols on oxidized PDMS surface were crosslinked by heating at 110 °C. The coating process could be completed within half hour. Thermal immobilization of polymers onto surface have been initially presented by Gilges et al., [134], who grafted poly(vinyl alcohol) (PVA) onto fused silica capillary surface at high temperature without any pre–coated surface anchoring layer. A hydrophilic silicate glass modified PDMS microchannel designed for glass–like performance was fabricated by channel coating of the preceramic polymer allylhydridopolycarbosilane (AHPCS) and subsequent hydrolysis. A few hundred nanometer thick, hydrolyzed preceramic polymers in the channels resulted in a lowering of the contact angle from 102° to 35°. Furthermore, this facile approach could be applicable to convert various plastic–material–based microchannels for a variety of microfluidic applications, including separation [135].

Surface initiated polymerization (SIP)] is another powerful toll to produce polymer brushes on surface–anchored initiation sites. Active sites that help in polymerization process are generated on surface. Then after applying monomers, polymer chains grow on surface. In this way, monomers added to the growing polymer chains from the surface do not face extensive molecular hindrance, and thereby a thick and dense layer of polymer brushes can be formed (figure 6) [126]. Hu et al., [136] established a simple one step UV mediated polymerization technique to coat PDMS surface with various polymers. PDMS pieces immersed in aqueous solution containing monomer, sodium per–iodate and benzyl alcohol were irradiated with UV source, which generated surface radicals to initiate polymerization. Sodium periodate was used as an oxygen scavenger and benzyl alcohol supported the diffusion of reactive monomers to the surface by decreasing solution viscosity. Hydrophilic polymer such as PEG monomethoxy acrylate (PEGMA) has been successfully coated onto the PDMS surface. Hu et al., [137] further modified this method for in situ surface coating inside assembled PDMS channel. A photoinitiator, benzophenone, in acetone solution was first adsorbed onto the PDMS channel wall before filling the channel with monomer solutions. The adsorbed photoinitiator significantly accelerated the polymerization rate on the surface and prevented gel formation in the solution, which may clog the channel.

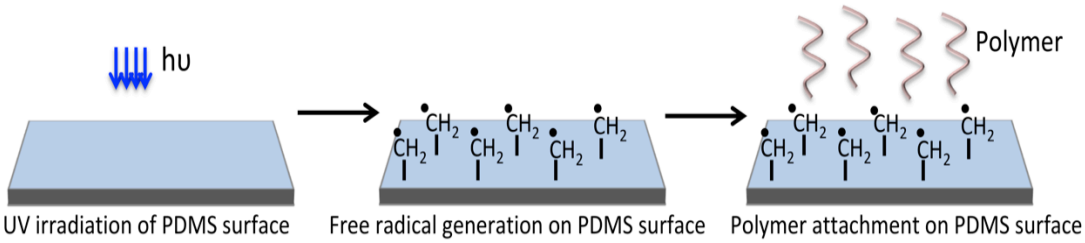

Figure 6: Schematic illustration of UV free radical based polymerization on PDMS surface.

Besides polymeric grafting, work has been also done to generate surface functional groups, which can be used for further reactions. He et al., [138] generated cyano (CN) functional groups on PDMS surface by using a two–step process. PDMS activated by microwave plasma in a mixed gas of Ar and H_2 was immersed in acrylonitrile solution to generate the hydrophilic functionalities on the surface. The grafted surface exhibited a low water contact angle (35° ± 15°) and was stable for at least one month at room temperature. Pruden et al., [139] modified PDMS surface with primary amine groups by using microwave ammonia plasma. A variety of nitrogen containing groups were formed in the reaction. At higher plasma power and higher temperature more amine groups are formed as compared to oxygen groups. Furthermore, functionalized dextran was successfully attached to the primary amine sites.

Living radical polymerization (LRP) or controlled radical polymerization has also attained considerable attention in surface chemistry. LRP basically relies on a continuous activation/ deactivation process of surface–anchored. Activated polymer chains (capping agents removed), in the presence of monomers, propagate for polymerization until it is randomly deactivated back by the capping agents [140, 141]. For example, Xiao et al., [142] described surface initiated ATRP to graft poly(acrylamide) on PDMS surface. ATRP initiator was first immobilized by vapor deposition of (1–trichlorosilyl–2–m–p–chloromethylphenyl) ethane onto UV/ozone oxidized PDMS surface. The silanized channel was then filled with oxygen free polymerizing solutions containing acrylamide monomer, Cu(I)Cl, $Cu(II)Cl_2$, and Tris[2–(dimethylamino)ethyl]amine and polymerization was allowed to proceed. The grafted surface maintained the hydrophilicity for at least one month.

B: Protein immobilization techniques.

Protein immobilization methods depend upon type of surface, protein properties, and the purpose of study. PDMS surface is relatively inert and lack functional groups (i.e., sites for protein attachment). Therefore chemical surface preparation is normally required to induce surface functional groups for protein immobilization [143].

The protein immobilization methods on PDMS surfaces can be mainly divided into three categories.

1- Physical adsorption/ physisorption
2- Bioaffinity interaction
3- Covalent modification

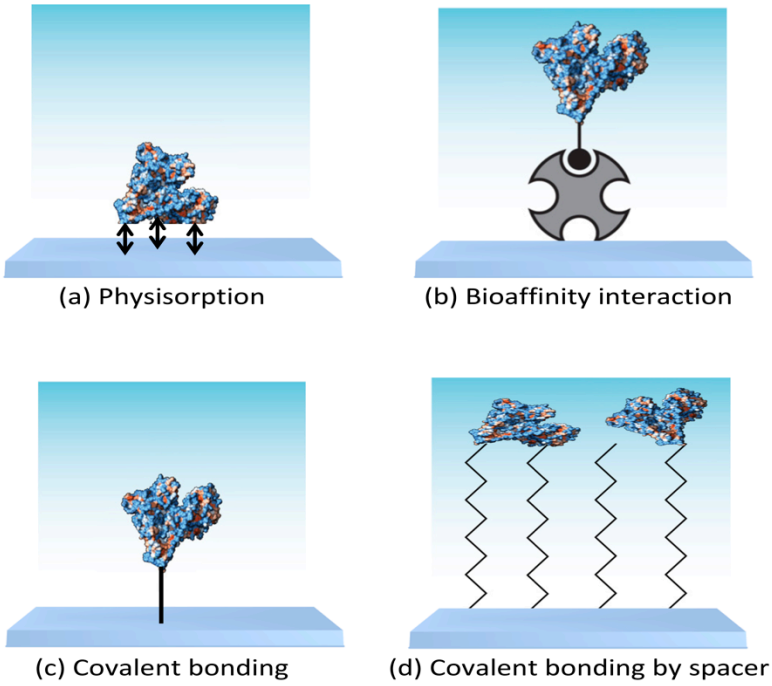

Figure 7: Various methods for protein immobilization on PDMS surface. Reproduced from [144] with the permission of AIP Publishing.

1.6.4. Physical adsorption/ physisorption:

Physisorption is a simplest approach to immobilizing protein on a surface. Protein can be conveniently adsorbed to surface by intermolecular forces such as electrostatic, hydrophobic, van der Waals, hydrogen bonding or combination of those (figure 7a). Incubating substrate in protein solution or continuous flow of solution through microfluidic channels will achieve the attachment of protein onto the surface, without any complex chemistry [145]. As immobilized protein is randomly oriented on the surface, thus a reproducible coating of protein is difficult to attain by this method. Because some fraction of the same binding sites within a population of proteins are likely not accessible. Furthermore, protein can be immobilized to the surface via multiple binding sites, which may result in conformational change and reduction of protein activity. In case of high protein density, active sites could be sterically blocked. In this type of cases, use of a spacer (e.g., PEG) between surface and protein has been widely used to reduce steric hindrance [125, 145, 146].

Proteins oftenly adsorbed or can be attached to PDMS surface by hydrophobic–hydrophobic interaction. Xiang et al. [147] designed an “H”–channel glass–covered PDMS chip as an immunereactor. An Escherichia coli antigen was physisorbed to PDMS surface and then later detected by primary and secondary antibodies. Hydrophobins are surface–active proteins of small molecular weight (7–15 kDa), could improve the physical and chemical properties substrate and might immobilize other proteins at surfaces simultaneously. Hydrophobins, group of cysteine–rich small proteins (≈ 100 amino acids), are typically used to attach on PDMS surface by hydrophobic–hydrophobic interaction to build the surface compatible for further functionalization [148, 149].

Spurlin et al., [150] prepared a collagen I thin film inside PDMS microfluidic devices after the hydrophobic recovery of PDMS surface. AFM characterization indicated that collagen fibril formed after 18 hour of incubation on PDMS surface have similar film thickness, fibril size, fibril coverage and physiological structure when compared to films on gold substrate. This method was further proposed for its applications for cell culturing on PDMS surface. In another study, Razafiarison et al., [151] reported remarkable effects of initial collagen self–assembly on PDMS surface that have important consequences for early stem cell signaling events and osteogenic differentiation. However, protein coatings based on self–assemblies due to hydrophobic interactions or simple adhesion onto the surface are not well appreciated in case of dynamic systems and under shear stress conditions in microfluidics.

Electrostatic or ionic interaction is very common to biomolecular attraction (e.g., protein– protein interaction and DNA hybridization. Thus, electrostatic interactions are frequently exploited in the biochemical assays, for example, cell adherence to positively charged poly–L–lysine (PLL) treated PS surfaces or protein blot to positively charge nylon membrane. Typical positively charged functional groups in biochemistry are protonated amine (NH^+) and quaternary ammonium cations (NR_4^+). Negatively charged functional groups are carboxylic acid ($-COO^-$) and sulfonic acid ($-RSO_3^-$). These functional groups are involved in the electrostatic interaction between protein and a surface [128, 152]. As mentioned before that PDMS is electrically neutral and contains no surface charges. Therefore typically the surface of PDMS is activated with O_2 plasma [97, 98] corona discharges [99, 100] or UV/ozone [101, 102] before growing cells onto the surface or before any protein/biomolecule attachment. So that an electrostatic interaction of proteins can be develop on PDMS surface for better attachment. Researchers showed that treating PDMS surface with O_2 or Ar^+/ O_2 plasma enhanced cell attachment and proliferation on surface [15, 153, 154]. It is demonstrated that plasma treated PDMS surface exhibits charged moieties (normally $-OH^-$) on surface that assist the better adhesion of ECM proteins e.g. Collagen [155] and Fibronectin [156] on surface, ultimately helpful for studying normal as well cancer cell lines. Juárez–Moreno et al., [157] studied the collagen coating strength on O_2 plasma treated PDMS by varying plasma strength between 40–120 Wa for 5–15 min. T–peel tests, performed on PDMS treated at 80 W/13 min and covered with collagen showed maximum peel strength of 0.1 N/mm which was 3 times higher than that measured for the control (PDMS without O_2 plasma). In a following study, same research group compared the effect of different plasma (oxygen, nitrogen and argon) treatments on PDMS surface for better adhesion of collagen. Peel test described that oxygen and nitrogen plasma attributed to the better adhesion of collagen on surface, which was further verified by FTIR studies [158].

In a recent study, Waters et al., [159]described a novel application of PDMS thin membrane as a skin model. Researchers studied the penetration of almost sixteen pharmaceutical compounds through O_2 plasma treated PDMS thin membrane. After comparing results with non–plasma treated PDMS membranes, it is that suggested that plasma modified membranes could be considered as suitable *in vivo* replacement to study clinical skin permeation.

1.6.5. Bioaffinity interaction:

The bioaffinity interaction or biospecific adsorption exploits precise binding phenomena already existing in nature. A bioaffinity interaction yields relatively stronger, very specific, and oriented protein immobilization thus advantageous over physisorption. Immobilized protein offers better approachability to binding partners than random orientation strategies. Additionally, bioaffinity immobilization can be reversed using chemical treatment, pH change, or heat treatment. In most of cases, bioaffinity interactions are used in conjunction with other immobilization mechanisms (i.e., physisorption and covalent bonding) with the bioaffinity reagent used as an intermediate binding molecule between the surface and proteins [125, 160, 161]. Figure 7b explains that how bio affinity interaction and immobilization works.

One of the most widely used immobilization pair is avidin (66–69 kDa tetrameric glycoprotein) and biotin (water–soluble vitamin B). Avidin binds to biotin via an exceptionally strong non–covalent interaction. The binding interaction is fast and nearly insensitive to pH, temperature, proteolysis, and denaturing agents. Biotin is a small molecule and conjugation to proteins does not significantly affect protein functionality or conformation. One shortcoming of using the avidin–biotin system is the high cost [162].

Due to the popularity of the avidin–biotin immobilization strategy, streptavidin coated polystyrene, agarose, and glass beads are commercially available for the microfluidic assays. PDMS-based microfluidic devices were used to immobilize streptavidin–coated polystyrene followed by a biotinylated glucose peroxidase (GOX) and horseradisch peroxidase (HRP) coating. The system was used to study the mixing efficiency of enzymatic substrate in a bead–packed microfluidic channel [163].

Moreover, protein A and G are two popular antibody (IgG) immobilizing reagents, obtained from bacteria. Protein G is known to have a wider immunoreactivity to mammalian IgGs than protein A. Surface coated with protein A or G specifically binds to the constant Fc region of IgG and the variable Fab region of IgG is accessible to antigen binding [160].

DNA–directed protein immobilization is also used for anchoring proteins onto the surface. Specific hybridization of single strand DNA (ssDNA) with the complementary DNA (cDNA) has been used to immobilize proteins. An ssDNA can be attached to the protein via covalent linkage or a biotin–streptavidin linkage. Protein is first joined to ssDNA and then this is hybridized to the surface where complementary ssDNA are already attached [164-167].

Despite this, antibodies are also used as universal intermediate biomolecule for proteins functionalizations. Microbeads coated with antibody exhibiting immunoreactivity towards an IgG of a specific animal species are commercially available to attach on PDMS surface, creating a site for further immobilizations. But high cost, variable affinity, and short shelf life of antibodies motivate the researcher to use other biomolecules [168, 169].

1.6.6. Covalent modification:

One of the frequently used protein immobilization mechanism in the microfluidic assays is by covalent bonding. The surface used for protein coating is activated with the help of reactive reagents. The activated surface reacts with amino

acid residues on the protein exterior and develops an irreversible linkage (figure 7c). Thus if highly stable protein coating is required, one can rely on covalent immobilization. Bifunctional spacer molecules are a common approach to develop an irreversible bond between proteins and the surface. In such an approach, one end of a spacer molecule is covalently linked to an activated surface, and then a protein is covalently linked to the other end of the spacer (figure 7d). The covalent attachment is mostly slow therefore covalent linking is normally performed as a preparatory step before performing microfluidic assays [144]. Huge varieties of covalent bonding chemistries are available. One of the most commonly used surface linkages is by using aldehyde intermediates. Amino groups ($–NH_2$) of lysine are the most common covalent binding sites because lysine residues are usually present on the exterior of proteins. Aldehyde is a reactive compound that forms the labile Schiff base with the amine and can be further reduced to form a stable secondary amine bond by using $NaCNBH_3$ or $NaBH_4$. Glutaraldehyde is a bis–aldehyde compound that has two reactive ends. GA can crosslink two amine functional groups, which may belongs to two proteins or a protein and a surface–immobilized polymer with amine groups (e.g., PEI). The Schiff bases formed on proteins are stable without further reduction by $NaCNBH_3$ or $NaBH_4$ [170]. For glass and PDMS-based surfaces, aminosilanes are normally used to bind with hydroxyl group of surface from one end (with $–NH_2$) and offering other end free for GA attachment followed by a covalent linkage with proteins.

Yu et al. [171] used an intermediate PVA [poly(vinyl alcohol)] layer to minimize nonspecific protein adsorption to PDMS. The researchers silanized an oxygen plasma treated PDMS surface with APTES. In order to form the hydrophilic layer, the amine group on APTES was activated with GA to attach PVA (via hydroxyl group of PVA) to PDMS. Then, GA was used once more to covalently link proteins such as IgM, BSA, and IgG to the PVA layer. So a sandwich immunoassay was demonstrated. Compared to the native PDMS surface, the SNR (signal– to–noise ratio) was improved due to low nonspecific adsorption and high antibody binding capacity.

Kuddannaya et al., [172] functionalized PDMS surfaces with APTES ± GA followed by the attachment of collagen type 1 and Fibronectin in order to improve the biocompatibility of PDMS substrate for long–term cell culture. Chemical functionalization was shown to reduce the hydrophobicity of the native PDMS surfaces. APTES and GA cross–linking chemistry showed stable covalent attachment of the matrix proteins on the basis of the available active surface functional groups. PDMS surface modified with APTES + GA + protein showed significant enhancement of mesenchymal stem cells (MSCs) adhesion and proliferation. In a following study by the same group, PDMS surface was coated with APTES and cross–linker glutaraldehyde chemistry to immobilize collagen type 1 (Col1) for MSCs growth. Gene expression of β–Catenin was evaluated during the early stage of MSCs sheet formation (1 week). β–Catenin is a protein within the cells that is responsible for the regulation of cell growth and cell–cell adhesion. Compared to the unmodified PDMS, a significant increase in the gene expression of β–Catenin on silanized PDMS surfaces lead to higher protein level of β–Catenin, which could enhance the cell–cell adhesion to maintain the integrity of the formed MSC sheet [130].

Another aminosilane coupling reagent, 3–(aminopropyl)trimethoxysilane (APTMS), is also widely used because of its better reactivity than APTES [127]. Sometimes a spacer of APTES or APTMS may be too short to properly immobilize large proteins (such as antibodies and enzymes) to planar channel surfaces in high capacity owing to steric hindrance [173]. The scheme may also cause reduced activity owing to partial physisorption to channel surface. Therefore, a hydrophilic polymer matrix such as dextran [161], chitosan [174], and polyethylene glycol [127] are used as longer spacers for improved assay sensitivity. There are many functional groups, which can be generated or attached on PDMS surface to develop a stable linkage to amine group of proteins. For example, N–hydroxysuccinimide–Amine [175], sulfhydryl–epoxide–Amine [176], isothiocyanate–Amine [127] are some individually reported methods/ linkages to covalently bond proteins on surface.

In order to enhance the stability of protein coatings, it has become very common to use more than one immobilization techniques simultaneously. Keranov et al., [177] described a multistep surface coating to bond collagen on PDMS surface. In this multistep procedure to an Ar^+ plasma treated PDMS surfaces was used for acrylic acid grafting followed by flexible PEG spacer coupling prior to the collagen immobilization. An improved cell growth was observed after growing on this biofunctionalized PDMS surface. In another study, Hou et al., [178] developed a fully biocompatible approach for patterning of cells on the PDMS surface by hydrophobin (HFBI) and collagen modification. HFBI and collagen were immobilized on the PDMS surface one after another by using copper grids as a mask. HFBI self–assembly on PDMS surface converted the PDMS surface from hydrophobic to hydrophilic, which facilitated the following immobilization of collagen. Consequently, the HFBI/collagen–modified PDMS surface could promote cell adhesion and growth. The patterning of cells was achieved by directly culturing 293T cells (the human embryonic kidney cell line) on the PDMS surface patterned with HFBI/collagen while native PDMS surface did not support cell growth.

1.7. Cell growth in PDMS microfluidic devices:

PDMS is a well–recognized biocompatible polymer but needs surface modification for cell adhesion and growth for almost all cell lines. In order to modify PDMS surface with improved biocontact properties, it is very important to understand the mechanism of cell/surface interaction. General theory of bio–adhesion does not exist up to now despite the fundamental understanding of its molecular mechanisms can lead to the creation of material surfaces that can support the cell–surface interaction [179].

It is already known that different cell types use different mechanisms when attaching to different surfaces and as a rule, cells do not interact with the surface directly but via proteins secreted by them and adsorbed on the surface adhesive, forming their own nonorganized layer. According to a “classical scheme”, adhesive factors, like fibronectin and vitronectin are present in the serum adsorbed on the substrate and the adhesion is in fact an interaction with them. Although the cell–surface interaction mechanisms are not fully understood but it depends significantly on different biomaterial surface parameters, such as hydrophilicity, chemical composition and charges [180].

The process of cell culture involves the removal of cells from their natural (in vivo) location and their subsequent growth in an artificial (in vitro) environment. To reproduce a culture environment is critical to enable cells to grow, function and survive in a realistic manner. Within a tissue, cells are in contact with the neighboring cells and ECM. The ECM is a complex environment of molecules consisting of proteoglycans and insoluble fibrous proteins. Interactions between cells and ECM components are important in many biological processes such as cell growth and development [181, 182].

Although, the ECM is basically composed of water, proteins and polysaccharides, but each tissue has an ECM with exceptional composition and topology that is generated during tissue development. The ECM is composed of two main classes of macromolecules: proteoglycans (PGs) and fibrous proteins. The main fibrous ECM proteins are collagens, elastins, fibronectins and laminins. PGs fill the majority of the extracellular interstitial space within the tissue in the form of a hydrated gel. PGs have a wide variety of functions that reflect their unique buffering, hydration, binding and force–resistance properties [183, 184]. Figure 8 is representing basic components of ECM, which are common to many of the tissues and organs.

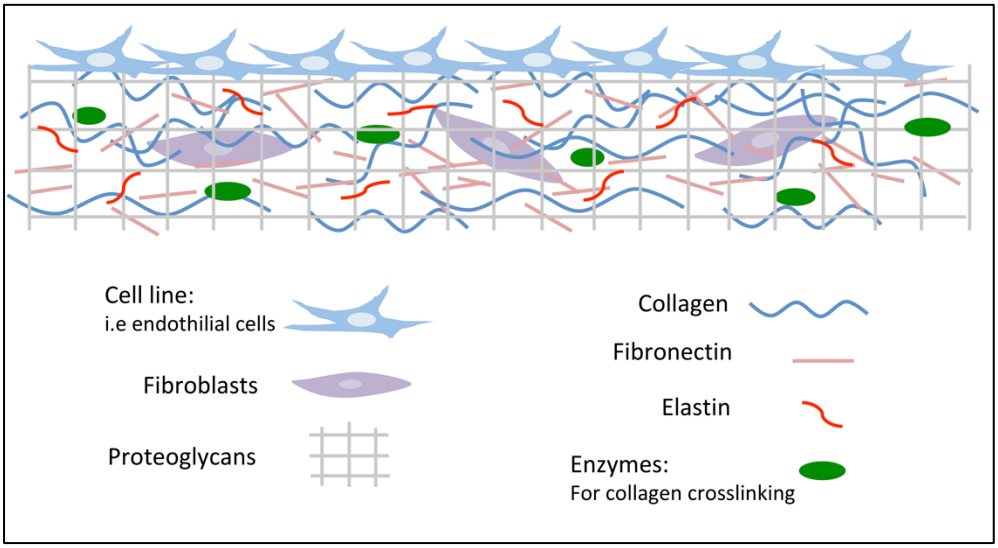

Figure 8: Representation of very basic units of ECM and cell–ECM interaction.

The transmembrane proteins, known as integrins, attach to the ECM and connect indirectly to the actin filaments through protein assemblies of talin– paxillin–vinculin. These protein assemblies stabilise the focal adhesion structure, as well as relaying signals from the ECM to the nucleus [185]. Focal adhesions were first observed to form between cells and solids by Ambrose [186] using the surface contact light microscope and later by Curtis [187]. Two morphological variants of the focal adhesion exist; the ‘dot’ and ‘dash’ variants ‘Dot’, or small initial, contacts are composed of transmembrane and some linker proteins but are not associated with actin bundles. These are the predominant contact type, with dimensions of 0.2–0.5μm, and are mainly located at the active edge of the cell. Elongated large mature, or ‘dash’, contacts are also composed of transmembrane and linker proteins but differ due to their association with the cytoskeletal actin bundles. Dash contacts are 2–10μm

in length and 0.5μm in width and are located centrally in parts of the lamellae, areas of the endoplasm and under the nucleus [188].

Cell attachments to the ECM or to the other cells contribute not only to the organization of tissues and organs but also to the capacity of a cell to recognize and be regulated by microenvironments. For example focal adhesions physically link the actin–myosin cytoskeleton to ECM proteins – collagens, fibronectin and laminin and provide a means to transmit forces during cell migration and stationary contraction. Cellular dynamisms are known to regulate focal adhesion size, shape and composition [182].

Many ECM proteins can be involved in cell adhesion and all include domains that contain a specific amino acid sequence, each sequence is a signal for a specific integrin complex attachment site. Signals from the integrins are communicated to the nucleus by the bridging proteins and the actin fibers. These signals initiate nuclear gene expression that subsequently sends the corresponding response signal [189].

Surface chemistry has been reported to modulate the structure and molecular composition of cell–matrix adhesions as well as focal adhesion kinase (FAK), a focal adhesion associated protein signaling. It is reported that FAK also shows different sensitivity to surface chemistry. For example, surfaces with neutral hydrophilic –OH groups supported the highest levels of recruitment of talin, α–actinin, paxillin and tyrosine–phosphorylated proteins to adhesive structures. Positively charged $–NH_2$ and negatively charged –COOH terminated SAMs exhibited intermediate levels of recruitment of these focal adhesion components, while hydrophobic $–CH_3$ substrates displayed the lowest levels [190].

In general, the cells utilize integrins, a family of transmembrane glycoproteins, to attach to specific cell binding sites that are displayed by ECM proteins. The integrins are able to link the cell cytoskeleton to a material surface via these proteins present on the surface. Adsorption or immobilisation of specific ECM proteins can therefore be used to enhance cell attachment. It is widely recognized that adsorbed ECM proteins assist in specific cell adhesion and spreading through integrin binding and regulate other subsequent signaling events including proliferation, differentiation motility, gene expression, survival and even cell death [191-193].

Considering the importance of ECM to many of basic cellular processes it has become fundamental step to coat substrate surface with ECM proteins to get more precise information about cell behavior.

Fibronectin has been widely studied in this role. Adsorption of fibronectin onto substrates of varying surface chemistry alters its conformation/structure and therefore the ability of the molecule to support cell adhesion. In a previous study, fibronectin was coated on variously functionalized surfaces. The contrasting surface chemistries exhibited variation in fibronectin adsorption, which ultimately provided the differential cell adhesion characteristics [194].

Hence, collagen is highly preferred ECM protein used for *in vitro* cell adhesion and growth models. It is the most abundant fibrous protein of ECM and constitutes up to 30% of the total protein mass of a multicellular animal. Collagens, which constitute the main structural element of the ECM, provide tensile strength, regulate cell adhesion, support chemotaxis and migration, and direct tissue development [195].

There are twentyeight different types of collagen composed of at least 46 distinct polypeptide chains have been identified. In 1940, Astbury and Bell [196] proposed that the collagen molecule consists of a single extended polypeptide chain with all amide bonds in the *cis* conformation. A significant advance was achieved when later on, Pauling & Corey [197] proposed a structure for collagen in which they described the correct structures for the α–helix and β–sheet. In that structure, three polypeptide strands were held together in a helical conformation by hydrogen bonds. In 1955, this structure was refined by Rich and Crick [198] and by North and colleagues [199] to the triple–helical structure accepted today, which has a single interstrand $N–H_{(Gly)} \cdots O=C_{(Xaa)}$ hydrogen bond per triplet and a tenfold helical symmetry with a 28.6–Å axial repeat.

Triple helix structure and internal bond nature of collagen provides more stability to the collagen fibers. Moreover, being the most abundant part of ECM it is obviously a most available/in contact protein to the cells *in vivo*. Therefore, the use of collagen coatings on various substrates including PDMS, prior to cell culturing, has become popular.

Zhang et al., [155] demonstrated that coatings of fibronectin, bovine serum albumin (BSA), or collagen on PDMS surfaces dramatically impacted the phenotypic equilibrium of breast cancer stem cells, while the variations of the PDMS elastic stiffness had much less such effects. Moreover, the surface coatings of collagen and fibronectin on PDMS maintained breast cancer cell phenotypes to be nearly identical to the cultures on commercial polystyrene petri dishes. While, the surface coating of BSA provided a weak cell–substrate adhesion.

Therefore, the ECM proteins coating, generally with collagen, is not only used for modification of PDMS surface but has also become obvious for microfluidic cell culture. Principally when PDMS microfluidic devices are used to study vascular model or vascular disease models it is important to provide the cells a natural habitat to develop more precise understanding.

The endothelial cells (ECs) covering the luminal surface of the blood vessel wall are continuously exposed to fluid shear stress, generated naturally by blood flow. The ECs respond to shear stress and change their morphology, function, and gene expressions to regulate blood flow and maintain tissue homeostasis. The responses of ECs to shear stress are also associated with blood flow–dependent phenomena, including vascular remodeling, angiogenesis, atherosclerosis, and thromboembolism [200].

As described above, due to hydrophobic recovery of PDMS, many of protein grafting techniques have been developed to stably coat PDMS surface with collagen or fibronectin. In microfluidic devices, system become more dynamic because of continues fluid flow, which can cause protein detachment from channel walls ultimately leads to cell death.

Other than blood flow, Interstitial fluid, flowing within the interstitium of the extracellular matrix (ECM), transports nutrients and signaling molecules between blood vessels, lymphatic capillaries, and ECM. Although the velocity of interstitial fluid flow (IFF) is relatively slow. Besides its role in mass transport, IFF provides a specific mechanical environment for the cells, which is significant to cells' physiological and pathological activities. Low shear stress (mPa) generated by IFF

plays an important role in the cellular mechanotransduction, by which the cells transduce mechanical stimuli into a biochemical response [201]. In a study, Delaine–Smith et al., [202] reported that alkaline phosphatase activity, collagen production and calcium deposition were enhanced in human progenitor dermal fibroblasts by FSS when these cells were cultured in osteogenic media.

Thus it is assumed that including endothelial cells, many of the other cells in the body like fibroblasts and osteoblasts, smooth muscle cells etc. are continuously exposed to shear stress.

Yang et al., [203] developed a PDMS-based microfluidics to create a microenvironment that can incorporate both nanotopography and flow for studies of cell–matrix interactions. Microfluidic channels were fabricated endowed with nanopatterns suitable for dynamic culture. The cellular study showed that both nanotopography and fluid shear stress played a significant role in adhesion, spreading, and migration of human mesenchymal stem cells. The orientation and deformation of cytoskeleton and nuclei were regulated through the interplay of these two cues. Figure 9 is demonstrating the simple model of cell growth inside a microfluidic channel.

The magnitude of shear stress in our body ranged 0.02 dyne/cm^2 (in gut) to ≈ 650 dyne/cm^2 (in neurons), whereas the arterial shear stress ranges from 0.07–13 dyne/cm^2. So far, a number of microfluidic assays have been developed to study cell response and behavior under shear stress and most of them used arterial shear stress range to investigate cell response [204].

In order to increase the experimental efficiency, many microfluidic shear flow assays have been developed so that multiple shear stress levels can be simultaneously applied to ECs cultured in a single chip. In this regard, Song et al., [205] conducted a preliminary study to recreate physiological conditions of EC environment *in vivo* in terms of shear stress. The integrated microfluidic valving and pumping system allowed primary EC seeding and differential shearing in multiple compartments to be performed on a single chip. The microfluidic flows caused ECs alignment and elongation significantly in the direction of flow according to their exposed levels of shear stress (5–20 dyn/cm^2, pulsatile) for maximum of 24 h.

Chau et al., [206] introduced a multichannel microfluidic design to study the stress dependent elongation and alignment of endothelial cells. This fibronectin coated PDMS device covered the range from physiological shear stress at rest (1–70 dyn/cm^2) to shear stress during exercise or thrombosis (70–100 dyn/cm^2). HUVECs under shear stresses ranging from 1–3 dyn/cm^2 (0.1–0.3 Pa) showed similar vWF content, cell and nuclear size and perimeter to static cultures, while the cells under shear stresses above 5 dyn/cm^2 (0.5 Pa) showed significantly higher vWF secretion and were at least 30% smaller in cell size. The data observation time in experiment was selected as 6 hours because after 6 hours cells started detaching and after 24 h 90% of the cells were detached from the channels.

These studies indicated the fact that long–term studies are limited by instability of protein coatings and cell adhesion inside PDMS microfluidic devices at high shear stress.

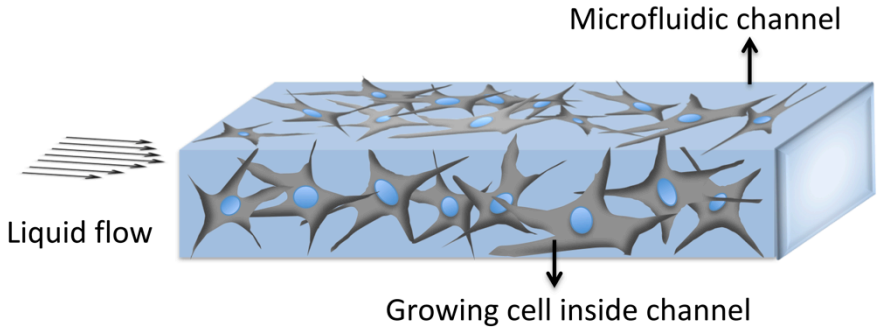

Figure 9: Schematic illustration of cell growth inside a simple microfluidic channel

Tsai et al., [12] developed a very nice and explanatory model of in vitro "endothelialized" microfluidic microvasculature. The model describe the development and characterization of a microfluidic device consisting of key aspects of the microvasculature that includes size scale (30µm–wide), an endothelial monolayer cultured throughout the entire fibronectin coated 3D inner surface of PDMS system. Moreover, physiologically relevant hemodynamic parameters were tightly controlled and varied. This in vitro microvasculature presented an experimental recapitulation of collective of physiological processes, including platelet, leukocyte, and endothelial activation, adhesion molecule expression, cell aggregation, cytokine production. Furthermore, the interactions among many different cell types as well as biophysical and rheological interactions among hemodynamics, microvascular geometry, and multiple cell types was also described. This microsystem was ideally suited for studying hematologic diseases involving microvascular occlusion and thrombosis in which interplay among those processes affects pathophysiology. The system was used in a continues study for 2–3 days but at very low shear stress (1.25 µL/min).

Therefore, the development of protein grafting technique on PDMS surface has become essential to achieve stable protein coating.

In some cases, the monolayer of protein may not adequately mimic the structural, chemical and mechanical features of an in vivo three–dimensional (3–D) environment, which limits the cell attachment, proliferation and stability. This is normally happens when surfaces are coated with native collagen due to its complex 3D structure. Surface charge, functional groups, pH of the solution, ionic concentration of solution are some of the basic influencing factors for collagen self assembly which can promote stable cell adhesion [207]. For example, Jiang et al., [208] explained the dependency of fibril formation on pH of the solution and reported that collagen fibril formation starts after pH 5 and nice fibers can be obtained at pH 7–9. He et al., [209] described the dependency of thermal stability of collagen on ionic concentration of solution. Reports are also available to described that collagen structure and fiber formation can be controlled by surface/substrate chemistry and surface functional groups [207, 210].

Though these all procedures are studied to develop better understanding about collagen assembly and correct orientation on surfaces but can also be applied to

anchor PDMS surfaces inside microfluidic devices for better cell adhesion. Meanwhile thin layer protein coatings are always preferred in microfluidic channels with small dimensions. As described earlier that collagen assembly and fiber formation can be rather controlled on surface by varying various factors. But still the establishment of thin layer protein coating under long term high shear stress conditions in PDMS-based microfluidic devices is still challenging due to less binding forces between PDMS proteins, hydrophobic recovery of PDMS surfaces and dynamicity of the system.

The current work aimed to develop thin layer protein coatings inside PDMS microfluidic devices with narrow dimensions, where the influence of applied shear stress on protein coatings and growing cells is more dominant.

Chapter 2. Materials and Methods

2.1. Techniques used for studies

2.1.1. Water Contact angle (WCA):

Water contact angle is a measurement of the extant of hydrophobicity/hydrophilicity and surface energy of a material. When a liquid/water is placed on a solid, it forms a drop or it spreads on the surface, the angle between the liquid–solid interface is called its contact angle θ.

There are three general cases can be seen (figure 10) during liquid spreading onto a surface contact angle

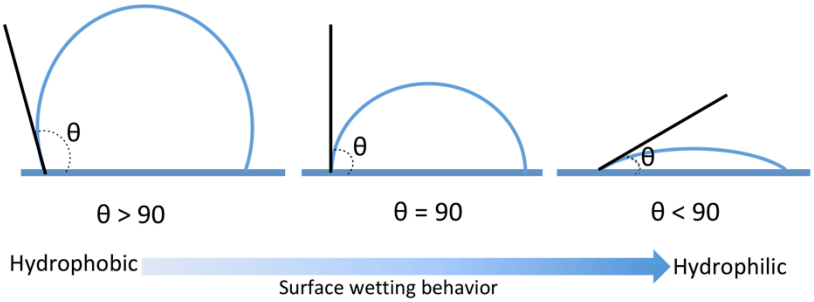

Figure 10: Basic concept of contact angle formation on solid surface.

When a liquid drop forms a contact angle below 90°, it is referred as 'good wetting' and when it forms a large contact angle i.e, 90° – 180°, it is said to be non–wetting. Wetting of a surface with water means that the surface has a high surface energy and is hydrophilic whereas non–wetting surface has a low surface energy and is hydrophobic. This signifies that the higher the contact angle, the higher the water repelling properties of the surface. Small contact angles can occur, for example, when surfaces are electrostatically charged. Such surfaces can bind water via hydrogen bonds, which results in a spreading of water and therefore in an easy water–coverage of the surface [211, 212].

In 1805 YOUNG had already formulated a relationship between the interfacial tensions at a point on a 3–phase contact line (figure 11) [213].

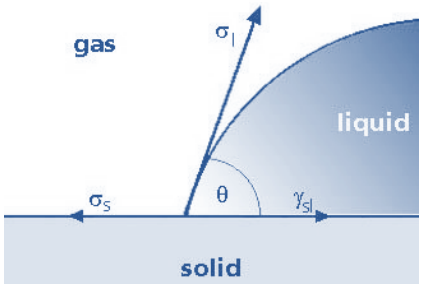

Figure 11: Contact angle formation on solid surface according to Young's 3–phase contact line.

Where “s” and “l” stand for “solid” and “liquid”; the symbols σ_s and σ_l describe the surface tension components of the two phases; symbol γ_{sl} represents the interfacial tension between the two phases, and θ stands for the contact angle corresponding to the angle between vectors σ_l and γ_{sl} .

YOUNG formulated the following relationship between these quantities,

$$\sigma_s = \gamma_{sl} + \sigma_l \cdot \cos\theta \qquad (2)$$

So that the surface energy can be calculated by measuring the contact angle between liquid and surface.

2.1.2. Light Microscopy:

Microscopes are specialized optical instruments designed to produce images of objects or specimens that are too small to be seen with the naked eye. Starting from hand–held instruments such as photography loupe or common magnifying glasses to a compound microscopes include multiple–lens, designs featuring objectives and condensers. In its simplest form, the instrument is composed of two convex lenses aligned in series: An objective closer to the object or specimen, and an eyepiece (ocular) lens closer to the observer's eye (with means of adjusting the position of the specimen and the microscope lenses). The compound microscope achieves a two–stage magnification where the objective projects a magnified image into the body tube of the microscope and the eyepiece further magnifies the image projected. The total magnification equals the magnification of the objective multiplied by the magnification of the eyepiece:

Total Magnification = Objective Magnification x Eyepiece Magnification

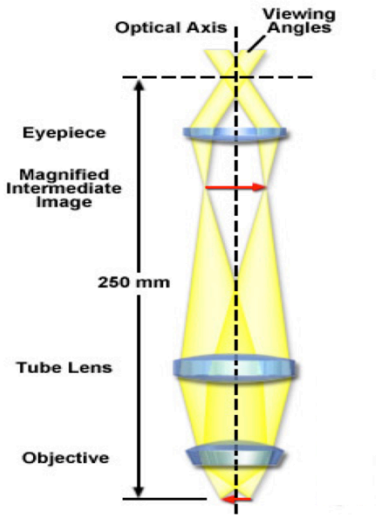

Figure 12: Basic principle of light microscopy. Image is reprinted with permission from Zeiss microscopy GmbH.

In modern microscope contains a tube lens as added support for the objective. The light rays originating from one point of the specimen travel in straight, parallel lines behind the objective. The tube lens then functions in a similar way to a camera to focus the parallel ray bundles, producing a magnified intermediate image located inside the eyepiece at its front focal plane (figure 12).

At a selected numerical aperture, where the microscope presents a magnified image with a magnitude equivalent to the resolution limit of the human eye, further magnification beyond this point does not result in the resolution of even finer specimen detail. The numerical aperture of a microscope objective is the measure of its ability to gather light and to resolve fine specimen detail while working at a fixed object (or specimen) distance.

In a simple microscope system consist of an objective and specimen being illuminated by a collimated light beam. Light diffracted by the specimen is presented as an inverted cone of half–angle (α), which represents the limits of light that can enter the objective. In order to increase the effective aperture and resolving power of the microscope, a condenser is added to generate a ray cone on the illumination side of the specimen. This enables the objective to gather light rays that are the result of larger diffraction angles, increasing the resolution of the microscope system. The sum of the aperture angles of the objective and the condenser is referred to as the working aperture (figure 13). If the condenser aperture angle matches the objective, maximum resolution is obtained.

The numerical aperture is defined as

$$\textbf{Numerical Aperture (NA)} = \eta \bullet \sin(\alpha)$$

where α equals one–half of the objective's opening angle and η is the refractive index of the immersion medium used between the objective and the cover slip protecting the specimen (η = 1 for air; η = 1.51 for oil or glass).

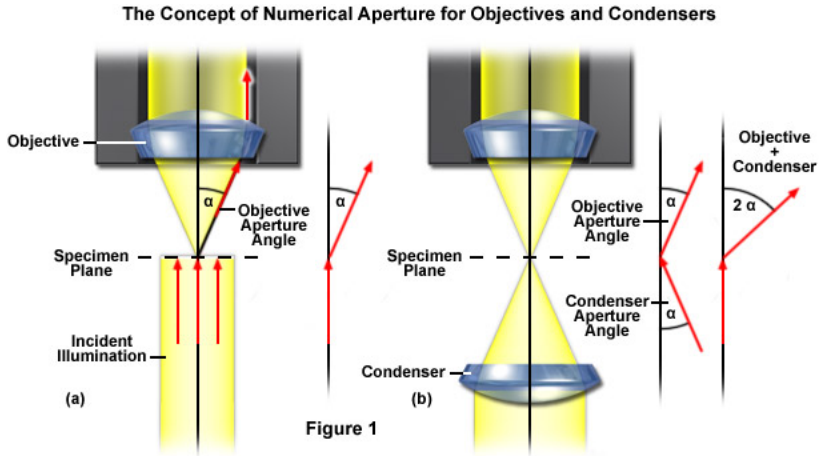

Figure 13: The concept of numerical aperture (NA) for objectives and condensers. Image is reprinted with permission from Zeiss microscopy GmbH.

The highest angular aperture obtainable with a standard microscope objective would theoretically be 180 degrees, resulting in a value of 90 degrees for the half–angle used in the numerical aperture equation. The sine of 90 degrees is equal to one,

which suggests that numerical aperture is limited by the angular aperture and definitely by the imaging medium refractive index. Practically, aperture angles exceeding 70 to 80 degrees are found only in the highest–performance objectives that typically expansive.

The range of useful total magnification for an objective and eyepiece combination is defined by the numerical aperture of the system. There is a minimum magnification necessary for the detail present in an image to be resolved by the eye, and this value is typically set at 500 times the numerical aperture (500 x NA). At the other end of the spectrum, the maximum useful magnification of an image is usually set at 1000 times the numerical aperture (1000 x NA). This limit is set by the wave nature of light imposed on the objective by diffraction. Magnifications higher than this value will yield no additional useful information of finer resolution of image detail, and will usually lead to image degradation. Exceeding the limit of useful magnification causes the image to suffer from empty magnification, where increasing magnification through the eyepiece or intermediate tube lens only causes the image to become more magnified with no corresponding increase in detail resolution [214, 215].

2.1.3. Fluorescence Microscopy:

The idea underlying fluorescence microscopy is the visualisation of fluorescent molecules by light excitation. Light with a certain wavelength is used to illuminate the specimen, which is already labeled with specific fluorophores. Electrons from the outer shell of fluorophores are excited by a specific wavelength, the absorption process is fast and only takes 10^{-15} s. At excitation state due to energy loss processes, light of certain wavelength is re–emitted by the electron, which falls down again to a first excited level. . Finally, this orbital electron relaxes to its ground state and a photon is emitted along with, hereby fluorescence is detected (figure 14). The emission takes place after 10^{-12} s to 10^{-9} s.

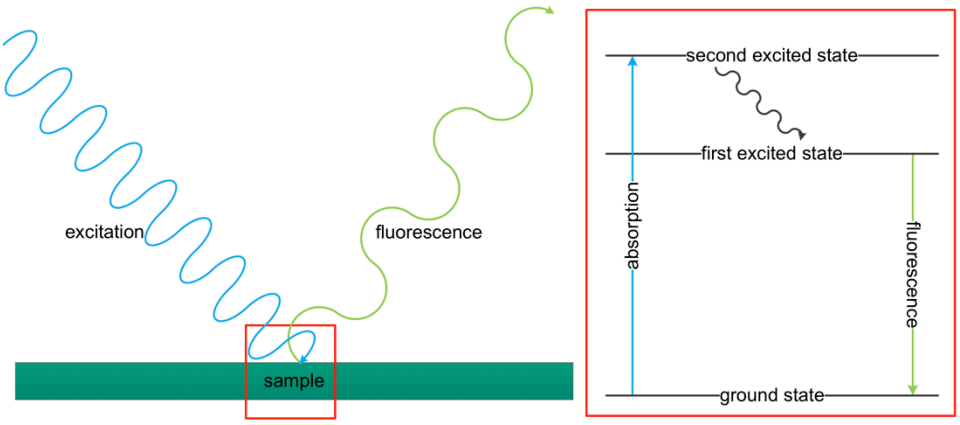

Figure 14: Basic principle of fluorescence microscopy

In a fluorescence vertical illuminator, light of a specific wavelength, often in the ultraviolet, blue or green regions of the visible spectrum is produced, by passing multispectral light from an arc–discharge lamp, high–powered LEDs or other source

through a wavelength selective excitation filter. Wavelengths passed by the excitation filter reflect from the surface of a dichromatic mirror or beam splitter, through the microscope objective to the specimen. If the specimen fluoresces, the emission light gathered by the objective passes back through the dichromatic mirror and is subsequently filtered by an emission filter, which blocks the unwanted excitation wavelengths. In this manner, the distribution of a single fluorophore is imaged at a time. Multi color images of several types of fluorophores can be composed by combining several color images [216, 217].

2.1.4. Atomic Force Microscopy (AFM):

Atomic force microscope was first invented in 1986 by Binnig and colleagues [218]. Since its invention, it has become one of the most important tools for imaging the surfaces of objects at nanometer scale resolutions. AFM is a type of scanning probe microscope (SPM), which uses a fine probe to scan surface rather than use electrons or a beam of light and a 3D maps of surfaces is created. AFM consists of four major parts: (i) a cantilever with a sharp tip, normally made of silicon or silicon nitride, mounted underneath it; (ii) a piezo–scanner that drives the cantilever; (iii) a laser diode; and (iv) a position sensitive detector. As the tip scans over the surface, the interactions between the AFM tip and the features on the surface cause displacement of the cantilever. This displacement is measured by detecting the deflection of a weak laser beam, generated by the laser diode, reflecting off the back of the cantilever with the photodiode detector. The atomic force microscope creates topographic images of the surface by plotting the laser beam deflection as its tip scans over the surface [219]. Figure 15 represents basic parts and working principle of a simple AFM mode.
The AFM technique can analyze any kind of samples such as polymers, adsorbed molecules, films or fibers whether in a controlled atmosphere or in a liquid medium at room temperature or at 37 °C.

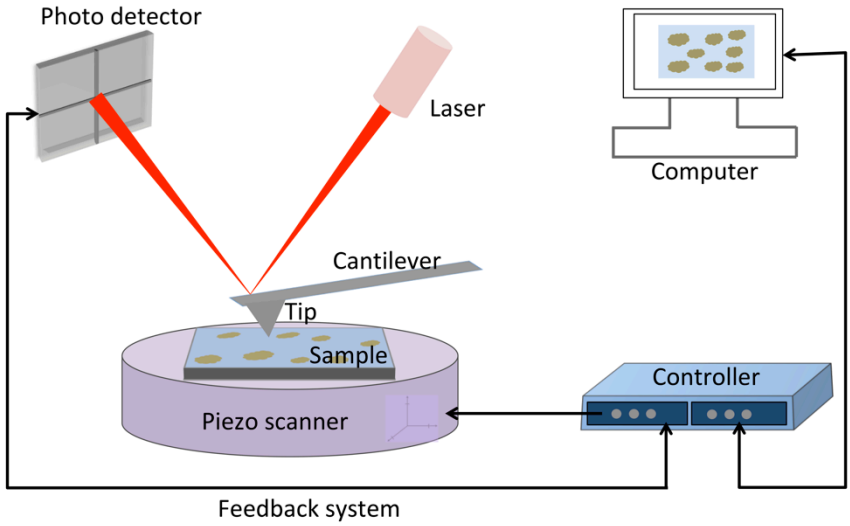

Figure 15: Basic principle of atomic force microscopy

AFM operates in different modes according to its application; the most famous modes for surface scanning are contact mode, non–contact and tapping mode. In the

contact mode, a force is applied by the AFM on the sample, and the interaction between the AFM probe and the sample is repulsive. As the scanner gently traces the tip across the sample, the contact force causes the cantilever to bend to accommodate changes in the sample's topography. Both the normal and the frictional force can damage exposed biological samples. To image these kinds of samples, the force applied must be carefully controlled.

In the non–contact mode, the cantilever is oscillated at a distance (normally 5–15 nm) above the sample surface. The working force between the tip and the surface are mainly van der Waals forces or Coulomb and dipole interactions. These attractive forces are varied during measurement, due to change in topography of surface. These force changes induce alterations in the resonant behavior of the oscillating cantilever [220].

In order to achieve the highest resolution, the cantilever is brought close enough to the surface to effectively detect the attractive forces. Thus, the oscillating probe very often slightly touches the sample surface, and becomes intermittent–contact or tapping mode AFM [219, 221].

2.2. Materials used for studies:

Name	Empirical formula	Company	Catalogue number	CAS number
Acetic acid	$C_2H_4O_2$	Roth®	7332.1	64-19-7
Acetone	C_3H_6O	Roth®	5025.2	67-64-1
APTES [(3–aminopropyl)–triethoxysilane]	$C_9H_{23}NO_3Si$	Sigma Aldrich®	G5882	919-30-02
Eosin methylene blue	—	Sigma Aldrich®	45250-10G-F	—
Glutaraldehyde solution	$C_5H_8O_2$	Sigma Aldrich®		111-30-8
Hydrochloric acid	HCl	Roth®	T134.4	7647-01-0
Live/Dead® viability kit (Molecular Probes)	—	ThermoFischer Inc.	L3224	—
Actin stain™ 555	—	Cytoskeleton, Inc.	PHDH1-A	—
LSGS [low serum growth supplement]	—	ThermoFischer Inc.	S00310	—
Medium 200	—	ThermoFischer Inc.	M200500	—
Normocin	—	InvivoGen	ant-nr-1	—
PBS	—	Sigma Aldrich®	D8537	—
PDMS Sylgard 184 kit Dow corning	C_2H_6OSi	Biesterfeld	5498840000	—
Rat tail collagen I	—	ThermoFischer Inc.	1.1. A1048301	1.2. —
Sodium acetate	$C_2H_3O_2Na$	Roth®	6773.1	127-09-3
Sodium bicarbonate	$NaHCO_3$	Sigma Aldrich®	S8761	144-55-8
Sodium hydroxide	NaOH	Roth®	9356.1	1310-73-2
Trypsin/EDTA	—	Biochrom GmbH	L2123	—
Trypsin neutralizer	—	ThermoFischer Inc.	R002100	—

2.3. Collective methods for studies:

Though many researchers worked on ECM protein grafting on PDMS surface to enhance its wetting ability and surface biocompatibility (Chapter–1, Introduction). However, it is still a challenge to produce a thin homogeneous layer of proteins and to evenly distribute the coating throughout the micro channel and to ensure the stability of the system under flow conditions. And it is also assumed that in many of the surface anchoring protocols the protein to surface bonding mechanism needs to explore in detail.

To address this issue, in current thesis, a simple and steadfast method for stable ECM protein coating inside PDMS micro channels using aminosilane chemistry is developed. Moreover, considering collagen as model ECM protein, a detailed comparison of various different PDMS functionalizations was established by using PDMS surfaces as well as inside the microfluidic channels.

2.3.1. PDMS preparation:

The PDMS was cross linked by gently mixing silicone elastomer and its curing agent (provided along with elastomer) with a ratio of 10:1 (w:w)) for 2 min (Figure 17). The curing agent contains platinum catalyst for polymerization [222]. The polymer was degased at room temperature for approximately an hour in a desiccator to remove air bubbles. After degasing, PDMS was poured onto the desired surface (petri plate, glass slide, glass coverslip or SU–8 wafer) according to its further usage.

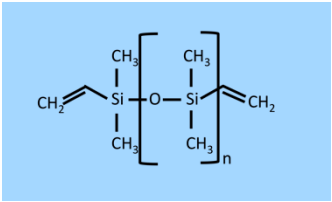

Figure 16: Structural formula of PDMS

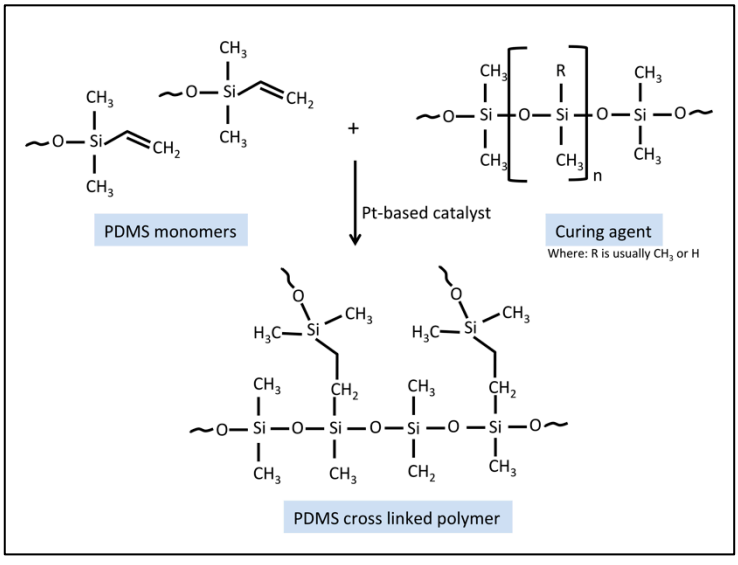

Figure 17: Basic mechanism of PDMS crosslinking reaction.

2.3.2. PDMS surface characterization methods:

PDMS surfaces before and after functionalizations were characterized by contact angle measurements and AFM surface topography.

(i) Contact angle measurements:

After functionalization, the change in hydrophobicity of PDMS and decrease in hydrophilicity of glass surfaces was evaluated by measuring water contact angles (CA) using a contact angle goniometer (OCA 20, DataPhysics Instruments, Germany). Briefly, a 2 µl sessile droplet of distilled water was placed on each treated and untreated PDMS and glass surface and the static contact angle was measured by Young–Laplace fitting. The CA value were averages of at least five droplets per sample.

(ii) AFM topography:

The topography of PDMS surfaces was studied with an atomic force microscope (Veeco Dimension^{TM} 3100 and Veeco Dimension Icon^{TM}) in tapping mode. The root mean square (RMS) surface roughness of differently treated PDMS surfaces was calculated by using NanoScope analysis software. PPP–ZEIHR–20 probes, with a nominal force constant of 10–60 N/m and a typical resonance frequency range of 98–177 kHz, were used for scanning. In each case two identical samples were scanned and an average over a total of ten measurements was taken.

2.3.3. PDMS microfluidic devices fabrication

The devices were fabricated using conventional microfabrication techniques involving SU–8 photolithography and PDMS soft lithography. The designs were created in AutoCAD and were used to yield master molds composed of SU–8 photoresist patterns on a silicon wafer. PDMS microstructures are fabricated by casting polymerized polymer these molds and cured at 80°C for 2 h – called soft lithography. Soft lithography represents a non–photolithographic strategy based on self–assembly and replica molding for carrying out micro– and nanofabrication. It provides a convenient, effective, and low–cost method for the formation and manufacturing of micro– and nanostructures [223]. Figure 18 explains the complete process of PDMS device fabrication from SU-8 master molds and figure 19 represents an indigenously prepared representative PDMS device.

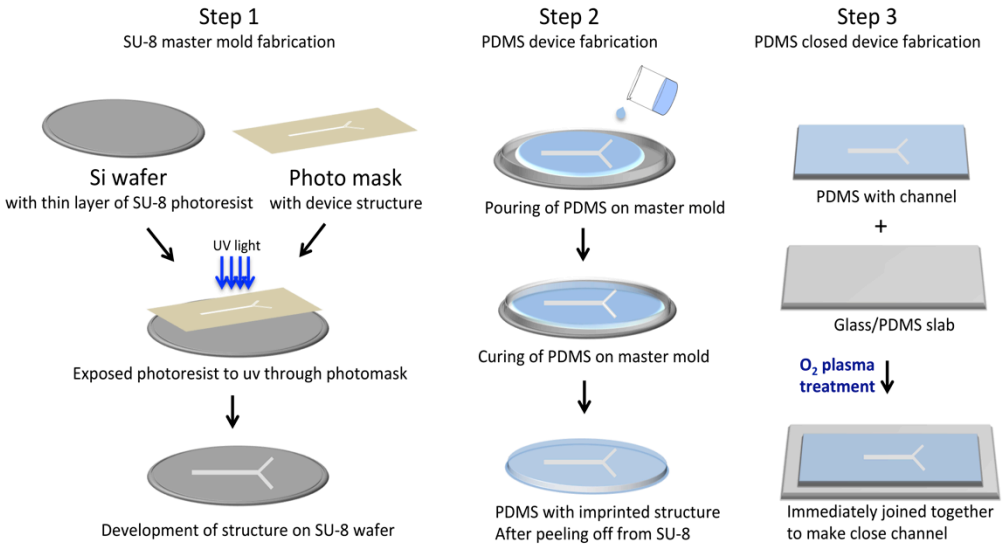

Figure 18: Schematic illustration of PDMS device fabrication from SU–8 master molds.

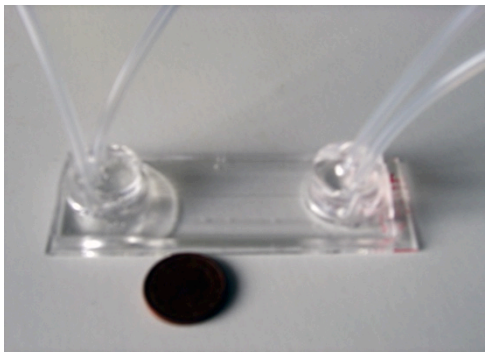

Figure 19: An indigenously prepared representative PDMS device.

2.3.4. PDMS device designs:

Four different PDMS microfluidic devices were designed for different studies (figure 20). Two of the devices were 100 µm wide (device A), and 900 µm wide (device C), straight channels while the other two devices (device B and D) exhibited two dimensions in terms of width. Device B consists of a 99 µm wide channel first divides into three equal channels of width of 33 µm each, which then rejoin again into a single 99–µm–wide channel at the outlet. The fourth device (device D) contained two different widths (device B) where a 198 µm wide channel further divides into three equal channels of 66µm width

The height of the devices was 55 µm, defined by the height of the SU–8 master molds. The height of the structures can be controlled by SU–8 spin coating parameters and were further confirmed by using Dektak XT profilometer from Brucker.

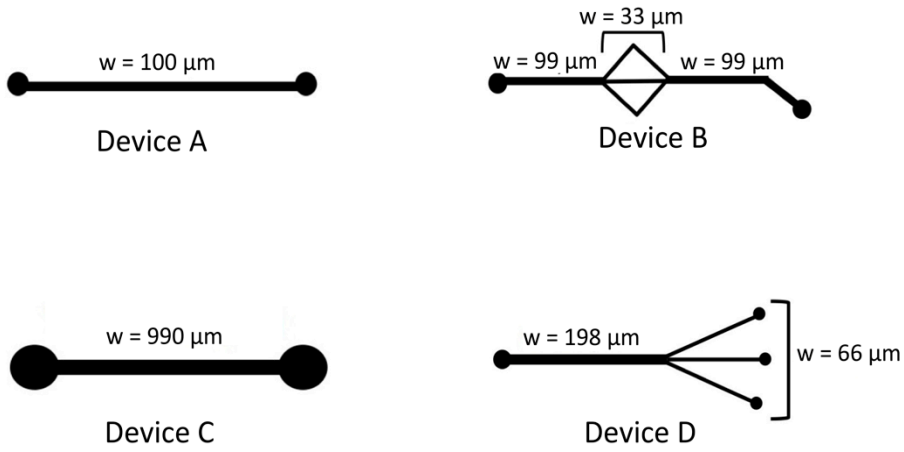

Figure 20: Designs of PDMS microfluidic devices used for various studies.

2.3.5. Shear stress calculation:

Assuming a parallel plate flow chamber, the wall shear stress (WSS) in a fully developed laminar flow can be calculated by given formula [224]

$$\tau = \frac{6\eta Q}{h^2 w} \quad (3)$$

Where, τ is the shear stress (dyn/cm^2), η the viscosity of DMEM at 37°C (0.0078 dyn/cm^2) [225], Q the flow rate (cm^3/s), h the height of channel (cm), and w the width of the channel (cm).

2.3.6. Mammalian cell culture:

The mammalian cells, either freshly isolated cells or taken from the culture bank, grown into a new dish or flask normally (only in case of adherent cells) stick down and begin to proliferate, with new cells adhering to unoccupied areas on the bottom of the vessel. As cell number increases, the cell monolayer becomes denser until no area remains available for new cells, a state known as "confluence". When the cells become confluent, in case of adherent cells, cell viability decreases. Thus, to keep adherent cells healthy they must be split and fed with fresh medium before they reach confluence. For this purpose, the cells must be loosened from their vessel and dissociated into a single–cell suspension.

This is usually accomplished in following steps

(i) Initial preparation is required before starting cell culturing. For example to create a complete sterile environment, laminar flow in turned on at least 30 min before starting cell culture and thoroughly sprayed with 70% ethanol or other commercial sterilizing medium. As the cells are temperature sensitive, so before starting cell culturing, growth media and buffer is pre warmed by placing at 37 °C.

(ii) The cells were taken out from CO_2 incubator into the laminar flow box, cell surface is washed with sterile buffer (normally PBS)

(iii) Adherent cells need to expose to a solution containing an enzyme such as trypsin, which disrupts cell attachment. Cell surface is covered with 0.25%

trypsin in 1 mM EDTA and keep them in CO_2 incubator at 37°C until the cell detachment.

(iv) The enzyme must be inactivated as soon as the cells are loosened from the culture vessel to prevent excessive digestion and cell damage. Trypsin is inactivated by adding serum or serum–containing medium.

(v) Gently centrifuge the cell suspension in sterile tubes at room temperature for 5 min to collect the cell pallet.

(vi) Supernatant is removed and pallete is suspended in fresh growth medium.

(vii) The cells are counted by using hemocytometer and from the fresh cell suspension appropriate cell density is added into fresh sterile flask and fresh growth medium is added.

(viii) Fresh flask is kept into CO_2 incubator at 37°C for cell growth

The cells are counted usually with the Neubauer chamber also denoted as hemocytometer. The full grid on a hemocytometer contains nine squares, each of which is 1 mm^2. The central counting area of the hemocytometer contains 25 large squares and each large square has 16 smaller squares. The four corner squares (identified by the red square) are further subdivided into 4 x 4 grids (figure 21). To count cells by using a hemocytometer, 15–20µl of cell suspension is placed on the hemocytometer and covered with a glass cover slip. Hemocytometer and glass cover slip should be cleaned with sterilizing solution before using them. And cell suspension must be diluted enough to avoid the overlapping of the cells.
The cells in all four outer squares are counted and divided by four to get the average number of the cells per square.

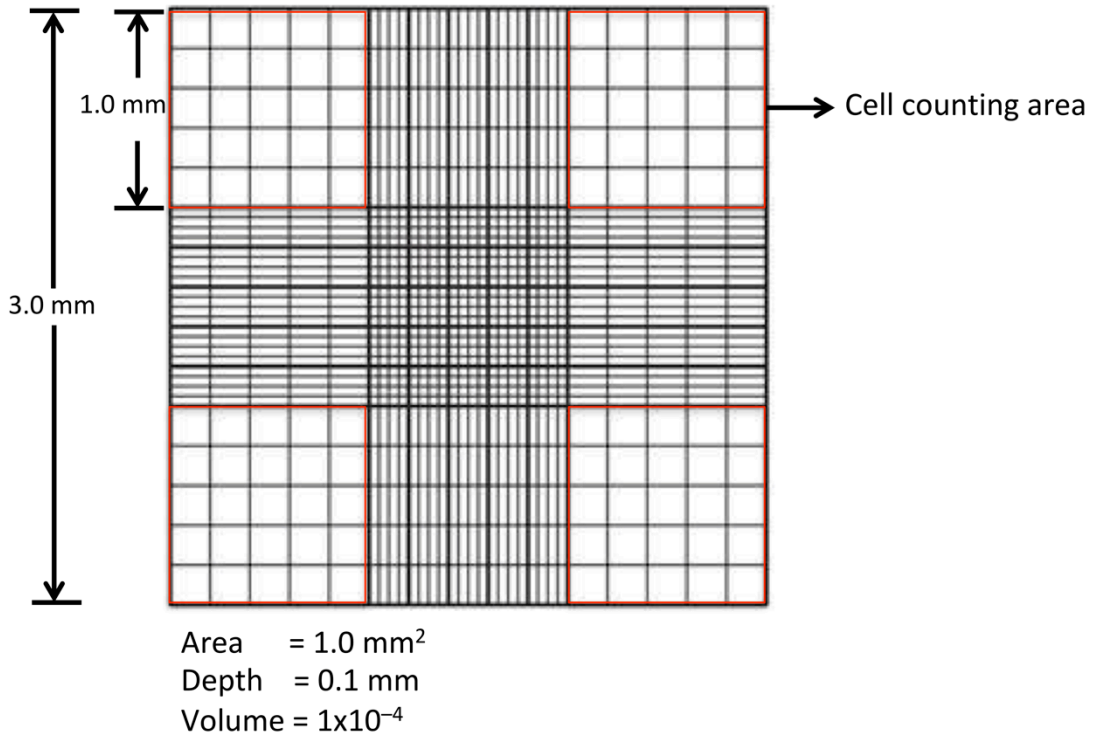

Figure 21: Principle of cell counting with a typical hemocytometer. Image adopted from reference 218.

As each square of the hemocytometer (with cover slip in place) represents a total volume of 0.1 mm^3 or 10^{-4} cm^3. Since 1 cm^3 is equivalent to 1 ml, the subsequent cell concentration per ml (and the total number of cells) will be determined using the following calculations [226].

Cells/ml = average count per square × the dilution factor × 10^4

Sandell and Sakai [227] published a very explanatory review about mammalian cell culturing techniques, can be consulted for more details.

2.3.7. Cell viability assay protocol:

The method is based on simultaneous determination of live and dead t by using cell viability kit. Viability kit comprise of two dyes, Calcein (A) with an excitation wavelength of 494 nm and an emitting wavelength of 517 nm and ethidium homodimer (B) with the wavelength of 538 nm and 617 nm, respectively.

According to manufacturer protocol staining was done as followed,

(i) 5 µL of substance A and 20 µL of substance B were mixed in 10 mL PBS.
(ii) After removing culture media, the cells were gently washed once with PBS at 37°C.
(iii) The mixture of substance A and B was used to cover the cell surface for 30 min at room temperature.
(iv) After washing the surface, fluorescent images were taken at above mentioned wavelengths.

Images were taken by using AXIO Observer, and processed by using Axiovision SE64 software (Carl Zeiss Microscopy GmbH, Frankfurt, Germany). The polyioninc dye Calcein is well retained within live cells, producing and intense green fluorescence in live cells. Ethedium homodimer enters cells with damaged cell membranes and produce a bright red fluorescence after binding with nucleic acid in dead cells. Images with green and red cells were used to count the number of live and dead cells by using ImageJ software.

2.3.8. Actin filament staining:

Actin filaments (F-actin) are linear polymers of globular actin (G-actin) subunits having mass of 42-kDa, with a diameter of 4 to 7 nm.
They commonly underlie the plasma membrane and are typically assembled at the cell periphery from adhesion sites or sites of membrane extension to form the dynamic cytoskeleton, which gives structural support to the cells and links the interior of the cell with its surroundings. Therefore cell morphology, proliferation and cell-cell contacts can be easily observed by visualizing actin filaments. Actin filaments are typically stained by fluorescently labeled phallodin. Phalloidin is a seven amino acid peptide toxin from the mushroom Amanita phalloides, which binds specifically to the polymerized form of actin (F-actin).

Following steps were performed to stain the actin filaments of the cells, as per manufacturer description

(i) Working stock of Acti-stain™ 555 phalloidin was prepared by diluting 14 µM labeled stock of phalloidin (ratio, 3.5 µl of phalloidin into 500 µl of PBS) and kept at room temperature in the dark.

(ii) After removing culture media, the cells were gently washed once with PBS at 37°C.

(iii) The cells were fixed by using fixative solution (provided with kit) for 10 min at room temperature followed by a washing with PBS at room temperature for 30 s.

(iv) The cells were permeabilized with permeabilization buffer (provided with kit) for 5 min at room temperature followed by a washing with PBS at room temperature for 30 s.

(v) Acti-stainTM 555 phalloidin was added to the cells as the complete surface of cells was coverd with the dye solution. Incubated at room temperature in the dark for 30 min.

(vi) The cells were washed thrice with PBS and imaged by using fluorescence microscope (excitation and emission spectra at 550 and 750 nm respectively).

Images were taken by using AXIO Observer, and processed by using Axiovision SE64 software (Carl Zeiss Microscopy GmbH, Frankfurt, Germany).

2.4. Development of PDMS surface functionalization method for improved cell growth under shear stress.

In this part of methodology, the development of stable collagen coating inside PDMS micro channels by using APTES mediation is illustrated. APTES-mediated linkage between PDMS and collagen was established in microfluidic device of small dimension where the effective shear stress becomes more dominant. Presence and absence of collagen, on surfaces as well as in micro channels, was determined by AFM measurements. To assess the stability of the cellular adhesion, the cells were forced in a shear flow until detachment. Moreover, the cellular adhesion and proliferation in devices with APTES-anchored collagen was compared to the devices with adsorbed collagen coating over a wide range of shear stress (10-300 dyne/cm^2) for 48 h [228].

2.4.1. PDMS Surface modification:

Immediately after bonding, the devices were incubated with freshly prepared 2% APTES (in acetone) for 15 minutes at room temperature and then washed with PBS. Another set of devices was treated in the same way with oxygen plasma but was prepared without APTES coating. Both sets of devices were further incubated with 50 µg/mL rat tail collagen in 0.1 M $NaHCO_3$ solution (in PBS) at 37°C in a humidified CO_2 incubator (BINDER GmbH, Tuttlingen, Germany), and finally washed with sterile PBS. Figure 22 gives a schematic explanation of the coating procedure inside the channel. The APTES concentration and incubation time (2% APTES for 15 minutes) were much reduced as compared to other protocols (e.g. 10% APTES for 2 h [130]).

While the incubation with small amount can generate monolayer of APTES with reactive functional groups (–NH) on the surface that can bind with collagen without clogging the micro channels.

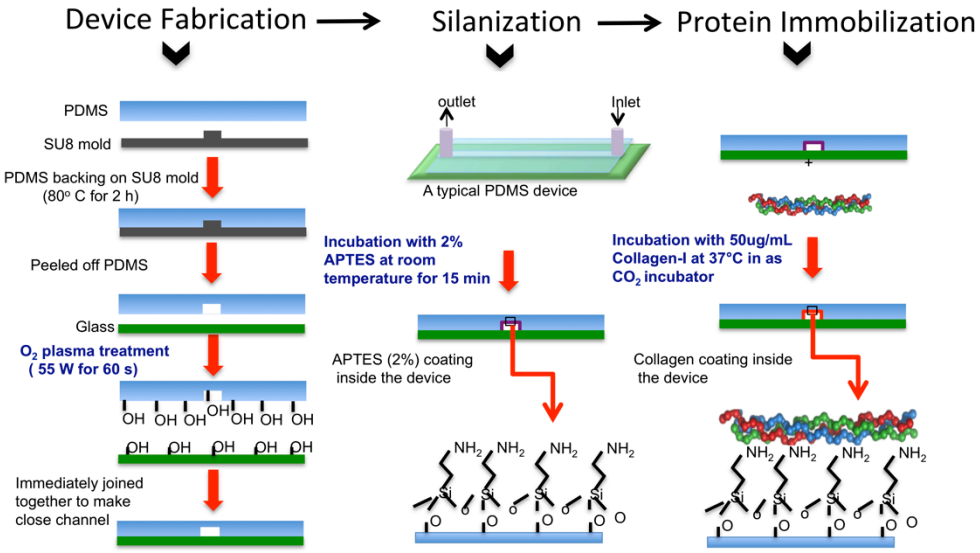

Figure 22: Schematic illustration of the APTES-mediated collagen coating inside a PDMS microfluidic channel.

The same procedure was expended to coat flat PDMS and glass surfaces for surface characterization and cell growth studies.

2.4.2. Surface characterization:

The variation in hydrophobicity of PDMS surfaces was evaluated by measuring water contact angles (CA) and surface morphology was studied with an atomic force microscopy technique (Veeco Dimension^{TM} 3100) in tapping mode (for detail methodology, refer to sec. 2.3.2).

2.4.3. Stability of APTES-mediated collagen coating on PDMS surfaces:

To verify the efficiency of APTES-mediated collagen on PDMS surface under *in vitro* cell culture conditions, differently treated (with and without APTES collagen coated) PDMS surfaces were incubated in cell culture medium (DMEM) in a CO_2 incubator at 37°C for 5 days. The surface topography was measured with AFM before and after incubation.

2.4.4. Cell growth and proliferation on PDMS surfaces:

To evaluate the efficiency of coated surfaces for cell growth and proliferation, FCOS–7 cell line was used to grow on PDMS surfaces. The cell line is derived from the kidney of the African Green Monkey *Cercopithecus aethiops* and resembles the fibroblast cells in humans. The FCOS–7 cell culture was maintained in DMEM/Ham's growth media supplemented with 15% FCS and 1 mL Normocin^{TM} (an antibiotic to avoid contamination) in Corning® CellBIND® tissue culture flask at 37°C in a CO_2 incubator. The cells from passage 20–30 were used for the experiments. 2×10^4 cells/mL were used to grow on APTES–collagen and O_2 plasma–collagen modified surfaces of PDMS in two parallel sets of experiment. After a maximum confluency on fifth day of growth, each surface was washed three times by gentle rinsing with 500 µL sterile PBS in each rinse. One set was used for bright field imaging, and images were taken before and after washing of the cells at 10 different areas of each surface. Images were taken by using AXIO Observer Z1 connected to HSM Axiocam camera and image processing and cell counting was done by using ImageJ program. Second set of surface with the growing cells was continued for cell viability study. The method is based on simultaneous determination of live and dead cells by using cell viability kit (method explained in section 2.3.7).

2.4.5. Cell growth in PDMS microfluidic devices:

To evaluate the efficiency of the APTES–collagen coating in microfluidic channels, two types of experiments were designed. In the first set of experiment, the cells were grown for 72 h under static conditions inside the PDMS devices (device A). The oxygen plasma treated PDMS channels (served as control to compare cell growth), APTES–collagen and only collagen (without APTES linkage) coated PDMS channels Were used to grow FCOS–7 (2×10^5 cells/mL) for 72 h. Growth media was provided through a needle via self perfusion. After 72 h of growth, the cells were washed by passing sterile PBS through the channels starting from a low flow rate of 1 µL/min and increasing it in a step of 5 µL/min after every 5 minutes. For example, the

cells were washed at 1 µL/min flow rate for the first five minutes and then the flow rate was increased to 5 µL/min for the next five minutes and so on, until the cells detached from the walls of device. The experiment was controlled under microscope and the shear stresses where the first and the last detachment of cells occurred were calculated.

In the second set of experiments, the cells were grown under dynamic conditions (in a continues flow of growth media at defined shear stress) for 48 h. For this purpose device A with two magnitudes of shear stress was used. FCOS–7 cells (2×10^5 cells/mL) were injected inside this microfluidic device and kept at *in vitro* culture conditions for one hour. After the cells attached to the surface in one hour, devices were connected to the syringes mounted on a syringe pump (KDS 210, KD Scientific, United State) for a continues flow of growth media. The cells were allowed to grow at defined shear stress by maintaining the flow rate of 5, 10, 15, 20 and 40 µL/min for 48 h. Bright field images were taken after 1 h of cell seeding i.e, before applying shear stress and then in every 24 h. Fluorescent images were taken for Actin filament staining of cells after 48 h of growth under shear stress (detailed staining method, section 2.3.8)

Applied shear stress was calculated by using formula given in sec. 2.3.4 and given in Table 1.

Table 1: Applied shear stress in device A and B

Flow rate (µL/min)	Shear stress (dynes/cm²)	
	Channel width 99 µm	Channel width 33µm
5	11.6	35
10	23	70
15	35	105
20	46	138
40	93	280

2.4.6. Stability evaluation if APTES-mediated coatings:

The stability of the APTES–collagen coating was verified by using two methods:

(i) Cell growth: The COS-7 cells were grown in the coated channels (device B), which were already exposed to a continuous flow of PBS before cell seeding. As collagen is required for a stable attachment and proliferation of cells on PDMS walls under flow conditions. This experiment indirectly indicated the presence or absence of collagen inside the micro channels after continues washing of channels at certain flow rate. In this experiment PBS was pumped continuously for 48 h through the coated channels at 37°C in a CO_2 incubator. The flow rate was maintained at 20 µL/min and after 48 h the COS–7 cells were allowed to grow in these channels at same flow rate for the next 48 h. Images were taken after 1 hour of cell attachment and after each 24 h.

(ii) AFM measurements: A device with a 990 µm wide channel (device C) was coated with APTES and without APTES-mediated collagen and exposed to continuous flow of sterile PBS at a flow rate of 180 µL/min (shear stress 46 dyn/cm^2) for 48 h in a CO_2 incubator at 37 °C. Then the PDMS channels were

carefully removed from glass surface. The channels were washed with sterile distilled water and surface topography of the coated channels was measured by scanning inside the channel with AFM.

2.5. Development and comparison of various surface chemistries for improved cell growth under shear stress.

Typically the charge distribution on protein molecules is defined by its isoelectric points (IEP), The isoelectric point is the pH at which a particular molecule contains no net electrical charge or is electrically neutral (figure 23). The net charge on the molecule is affected by pH of its surrounding environment and can become more positively or negatively charged due to the gain or loss, respectively, of proton (H^+).

Biological amphoteric molecules such as proteins contain both acidic and basic functional groups. Amino acids that make up proteins may be positive, negative, neutral, or polar in nature, and together give a protein its overall charge. At a pH below their IEP, proteins carry a net positive charge; above their IEP they carry a net negative charge.

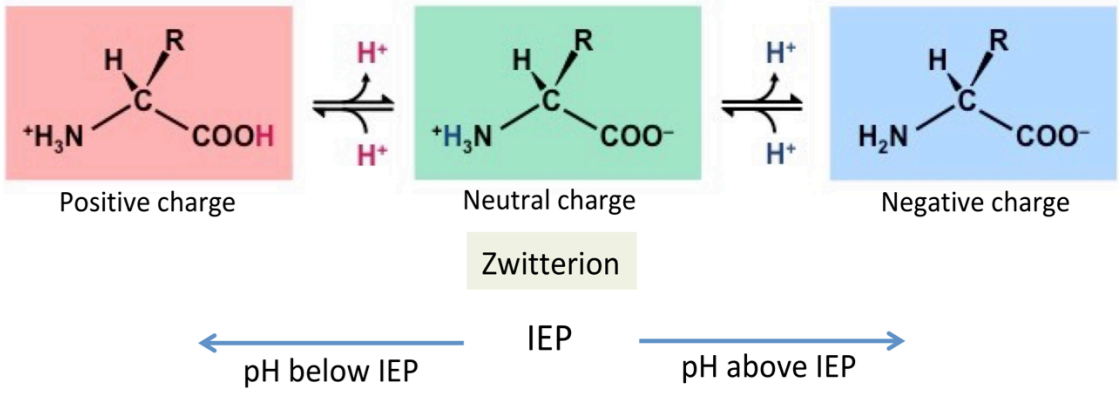

Figure 23: Description of isoelectric point

Thus the net charge on collagen can be varied buy changing pH of the solution to below and above to its IEP = pH 6.9–7.4 [209, 229]. Furthermore it has been already described that the fibrillogensis of collagen is also dependent on pH of the solution where the fibril formation started above pH 5 [208, 230].

Considering the effect of pH on fibril formation and charge distribution, in current study, collagen at three different pH values (5, 7 and 9) was use to bond on differently modified PDMS surfaces including (i) O_2 plasma; a negatively charged surface with $–OH^–$ functional group (ii) APTES; surface with $–NH_2$ functional group (iii) APTES–GA; surface with –COOH functional group and (iv) protonated APTES; positively charged surface with $–NH_2^+$ to develop various electrostatic and covalent linkages. Stability and biocompatibility of surfaces was examined by AFM studies inside microfluidic devices and cell (HUVECs) growth under shear stress.

2.5.1. Collagen solution preparation:

A solution of rat tail collagen I (100 ug/mL) was prepared in a sterile PBS/$NaHCO_3$ buffer. The pH of the solution was changed to pH 5 (< IEP), pH 7 (≅

IEP) and pH 9 (> IEP) by using 0.1 M NaOH and 1M CH_3COOH in order to develop positive, neutral and negative charges on collagen molecules respectively.

2.5.2. PDMS surface functionalization

PDMS surfaces were prepared as previously described method. The cured PDMS surfaces were divided into five sets consisting three surfaces each. One set of three native PDMS surfaces was incubated with three different collagen solutions (pH 5, 7 and 9) at 37°C in a CO_2 incubator for 2 h. Remaining four sets were treated with oxygen plasma at 55 W power for 60 s using a Femto plasma chamber (Diener electronic GmbH + Co. KG, Ebhausen, Germany) so as to activate the surface. From these plasma activated surfaces one set was used for collagen coating and remaining three for APTES coating by using one of our previously reported method [228]. A set of APTES treated surfaces was protonated by using 0.001M HCl solution for 10 min at room temperature in order to produce a net positive charge on surfaces [231]. In order to develop a covalent linkage of collagen to the surfaces, one set of APTES treated surfaces was incubated with 2.5% glutaraldehyde solution for 3h at ambient temperature [130]. And finally all three APTES treated sets were incubated with collagen solutions (pH 5, 7 and 9) as previously described. Figure 24 describes the complete concept of surface modification for collagen coatings at three pH values for a final microfluidic application.

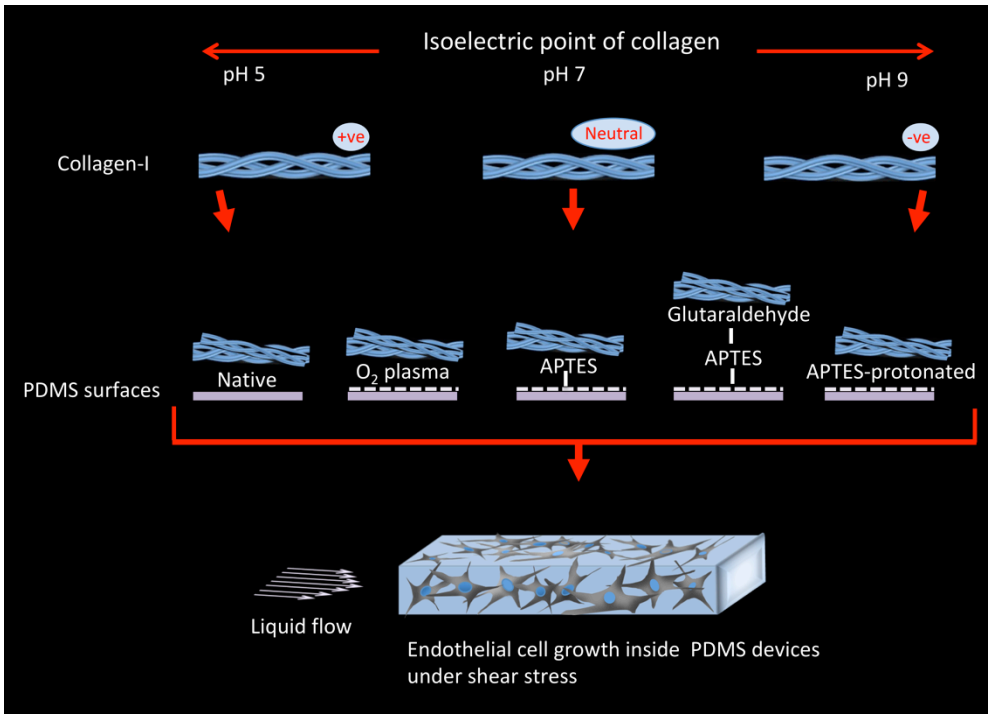

Figure 24: Schematic description of PDMS surface functionalization

2.5.3. Surface characterization:

The variation in hydrophobicity of PDMS surfaces was evaluated by measuring water contact angles (CA) and surface morphology was studied with an

atomic force microscopy technique (Veeco Dimension Icon^{TM}) in tapping mode (for detail methodology, refer to sec. 2.3.2).

2.5.4. Microfluidic device fabrication:

PDMS devices were prepared by soft lithography from SU–8 master mold. Two different PDMS microfluidic devices were designed as illustrated in Figure 19. One device contained simple 990–µm–wide straight channel (device C), while the other device exhibited two different widths (device D) a 198 µm wide channel dividing into three equal channels of 66µm width.

2.5.5. Stability of differently functionalized PDMS surfaces:

The stability of collagen on differently functionalized PDMS surfaces was studied by using two methods; (i) Surface studies: By incubating the surfaces in cell medium in a CO_2 incubator at 37° C for 5 days and AFM surface scanning before and after incubation. (ii) Microfluidic assay: For this purpose, all types of collagen coated microfluidic devices (device A) were perfused with sterile PBS buffer by using OB1 flow control system (Elveflow, France) at different shear stress values (10–40 dyn/cm^2) at 37° C for 48 h (Table 2). The channels were carefully removed from glass slides and presence or absence of collagen was verified by scanning with AFM in tapping mode. For control measurements the devices were kept at hotplate at 100 ° C for one week and then at room temperature for three months to recover the hydrophobicity of PDMS inside the channels [104].

Table 2: Applied shear stress in device C

Flow rate µL/min	Shear Stress (dyne/cm^2)
	Channel width 990 µm
40	10
90	20
125	30
170	40

2.5.6. Effect of different pH on APTES layer:

Incubation of APTES treated surfaces with three different collagen solutions (with respect to pH) values expected to vary the surface potential by varying the charge on amino functional groups of APTES. To determine the effect of buffers of pH 5, 7 and 9 on APTES monolayer on treated surfaces, charged Flouroshperes® of 0.2 µm size were used. Two sets, with three microfluidic devices in each set, were incubated with buffers at pH 5, 7 and 9, without collagen, for 2 h. After that, one set was incubated with Amine–modified, positively charged Flouroshperes® (ex/em ~580/604 nm) and the other set was incubated with carboxylate–modified, negatively charged, Flourospheres® (ex/em ~365/415 nm) for an hour at room temperature and finally washed with water. Amine–modified spheres attached to negatively charged

APTES surface and produce a red fluorescence while carboxylate–modified spheres attached to positively charged APTES surface to produce a blue fluorescence.

2.5.7. Cell culture:

Freshly isolated human umbilical vein endothelial cells (HUVECs) were obtained from Vascular Research Center (VRC), Frankfurt, Germany. Culture was maintained in growth medium M200 supplemented with growth supplement (LSGS) recommended by the company and 1mL Normocine at 37° C in a CO_2 incubator with 5% humidity. The cells from passage 3–6 were used for studies. Cell proliferation and morphology was observed by light microscopy and Actin filament staining (detailed method, section 2.3.8)

2.5.8. Cell growth and viability on PDMS surfaces:

To evaluate the biocompatibility of all functionalized surfaces, cell proliferation was studied by two methods, (i) time course study (ii) cell viability assay. For this purpose, fourty petri plates were coated with thin layer of PDMS. After sterilization with 70% ethanol followed by extensive washings with sterile PBS the surfaces were divided into two sets consisting equal petri plates and coated with collagen as described in sec. 2.3. HUVECs (2.5×10^5 cells/mL) were grown on all types of collagen coated and native PDMS surfaces at 37° C in a CO_2 incubator. In the first set of experiment, images were taken after 4 h and then after each 24 h of inoculation by using light microscope AXIO Observer Z1 equipped with Photometrics® Prime™ camera and Micro–Manager 1.4 software. For cell counting, seven images were taken from each surface including middle and periphery of the plates. After five days of cell growth and imaging, one set was kept at same conditions to observe cell proliferation after ten days of growth and for cell counting the images were taken on 10^{th} day. ImageJ software was used for cell counting. In the second set of experiment, cell viability was studied by using Iive/dead cell viability kit according to the manufacturer's protocol (method explained in section 2.3.7).

2.5.9. Cell growth under shear stress:

The selected biocompatible surfaces resulting from the biocompatibility assay, were used to further evaluate the cell adhesion and proliferation under flow conditions. PDMS microfluidic devices with two shear stress levels, a straight channel (device D) of 198 µm width, further divides into three channels of 66 µm width each, were used for this purpose. Applied shear stress at certain flow rate is calculated in Table 3. After biocompatible functionalizations, HUVECs (8×10^7 cells/mL) were injected to the devices and kept at *in vitro* conditions for initial cellular attachment. After one hour of incubation, devices were connected to a continues flow of growth medium with the help of a syringe pump (KDS 210, KD Scientific, United State) along with bubble trappers (Elveflow, France) to avoid air bubbles inside the devices. The cells were allowed to grow at various flow rates (12–32 µL/min) producing a wide range of shear stress (20–150 dyn/cm^2) for 48 h in two–shear device. Bright field images were taken before and after applying shear stress.

Table 3: Applied shear stress in device D

Flow rate µL/min	Shear Stress (dyne/cm^2)	
	Channel width 198 µm	Channel width 66 µm
7	10	30
12	20	60
18	30	90
25	40	120
32	50	150

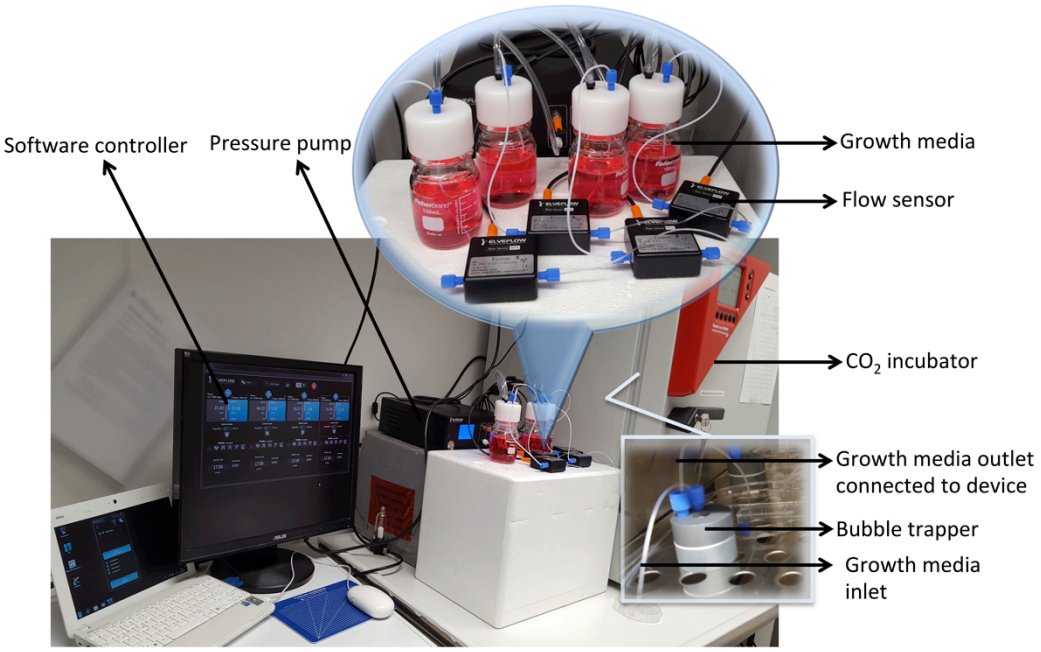

Figure 25: Microfluidic setup for cell growth

Chapter 3. Results and Discussion

3.1. Development of PDMS surface functionalization method for improved cell growth under shear stress.

In current chapter, the efficiency of APTES-mediated collagen coating on PDMS surface and inside PDMS microfluidic devices is described. APTES-collagen coating was compared with physically adsorbed collagen coating with the help of AFM measurements on surfaces as well as in micro channels. Moreover the results will be focusing on improved cell adhesion and proliferation inside PDMS microfluidic devices over a wide range of continues shear stress (10-300 dyne/cm^2) for 48 h.

3.1.1. Contact angle measurements:

Surface modification of PDMS and glass with O_2 plasma, O_2 plasma–collagen, APTES and APTES–collagen were measured primarily with water CA. The CA of PDMS significantly decreased from 108° ± 2° to 66° ± 2.4° after coating with APTES, which then decreased only slightly upon further coating with collagen protein (60° ± 2°). Plasma treated PDMS sample, coated with collagen, also showed a decrease in its CA value (Table 4). As the microfluidic device is made up of PDMS bonded to glass therefore CA of glass was studied in parallel. Since glass is inherently hydrophilic, contact angle was not decreased significantly after APTES coating, but after coating with collagen its CA decreased to 34° ± 2°. Trend in water contact angle variation on all modified surface can be seen in figure 26. The observed trend in decrease of CA of PDMS on silanization and ECM protein coating in our case matches with that already reported in the literature [173].

Table 4: Water contact angle values on differently functionalized glass and PDMS surfaces

Contact angle (°)				
Treatments / Surfaces	Before coating	APTES coating	APTES-collagen	O_2 Plasma collagen
Glass	54° ± 1.1°	50° ± 2.3°	34° ± 2.0°	22° ± 1.8°
PDMS	108° ± 2°	66° ± 2.4°	60° ± 2.0°	55° ± 3.1°

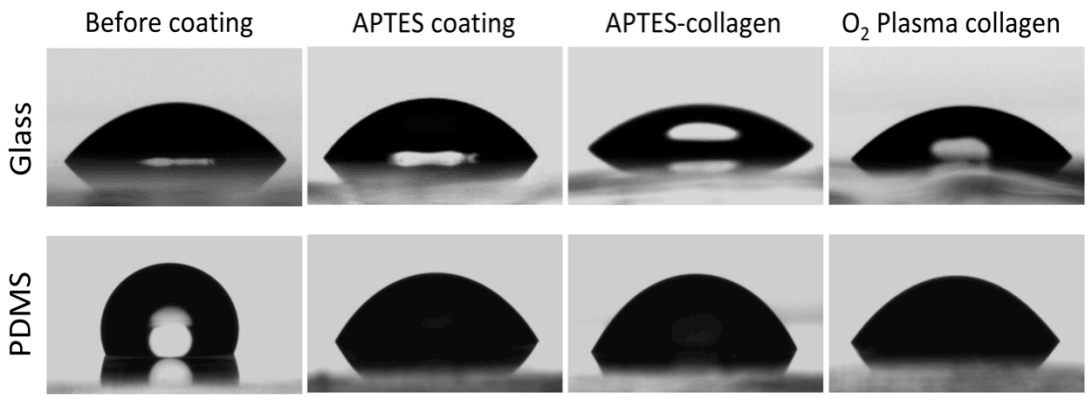

Figure 26: Water contact angle images on differently functionalized glass and PDMS surfaces

3.1.2. Collagen assembly on PDMS by light microscope:

Collagen fibers, after polymerization, can be seen simply on PDMS surface by using objectives of high magnification (≥ 40x). As it is clear from the figure 27 that initially both of the surfaces, O_2 plasma treated and APTES treated, exhibited collagen in the form of fibers. But the detail topography and stability of coating could not assume from light microscopy images.

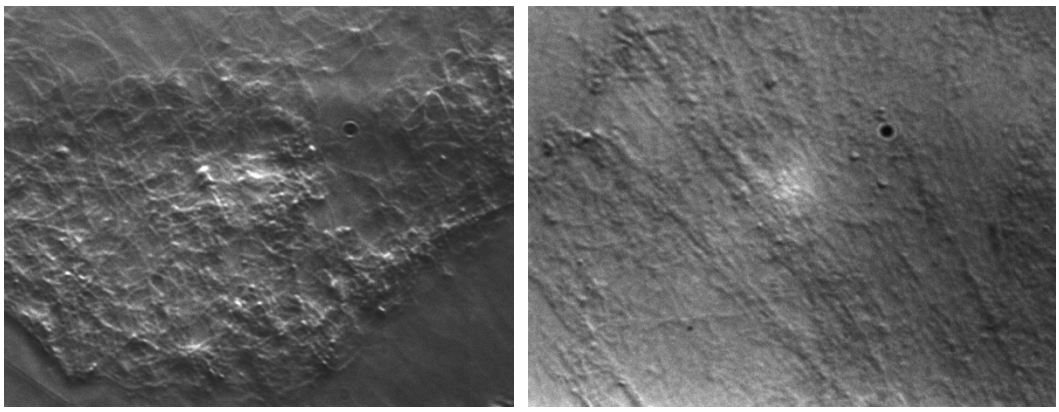

(a) **(b)**

Figure 27: Light microscopy images of collagen on PDMS surface (a) plasma treated surface, (b) APTES treated surface

3.1.3. Surface topography:

The topography images before and after incubating the differently treated PDMS surfaces in cell culture medium for 5 days are shown in Figure 28.

After plasma treatment, surface roughness of PDMS surface slightly increases (0.88 nm±0.03nm) as compared to smooth surface of untreated PDMS (0.61nm±0.01nm) but the APTES treated PDMS showed a rough and granular surface topography with an RMS roughness of (4.5 nm ± 0.4 nm) before and (1.40 nm ± 0.37 nm) after incubation. After coating with collagen both the APTES treated and O_2 plasma treated PDMS showed the presence of fibrillar collagen on their surfaces [177]. The surface

roughness values of both the surfaces were also in the same range indicating an initially similar distribution of the collagen fibers on both kinds of surfaces.

After incubation in the growth medium for five days, the surface roughness of the APTES–collagen coated PDMS was still comparatively higher than that of the bare PDMS and the O_2 plasma–collagen PDMS surface. The AFM height images confirmed the presence of collagen fibers on APTES-mediated collagen coating in contrast to few or no collagen fibers that were observed on PDMS that was only O_2 plasma treated. These results clearly suggest that the APTES linkage improved the stability of the collagen on the PDMS surface under in vitro conditions.

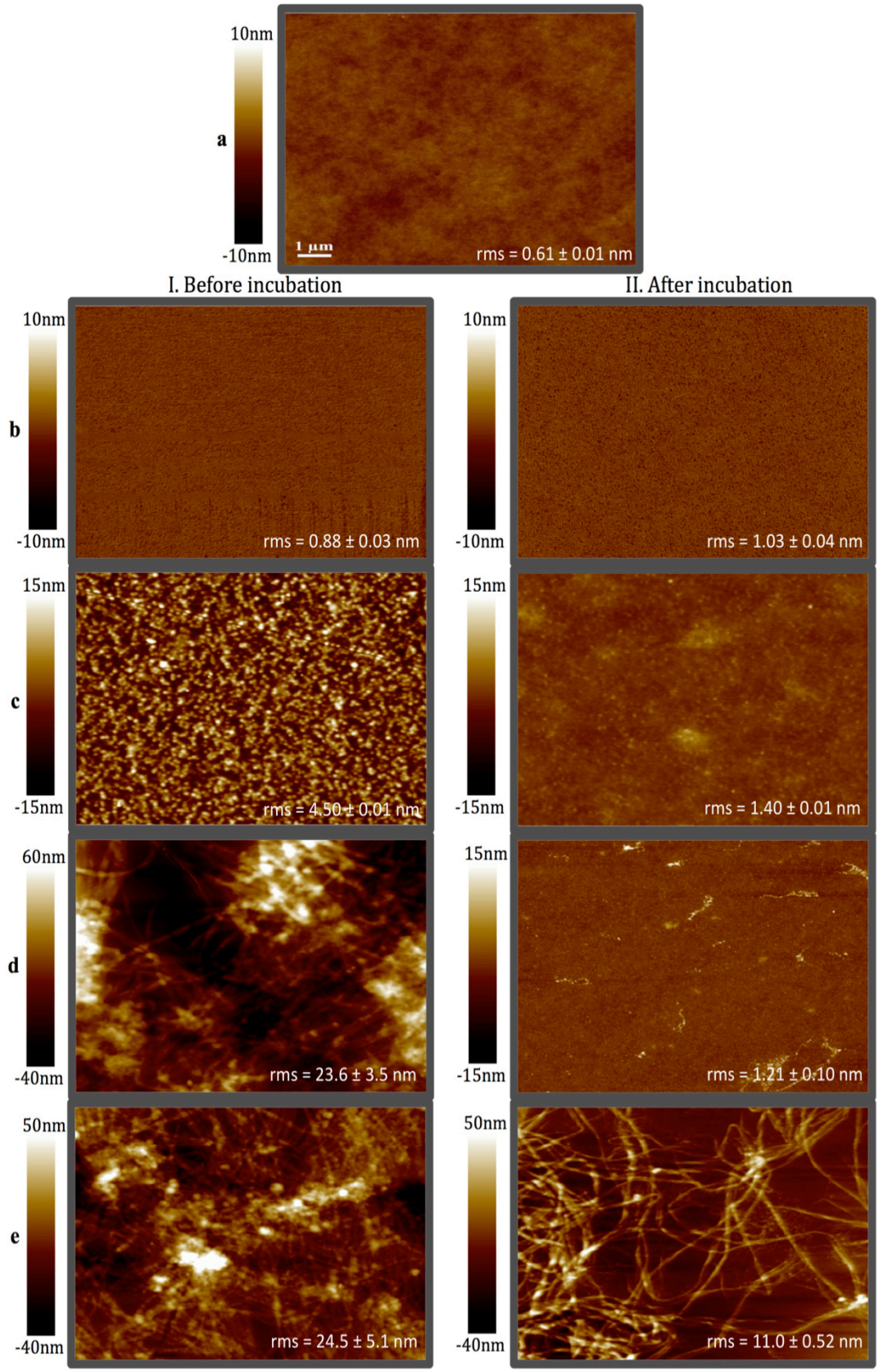

Figure 28: AFM topography (height) images of PDMS surfaces (10 µm x 10 µm) before and after incubation in cell culture medium, (a) native PDMS (b) O_2 plasma treated PDMS, (c) APTES-coated PDMS, (d) O_2 plasma–collagen PDMS, (e) APTES–collagen PDMS.

3.1.4. Adhesion of the cells grown on flat PDMS surfaces:

The FCOS–7 cell culture was maintained in DMEM/Ham's growth media augmented with 15% FCS and 1 mL Normocin^{TM} in Corning® CellBIND® tissue culture flask at 37°C in a CO_2 incubator. The cell morphology in control tissue culture flask is given in figure 29. 2×10^4 cells/mL cells were grown on APTES–collagen and O_2 plasma–collagen modified surfaces of PDMS. After 72 h of the cell growth a more confluent layer of cells was observed on APTES–collagen coated surface as compared to the other two types of surfaces. Upon rinsing with sterile PBS, there were only few cells left on the surface with the plasma–collagen coated surface, whereas a large number of cells was still attached to the APTES–collagen coated PDMS as shown in (Figure 30a). Figure 30b shows a clear decrease in cell number after washing in case of O_2 plasma–collagen treated surfaces. As all functionalized surfaces were biocompatible, therefore as per our expectations, the percentage of dead cells was small on all PDMS surfaces (Figure 31a,b). These results indicate an improved cell adhesion and biocompatibility due to APTES–collagen coating.

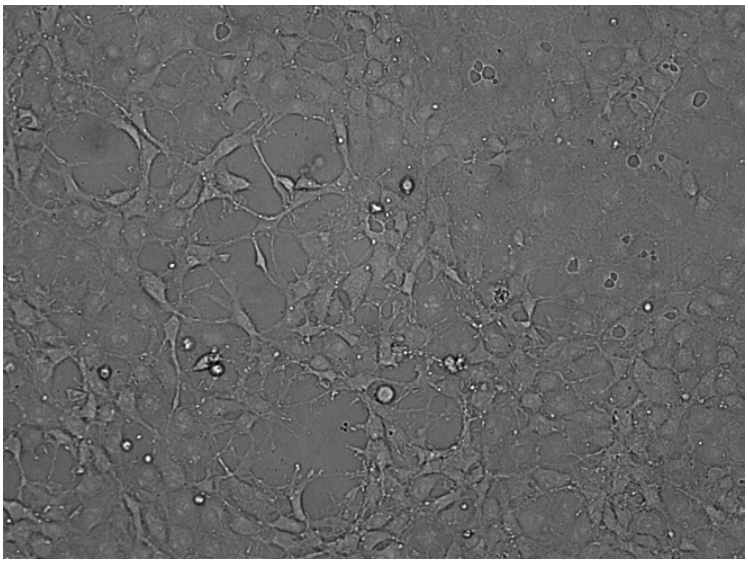

Figure 29: FCOS-7 growth and confluency inside a tissue culture flask

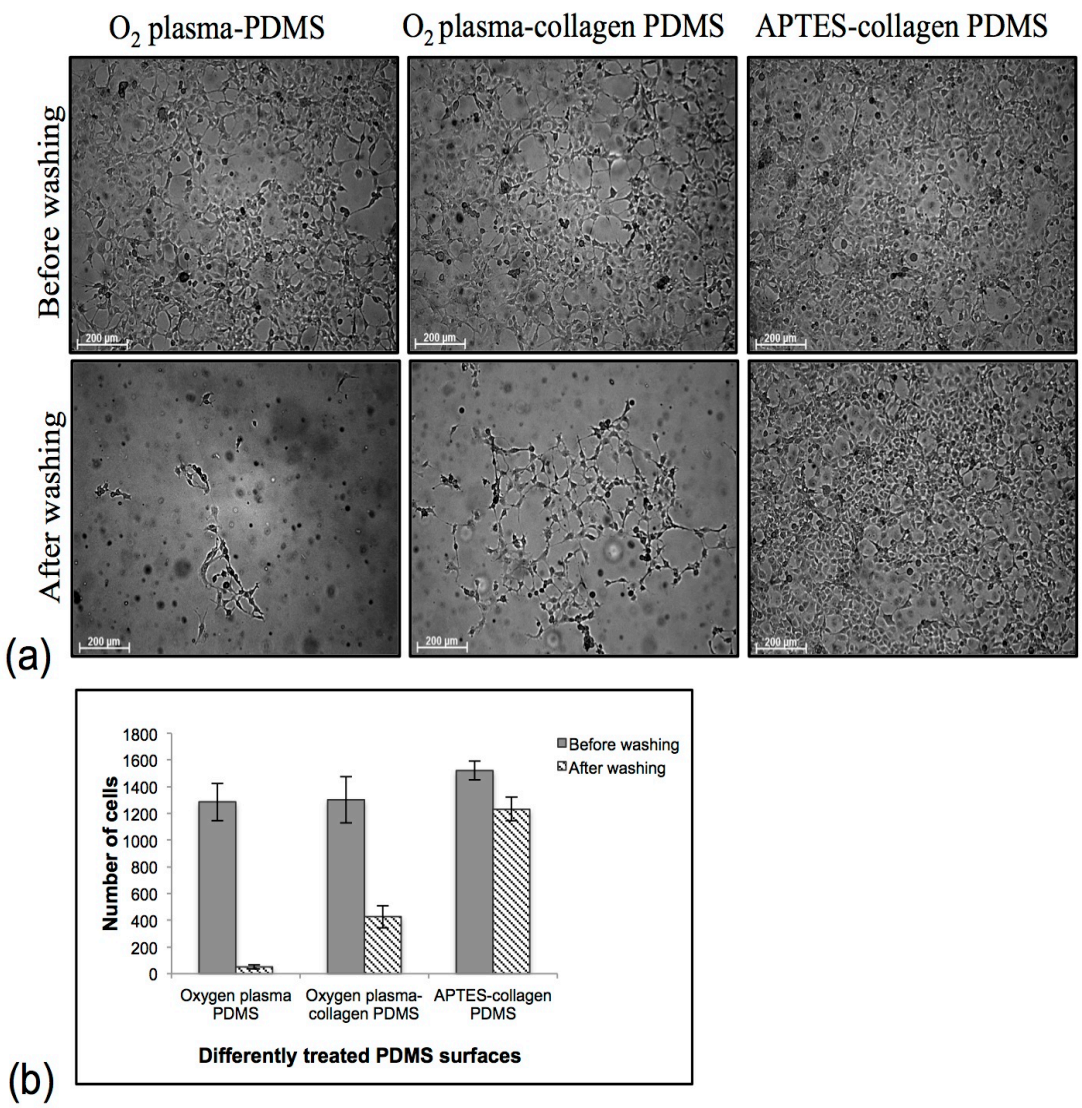

Figure 30: Cell growth and stability on differently treated PDMS surfaces before and after washing, (a) light microscopy images, (b) number of cells

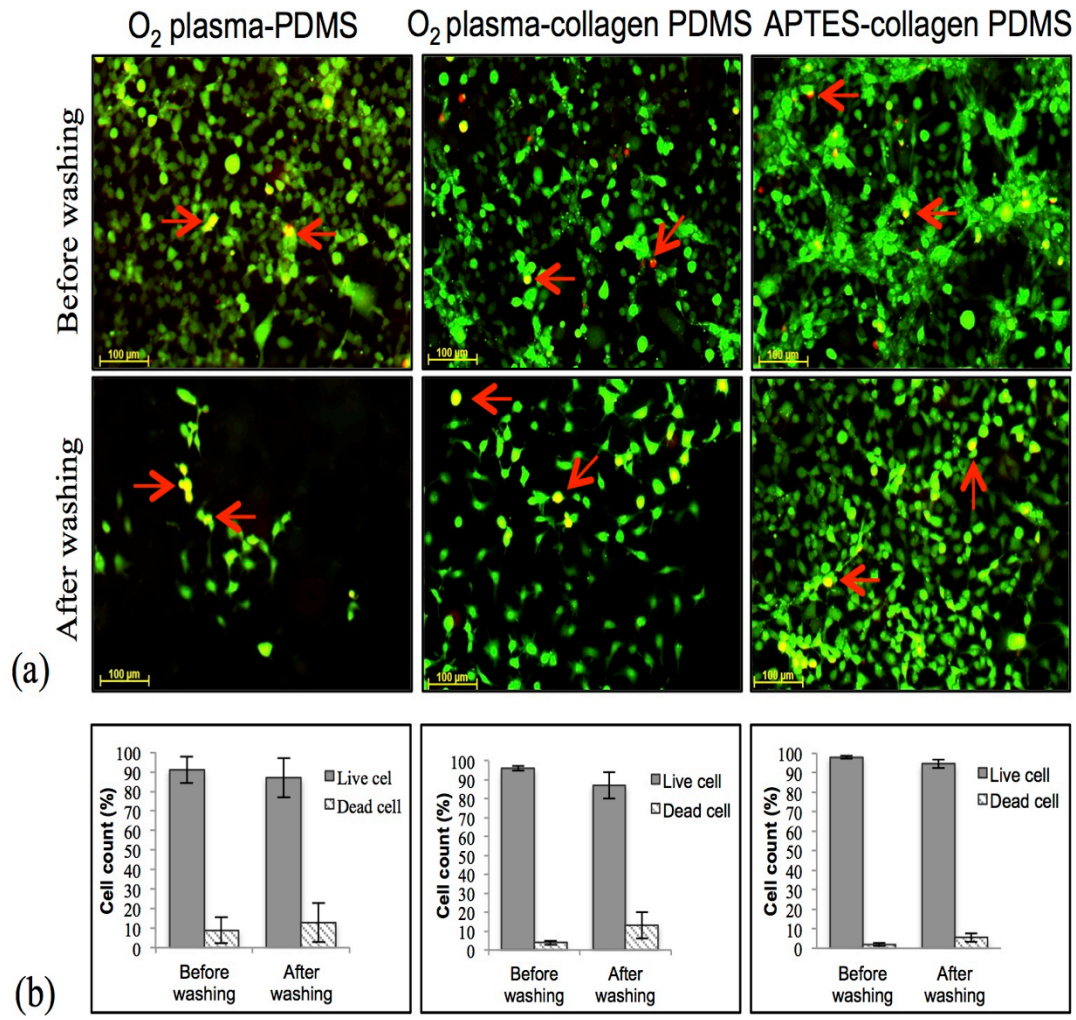

Figure 31: Cell proliferation, cell stability and cell viability on differently treated PDMS surfaces before and after washing. (a) Representative fluorescent images of live and dead cells. Red arrows point towards some examples of the dead cells (yellow or red). (b) Quantitative comparison of Live and dead cells. The experiment was performed in triplicate and 10 representative images were used for cell counting for each surface.

3.1.5. Adhesion of cells grown under static conditions in device A

A very good confluency of cells was observed after 72 h of growth inside both, the O_2 plasma–collagen coated and the APTES–collagen coated micro–channels as compared to channels that were only O_2 plasma treated. After 72 h the devices were subjected to an increasing shear stress by flowing media at controlled flow rates. In all the channels good cell stability could be observed for flow rates less than 10 µL/min. At an increased flow rate of 10 µL/min, individual cells started to detach from the plasma–collagen coated channel. The total detachment of all cells occurred at 40 µL/min flow rate (shear stress 93 dyn/cm^2). The cells in APTES–collagen coated channels showed a better stability against shear stress and the first detachment occurred at a comparatively higher flow rate of 40 µL/min and the full detachment occurred at 60 µL/min (Figure 32).

Analyzing the images and live videos obtained at cell detachment, it was hypothesized that the following two forces experienced by the detaching cells: (i) pushing force applied by the moving fluid, (ii) a pulling force transduced by the detaching cells. The detaching cells may be connected to the neighboring cells via intercellular junctions or, more important, via the delaminating collagen network. Thus, the overall stability of the cells exposed to shear stress depends on the balance between cell–substrate bond strength and the external pull/push force. For stable cell adhesion, the cell–substrate bond should be strong enough to resist against these two forces. In the case of the physically adsorbed collagen in the plasma–collagen coating the cells, presumably together with the collagen network, detached from the surface. The detaching cells are able to pull other cells off the surface leaving behind an empty channel. Whereas, in case of APTES–collagen coating, APTES acts as a stable linker between PDMS and collagen and the cell–substrate bond is strong enough to withstand the fluid shear stress.

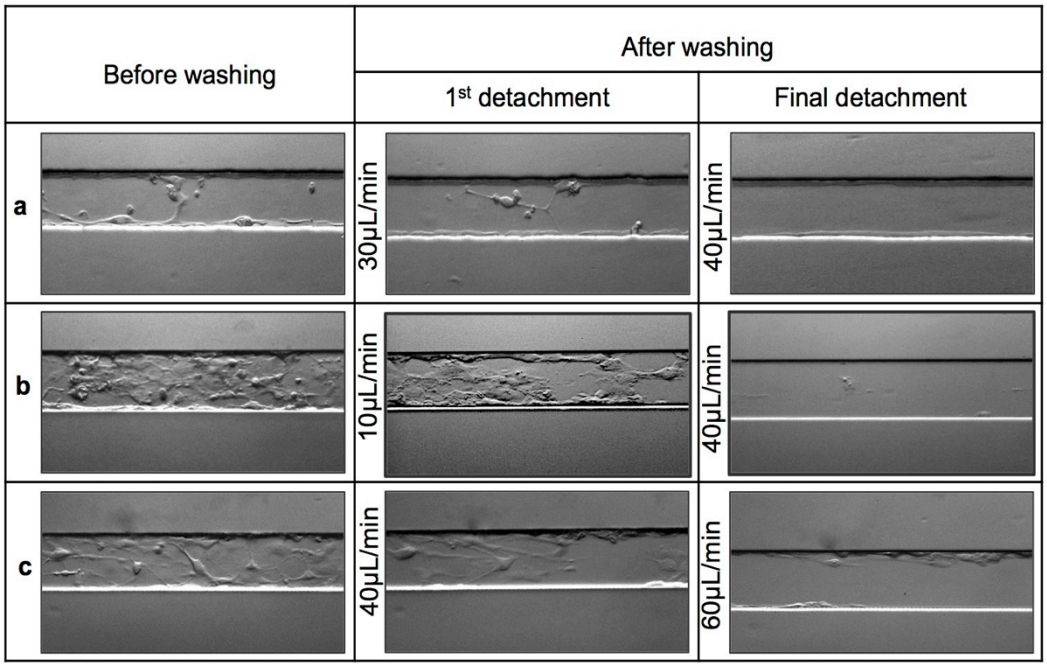

Figure 32: Cell growth and stability against shear flow inside differently treated PDMS microfluidic channels (device A), (a) O_2 plasma treated channel, (b) O_2 plasma–collagen coated channel, (c) APTES–collagen coated channel.

3.1.6. Adhesion of cells grown under continuous shear stress in micro channels

In this set of experiment F–COS7 cells were grown under different shear stresses (11.6 dyn/cm^2–280 dyn/cm^2) in a two–shear device (device B) for 48 h. The schematic of the device is shown in Figure 18, Table 1 gives the shear stress values in dyn/cm^2 experienced by the cells at different flow rates. The range of shear stress studied here is very high for fibroblast like cells but it well represents the stability of the adherent cells under continuous flow conditions beyond the physiological values, demonstrating the adhesion efficiency of our coating method. After 1 hour of seeding the cells into the channels, the proliferation and attachment of cells inside APTES–

collagen coated channels was found better than O_2 plasma–collagen coated channels, showing the influence of base coating even on the initial attachment of cells to the channel walls. After 48 h under continuous shear stress, the pattern of growth and adhesion of cells in both devices exposed to 5 µL/min and 10 µl/min flow rates were similar. Briefly, APTES–collagen coating supported cell growth and adhesion at both shear stresses but in case of plasma collagen coated device, no cells were observed soon after 24 h in the narrower channels (33 µm). Though the cells adhered to the wider channel (99 µm) in plasma–collagen coated device the number of cells were less than in the APTES–collagen coated channel. Increasing the flow rate to 15 µL/min, the induced stress was increased to 35 dyn/cm^2 and 105 dyn/cm^2 in the wider and in the narrower channels respectively (Figure 33a).

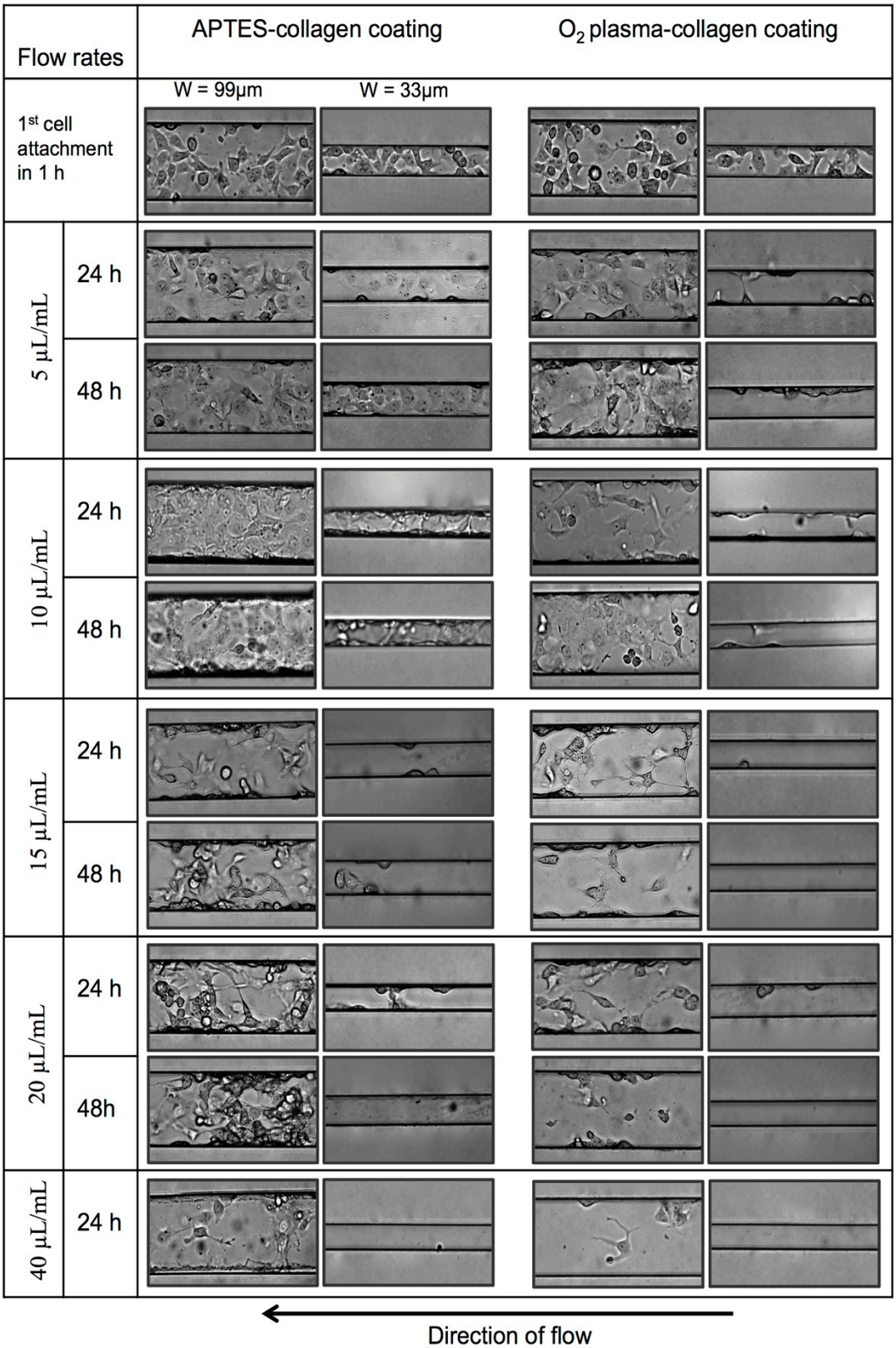
Flow rates
APTES-collagen coating
O2 plasma-collagen coating
W = 99μm
W = 33μm
1st cell attachment in 1 h
5 μL/mL
24 h
48 h
10 μL/mL
24 h
48 h
15 μL/mL
24 h
48 h
20 μL/mL
24 h
48h
40 μL/mL
24 h
Direction of flow

(a)

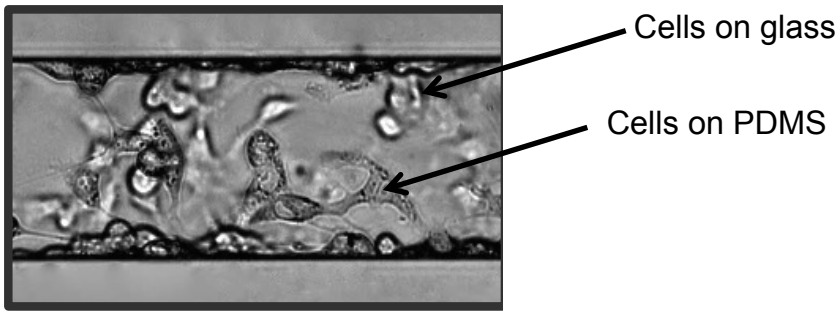

(b)

Figure 33: (a) Cell growth at different flow rates in collagen coated PDMS microfluidic devices with and without APTES intermediate (device B). All experiments were performed in triplicate and images of the complete channels were considered in each experiment. The given data are representative images. (b) Focal plane adjustment to capture glass as well PDMS surface in one image. Cells attached to glass appear bright those on PDMS dark because the focus plane was adjusted to the PDMS surface.

As per our expectations, there were no cells left at a high shear stress of 105 dyn/cm^2 in both kinds of modified channel surfaces, but at 35 dyn/cm^2, cells were found in both the devices. The representative images showed the cells attachment on both, glass as well as PDMS, walls of the channels as explained in figure 34b and decrease in cell count can also be seen quantitatively in Figure 34.

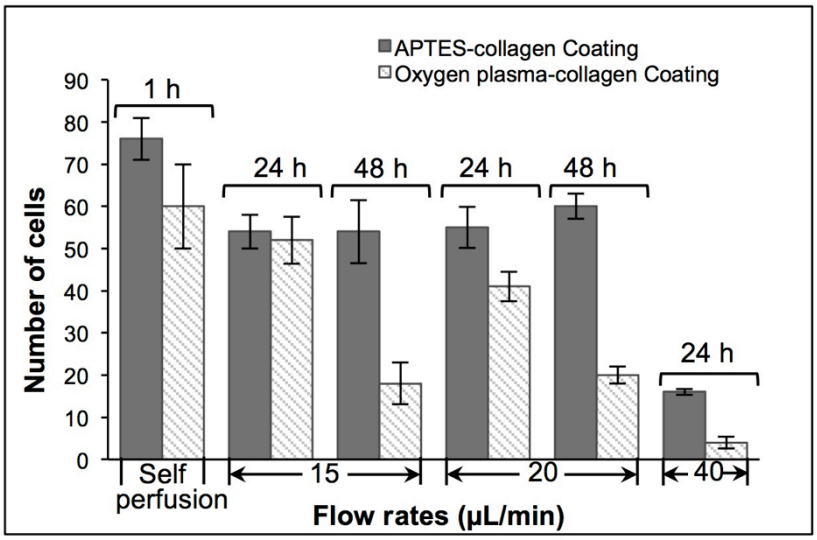

Figure 34: Number of cells counted in the wide channel of the PDMS microfluidic devices at different flow rates. Experiments were performed in triplicate and the given data represents the average cell counts in a channel area of 0.1 mm^2 from each experiment (shear stress: 35, 46 and 93 dyn/cm^2).

Interestingly, in case of plasma collagen coating, there was a difference in the number of adherent cells at the same applied fluid shear stress but generated in two different channel dimensions. This showed an influence of channel dimension on the effective shear stress experienced by the adherent cells on the channel wall. Gaver and

Kute [232] described that the effective shear stress felt by an adherent cell in a micro channel is highly dependent on the relation between cell size and channel dimension and is significantly different from the fluid shear stress in the absence of any cells. They mathematically showed that the force calculation is highly sensitive to the actual geometry of the channel which changes due to cell adhesion to the walls of channels and the actual magnitude of the effective shear stress felt by the cells in channels is greater than the calculated shear stress due to fluid flow through these channels. Thus, the narrower the channel the higher is the effective shear stress though the applied fluid shear stress is same. Therefore, the effective fluid shear stress in 33 μm channel width is higher than in the 99 μm channel width though the applied shear stress is 35 dyn/cm^2 in both the cases.

At flow rates of 15 and 20 μl/min, a significant decrease in the number of attached cells can be seen in case of O_2 plasma–collagen coated channels after 48 h of growth. From the images presented in figure 33a it is also clear that APTES-mediated collagen coating supported better cell attachment at 46dyn/cm^2 shear stress as compared to plasma collagen coating. Cell growth at flow rate of 15μL/min and 20μL/min was comparable in APTES collagen coated samples up to 48 h. But at these higher flow rates, it was observed that high shear stress changed the cell morphology after 48 h of growth and cells exhibited more filamentous structure in the direction of flow. This change in morphology and sensitivity of cells was also detected during Actin filament staining procedure. Cells after 48 h of growth at 5 and 10μL/min, showed very nice fluorescence images of actin filament but the cells grew at high flow rate were seemed to be very sensitive to labeling procedure (figure 35). Majority of the cells losses their morphology when fixative and permeablization solution was passed through the channels. This result showed that though fibroblast cells are still attach to the surface due to coating efficiency but at high shear stress, which is beyond the tolerance limit of this cell line, become more sensitive to any other stimuli.

At a flow rate of 40 μl/min, only few cell networks were observed in APTES collagen coated PDMS channels, which showed that the shear stress is then high enough to overcome the resistance of the cell–substrate bond strength. At such high fluid shear stress an orientation of the actin filament towards the flow direction can be observed in plasma–collagen coated channels, which was also reported by others, whereas on the APTES–collagen coating cells did not show a preferred orientation. This effect may be due to the formation of a stable cell–to–cell network on the APTES–collagen coating as compared to few individual cells observed on the plasma–collagen coating.

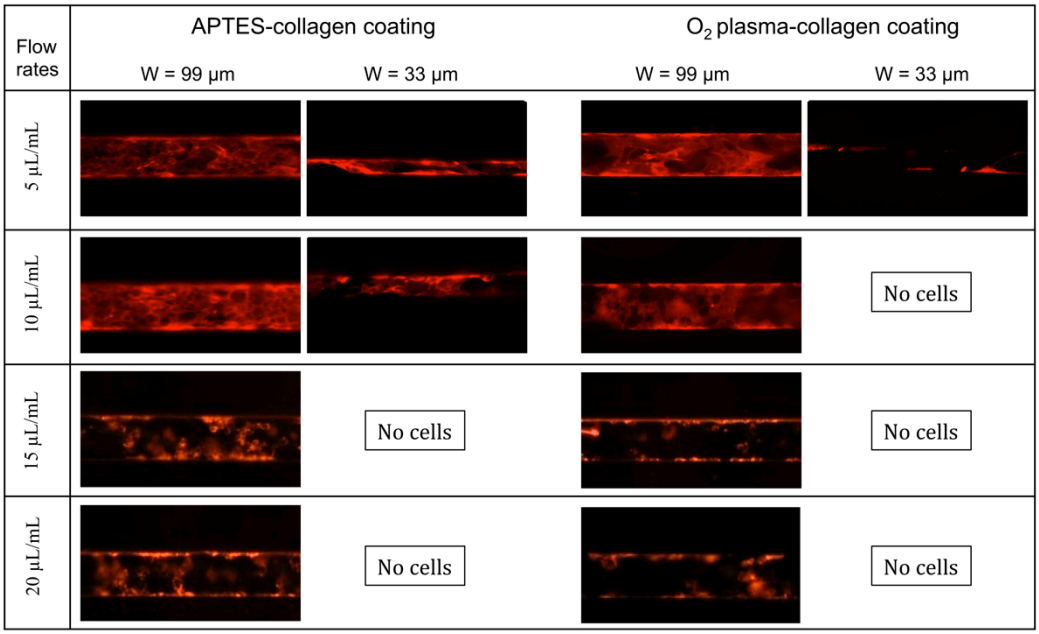

Figure 35: Actin filament staining of FCOS-7 cells inside microfluidic devices after applying shear stress for 48 h.

3.1.7. Stability of APTES-mediated collagen coatings

Stability of APTES-mediated collagen coatings was evaluated by two experiments

(i) By cell growth:

In this experiment, cells (FCOS–7) were grown in APTES–collagen coated and O_2 plasma–collagen coated channels (device B) which were already exposed to a continuous flow of PBS at 20 µL/min flow rate corresponding to 46 dyn/cm^2 and 138 dyn/cm^2 wall shear stress (in the 99–µm and the 33–µm–channel respectively) for 48 h in a CO_2 incubator at 37°C prior to cell seeding. A decrease in the initial attachment of cells after 1 h was observed in both the cases as compared to freshly coated channels. But the growth of cells on the APTES–collagen coating was comparable with that on the fresh device, while on the O_2 plasma–collagen coating, the number of cells was notably reduced after 24 h and 48 h (Figure 36a,b).

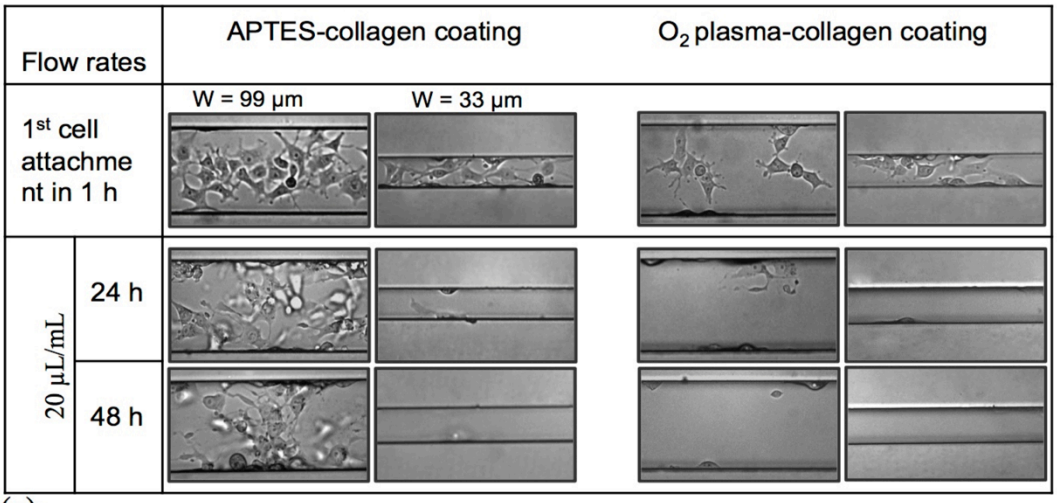

(a)

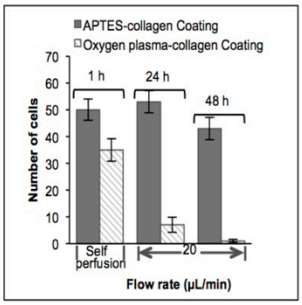

(b)

Figure 36: (a) Cell growth in collagen coated PDMS microfluidic devices with and without APTES intermediate that were perfused with a continuous flow of PBS prior to cell seeding. (b) Average cell count (± SD) in a channel area of 0.1 mm^2 in the wide channels of the microfluidic devices (shear stress: 46 dyn/cm^2). All experiments were performed in triplicates and multiple images were taken from each experiment.

(ii) By AFM scanning inside microfluidic devices:

The stability of the coatings also was investigated by means of AFM measurements inside the microfluidic channels after perfusion with a continuous flow at 20 µL/min flow rate (46 dyn/cm^2). Topographic data indicated a larger surface roughness value (rms = 24.6 nm ± 4.0 nm) for the APTES– collagen coating as compared to the O_2 plasma–collagen coating (rms = 1.1 nm ± 0.8 nm). Furthermore, the AFM images clearly show the presence of a collagen network on the APTES–collagen coated device even after washing the channels for 48 h, whereas there are no fibrillar structures on the O_2 plasma– collagen coating (Figure 37). These results further verify the stability of APTES-mediated collagen coating inside the PDMS microfluidic devices under shear stress conditions.

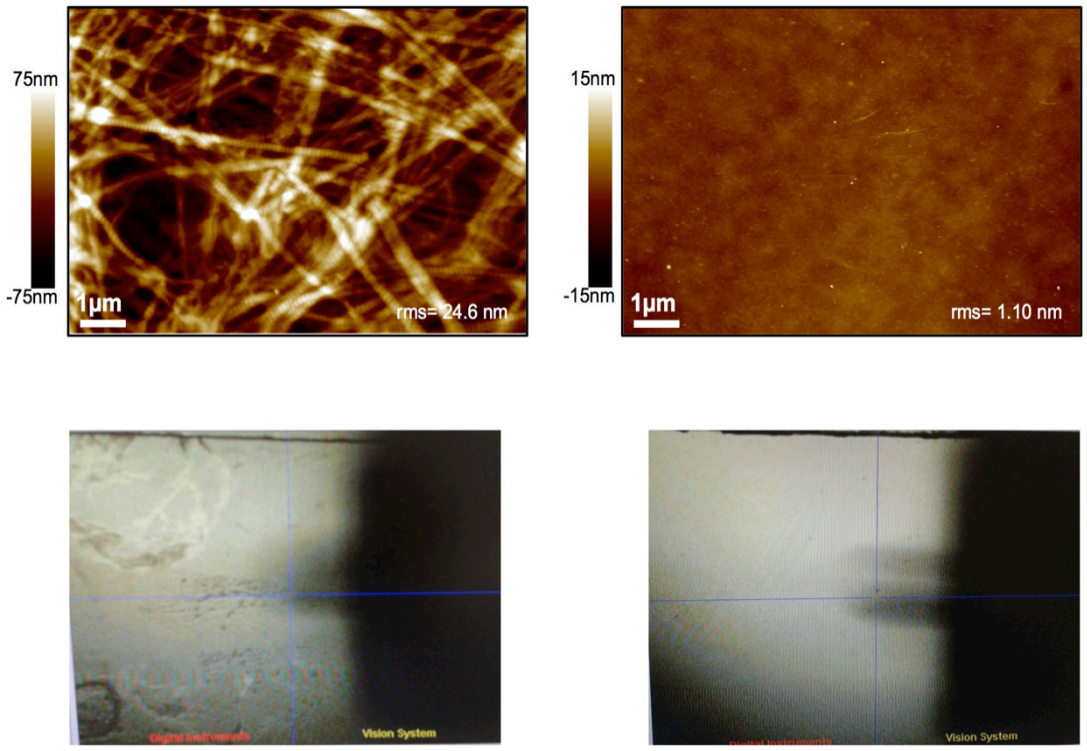

Figure 37: AFM images of the PDMS surface inside the micro–channels after 48 h perfusion at 180 µL/min flow rate in a 900–µm–channel (shear stress: 46 dyn/cm^2).

3.2. Development and comparison of various surface chemistries for improved cell growth under shear stress.

In this part of work, differently treated PDMS surfaces were used to bond collagen at three different pH values (pH 5, 7, 9). Various PDMS functionalizations attributed to distinct surface chemistries and surface charges so that expected to develop ionic interaction with charged collagen. For example, collagen at pH 5 probably bonds more stably to plasma treated surface due to a net positive charge on collagen and negative charge on surface. In the same manner collagen at pH 9 should contribute to a stable interaction when polymerized on protonated PDMS surfaces. Figure 38 explains PDMS surface chemistry after different treatments as well as our expected stable reactions with collagen.

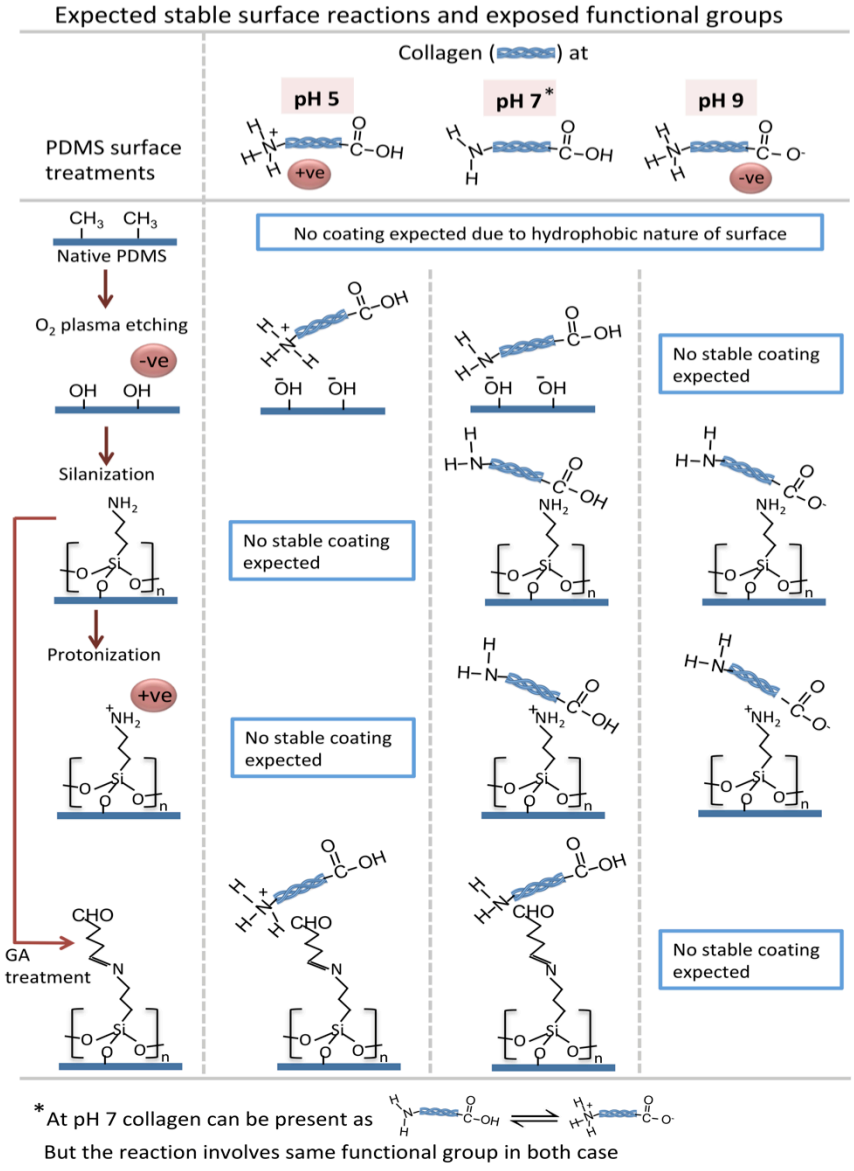

Figure 38: Schematic illustration of PDMS surface functionalizations and expected stable reactions after incubation with collagen at different pH values.

Moreover, after O_2 plasma treatment of PDMS surface, the surface can exhibit different reactive groups, for example Si–OH, Si–CH2–OH or Si–COOH but the Si–OH group is most abondentely present reactive group on surface [133]. As all other reactive groups, generated after O_2 plasma treatment, also exhibit –OH molecule therefore only –OH is mentioned as representative reactive molecule in figure 38.

The collagen coating efficiency by different surface functionalization methods for the development of endothelialized microfluidic channels at high shear stress is discussed in this chapter. Moreover, the effect of intermediate linkages on biocompatibility of surfaces is also explained by cell viability studies.

3.2.1. Water contact angle:

The decrease in hydrophobicity of differently treated PDMS surfaces, before and after collagen coatings, was determined by water contact angle. Contact angle of PDMS was decreased after treating surfaces with O_2 plasma (9.45° ± 2.77°), APTES (61.79° ± 0.14°), GA (66.14° ± 11.83°), and HCl (65.87° ± 14.89°). After coating all these surfaces with collagen at various pH, the contact angle values were observed between 33°–62° (Figure 39), which indicated that all the surfaces, coated with collagen pH 5, 7 and 9, are hydrophilic. The lowest contact angle among collagen coated surfaces was measured on APTES–GA–coll–9 (33.56° ± 4.24°) and the highest was on APTES–coll–9 (62.59° ± 3.20°). The decrease in contact angle of PDMS after coating with APTES, APTES–GA and collagen has been already reported in different studies [130, 177, 228]. Moreover, a decrease in hydrophobicity was also observed when PDMS, without any pretreatment, was coated with collagen pH 5 (CA: 81.93° ± 4.04°), collagen pH 7 (CA: 82.42° ± 4.63°) and collagen pH 9 (85.61° ± 2.61°)

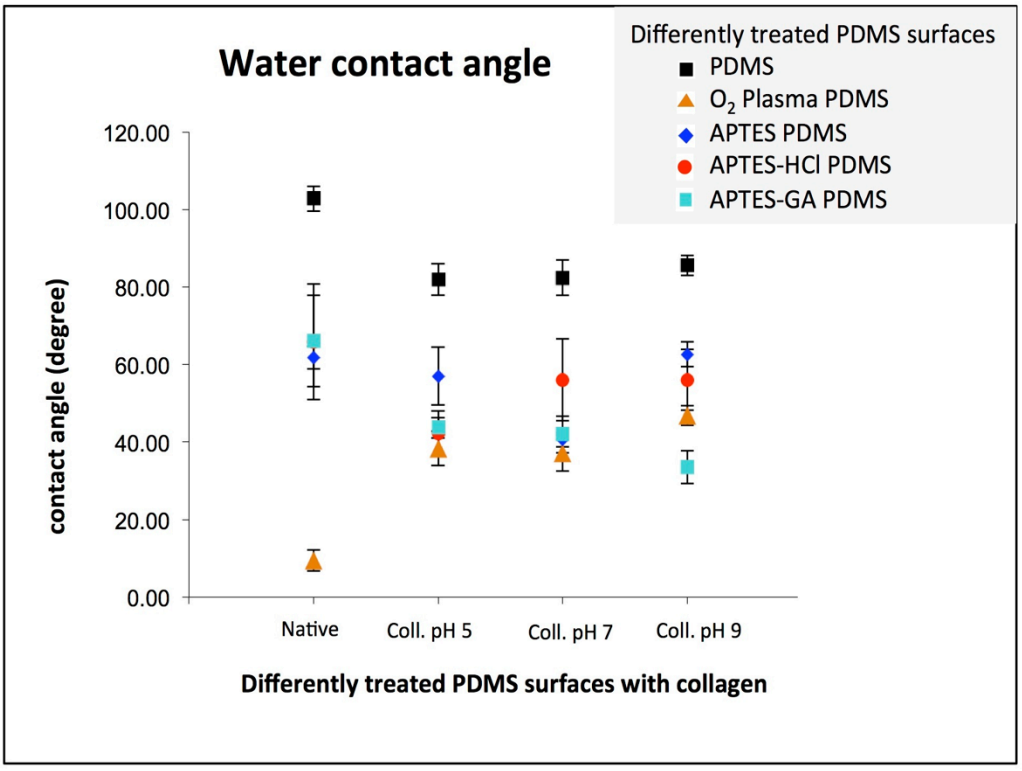

Figure 39: Water contact angle (± SD) of differently treated PDMS surface, before and after collagen coatings.

3.2.2. Surface topography:

The RMS roughness of all PDMS surfaces was increased after initial functionalization, and further increased after collagen coating when measured with AFM. After coating with collagen, different patterns of collagen fibril formation can be observed on all different types of surfaces (Figure 40). Long fibers of coll–7 have been observed on all PDMS surfaces with a maximum roughness on O_2 plasma treated PDMS (rms = 13.2 nm) and APTES treated PDMS (rms = 13.2 nm). PDMS surface after O_2 plasma treatment bears a negative charge [233] therefore more distribution of coll–5 and less of coll–9 can be seen on this surface. APTES and APTES–GA treated surfaces represented very nice collagen attachment at all three pH values. PDMS surface with APTES–HCl treatment was expected to contain more coll–9 and less coll–5 due to positive charge distribution on the surface. Expectedly the surface exhibited less coll–5 but in case of coll–9, although collagen formed long but distantly arranged fibers. In short, all differently treated PDMS surfaces and even the native one supported nice distribution of collagen except plasma treated surface with coll–9, this might be due to negative charge distribution on surface as well on collagen.

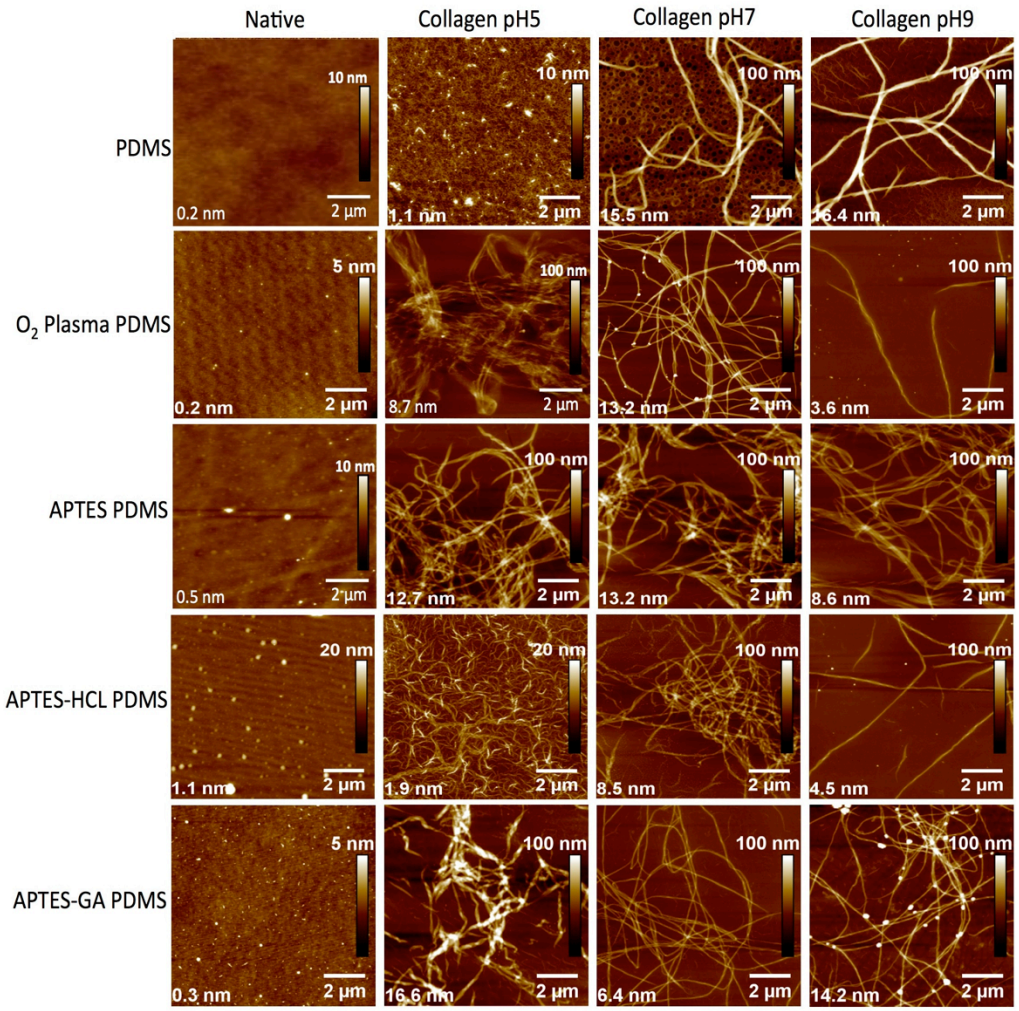

Figure 40: AFM topography (height) images of functionalized PDMS surfaces (10µm x 10µm) immediately after coating.

In two separate but related studies Denis *et al.,* and Elliot et al., [207, 234] discussed the fact that surface charged groups derive the distribution of collagen on the surface. Authors observed the better collagen attachment with long fiber like structures on a designed hydrophobic surface with $–CH_3$ functional groups as compares to hydrophobic surface with –OH functional groups.

It is also reported that fibrillogenesis of collagen is strongly dependent on pH of the medium; moreover the collagen fibril formation can be detected with the increase in pH value. It was observed that coll–5 contains more fibrous like structure while coll–7 and coll–9 exhibit more fiber like structure. These results matches to the observations reported by Yadavalli *et al*., about the effect of pH on fiber formation of collagen. Author reported a slow fibril formation at pH 5 but at pH 7 and pH 9 long fibers were observed however no fibrillation was observed at pH 3. The findings were argued as the charges on amino acids near to isoelectric point balanced at pH close to the isoelectric point of collagen which favored the fibrillation process [230]. Generally the rate of fibrillogenesis is increased by increasing pH from 6.9 to 9.2 perhaps no significant was observed in the size of the fibrils in this pH range [235]. After five days of incubation at 37° C the rms value of almost all surface was changed by a slight increase or decrease in the value but the entire surface still exhibited nice distribution of collagen (Figure 41). Dupont et al., (2004) reported that collagen fiber formation is enhanced by increasing its adsorption time on surface [210]. Surprisingly, collagen fiber growth was also enhanced on native PDMS surface after five days of incubation. Since collagen fibrous and fibers are free to move on smooth and hydrophobic surfaces in this case if the incubation time is prolonged, small fibrous contribute to the growth of long fibers [234].

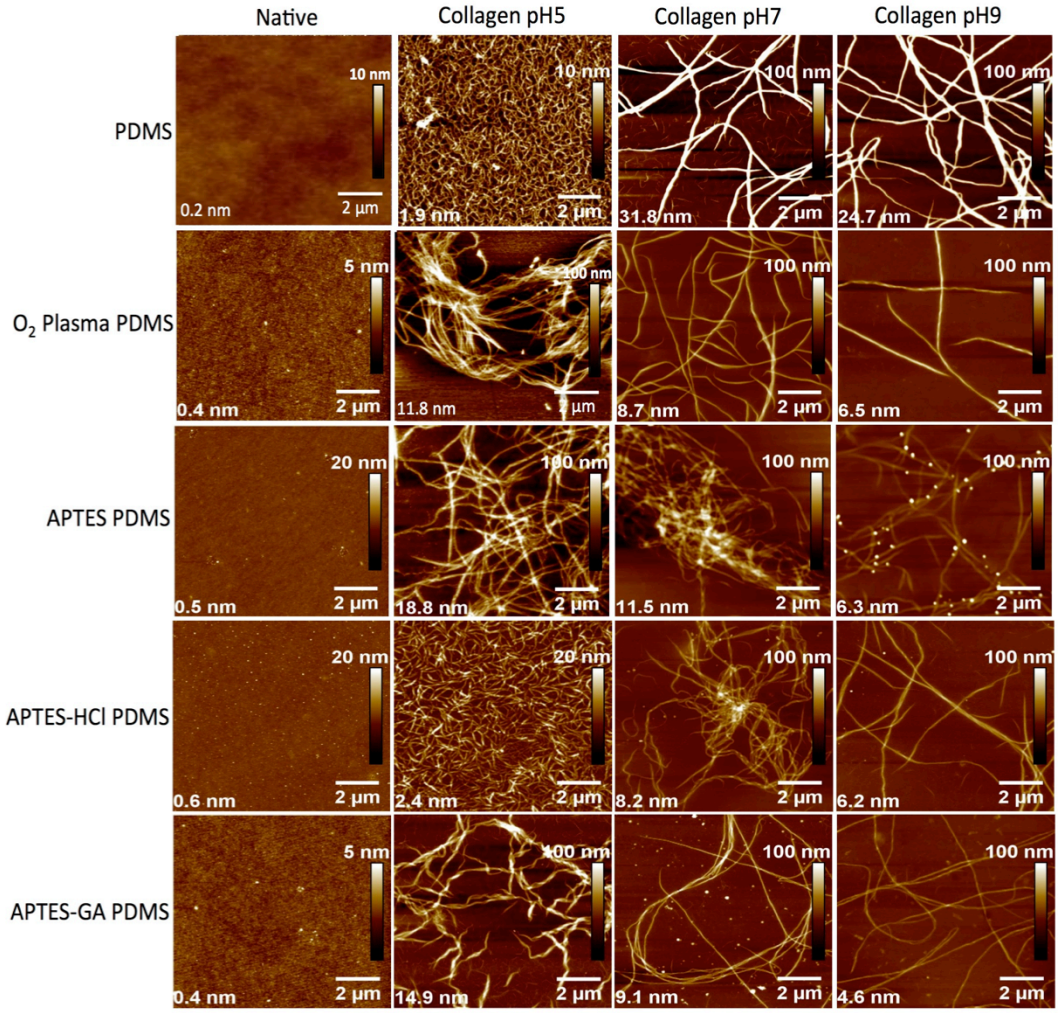

Figure 41: AFM topography (height) images of functionalized PDMS surfaces (10µm x 10µm) after five days of incubation in cell culture medium.

3.2.3. Effect of pH on APTES layer:

APTES monolayers are already reported to produce an amino functional group onto the surfaces with zero zeta potential at pH ≅ 6.7 [236, 237]. An increase or decrease in this pH value can also vary the surface charge on APTES layer. After incubation with buffer solution at pH 5, 7 and 9, PDMS devices exhibited positive charge at pH 5 and negative charges at pH 7 and 9. This charge distribution on APTES surface indicates the negative potential at high pH value (Figure 42).

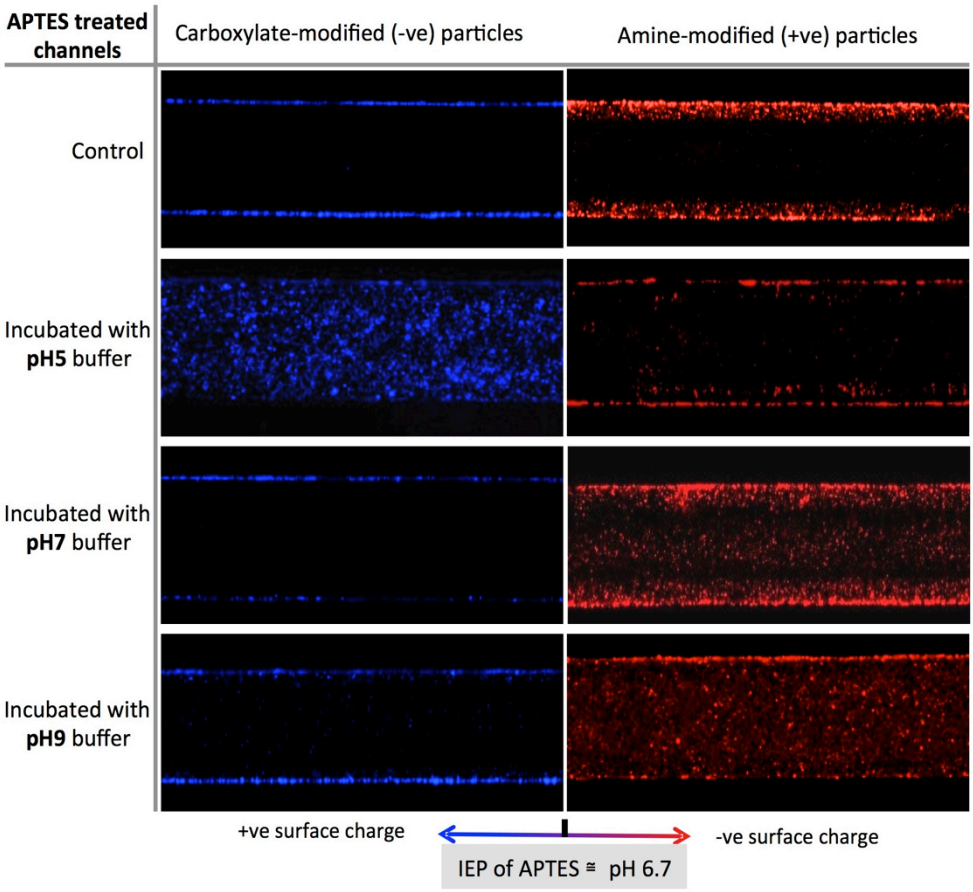

Figure 42: Charge distribution on APTES treated PDMS surfaces after incubation with buffers of different pH values.

3.2.4. Cell growth and viability on PDMS surfaces:

Freshly isolated human umbilical vein endothelial cells (HUVECs) were maintained in growth medium M200 supplemented with growth supplement (LSGS) in Corning® CellBIND® tissue culture flask at 37°C in a CO_2 incubator. After reaching passage three, cell growth and basic morphology was evaluated by Actin filament staining and finally used for experiments (figure 43a,b). Biocompatibility of all functionalized and native PDMS surfaces was assessed by growing HUVECs for a period of 10 days. Expectedly all collagen coated surfaces supported cell growth by a small increase in cell number with the period of time however an enhanced proliferation can be seen in APTES-mediated collagen coated surfaces (Figures 44–48). Related observations have been already reported for fibroblasts cells in one of our previous studies [228]. Collagen coated native PDMS surfaces exhibited cell attachment for 10 days of study though the numbers of cells were fewer. Razafiarison *et al*., (2016) described the stem cell growth and early osteogenic differentiation on collagen self assembled layer on PDMS surface [151]. However, our current study suggested that collagen assemblies on initially functionalized PDMS surfaces supported an improved cell growth than collagen assemblies on native PDMS surfaces. Collagen at all three pH (5, 7 and 9) showed considerably higher cell proliferation in case of initially APTES treated PDMS surface. Thus after cell

counting data, the purposed cell supportive surfaces can be ordered as "PDMS APTES–coll > PDMS APTES–HCl–coll ≥ PDMS APTES–GA–coll > PDMS O_2–plasma–coll ≅ PDMS–coll". Cellular attachment and proliferation mainly depends upon exposed functional groups on surface and "–CH_2NH_2" functional groups are reported to enhance cell adhesion as compared to "–CH_2OH" groups [92].

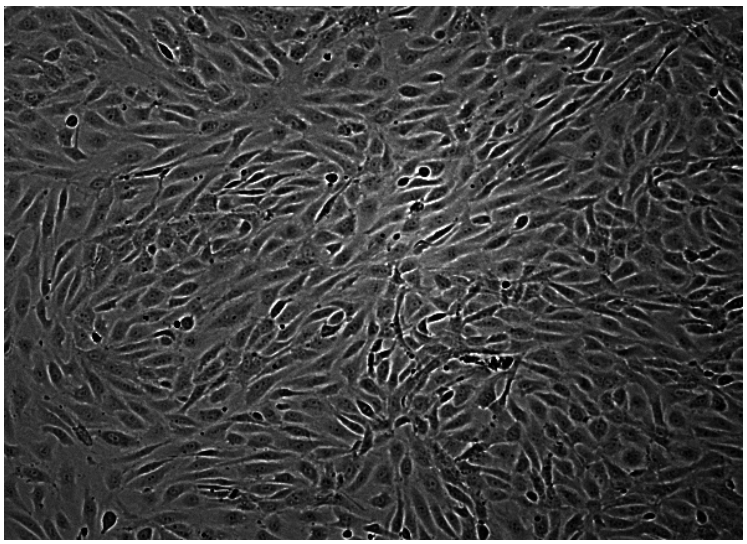

(a)

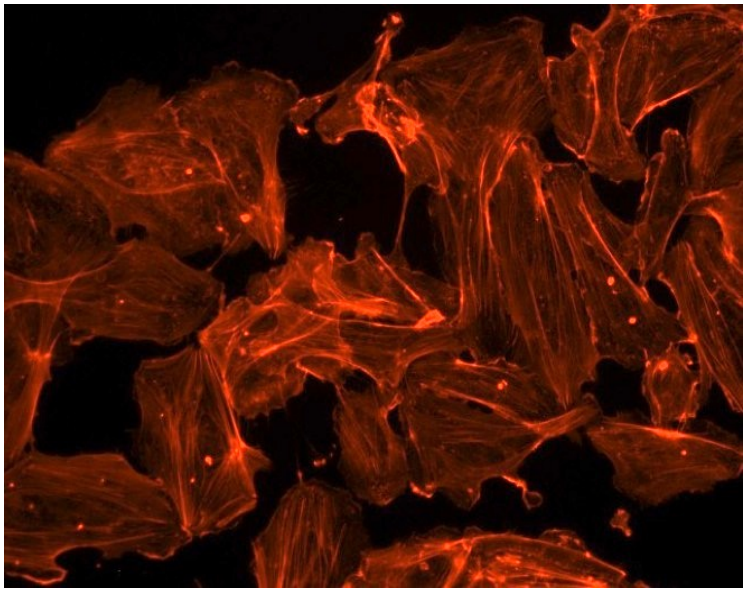

(b)

Figure 43: HUVECs growth and confluency (a) inside a tissue culture flask, image at 10x (b) Actin staining of cells in a polystyrene petri plate, image at 40x.

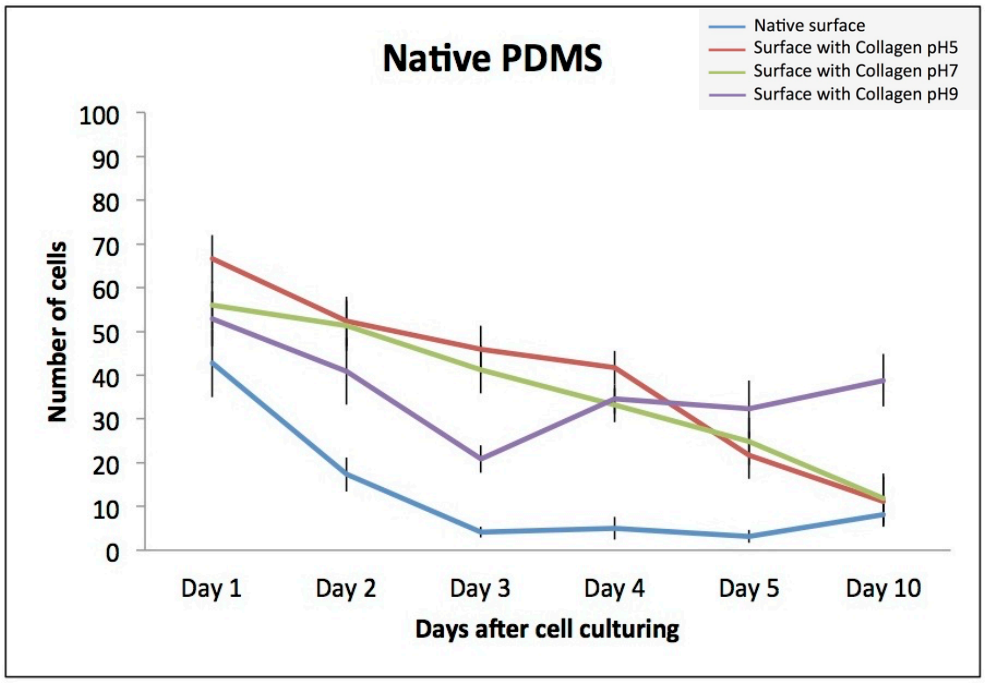

Figure 44: Quantitative analysis of cell growth and proliferation (± SD) on native PDMS surface coated collagen (pH 5, 7, 9).

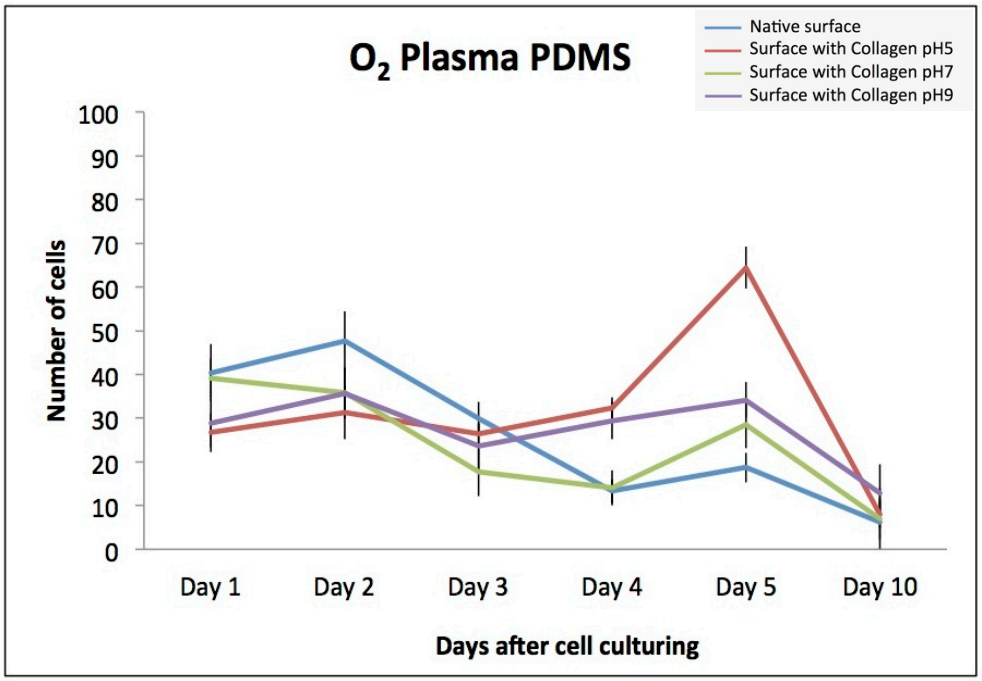

Figure 45: Quantitative analysis of cell growth and proliferation (± SD) on O_2 plasma PDMS surface coated collagen (pH 5, 7, 9).

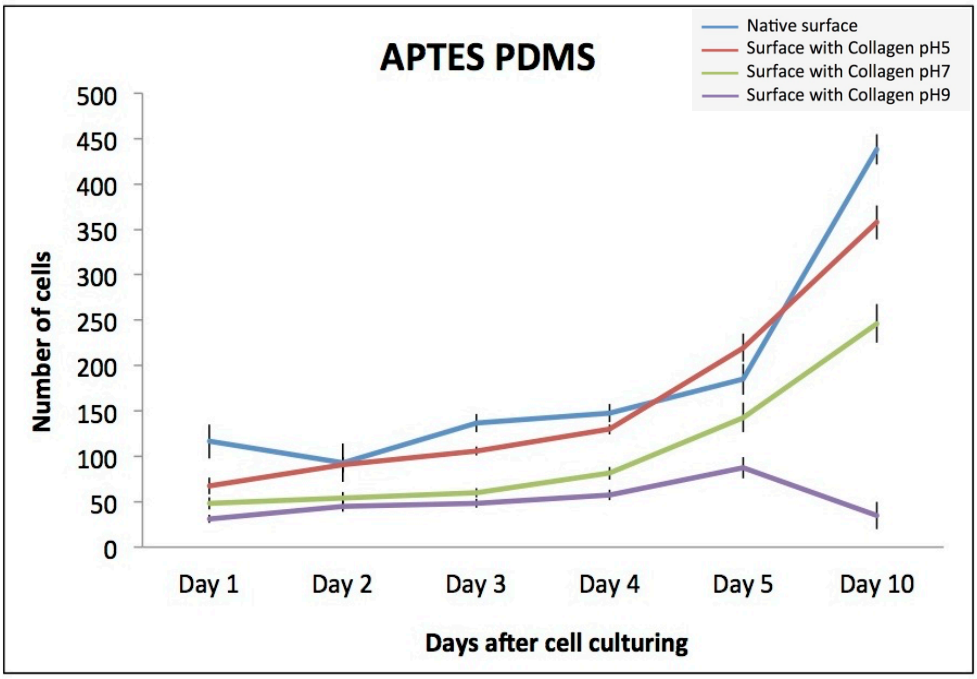

Figure 46: Quantitative analysis of cell growth and proliferation (± SD) on APTES PDMS surface coated collagen (pH 5, 7, 9).

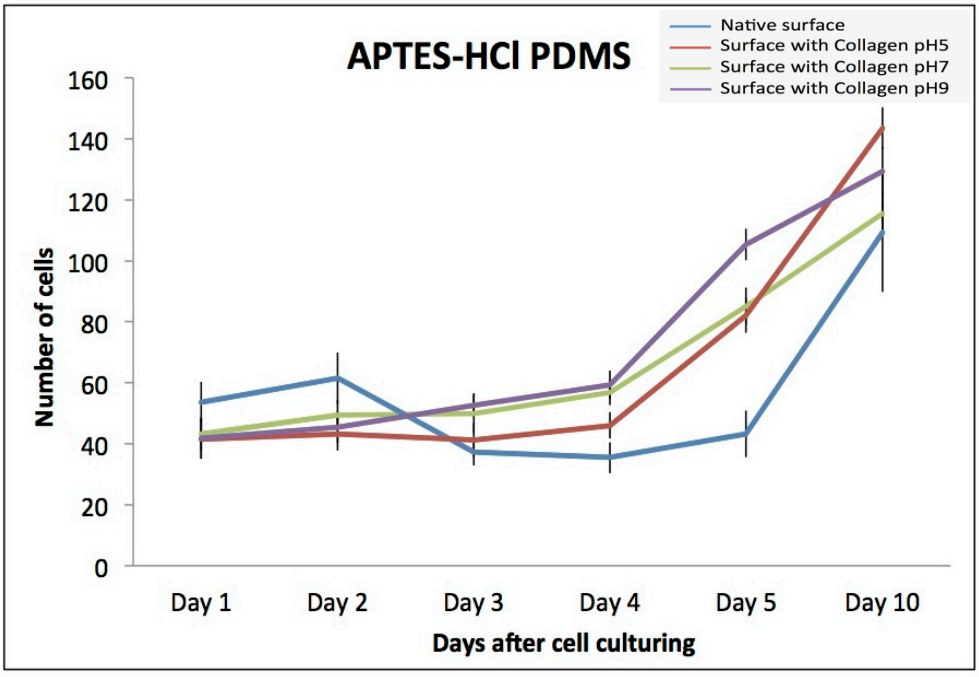

Figure 47: Quantitative analysis of cell growth and proliferation (± SD) on APTES–HCl PDMS surface coated collagen (pH 5, 7, 9).

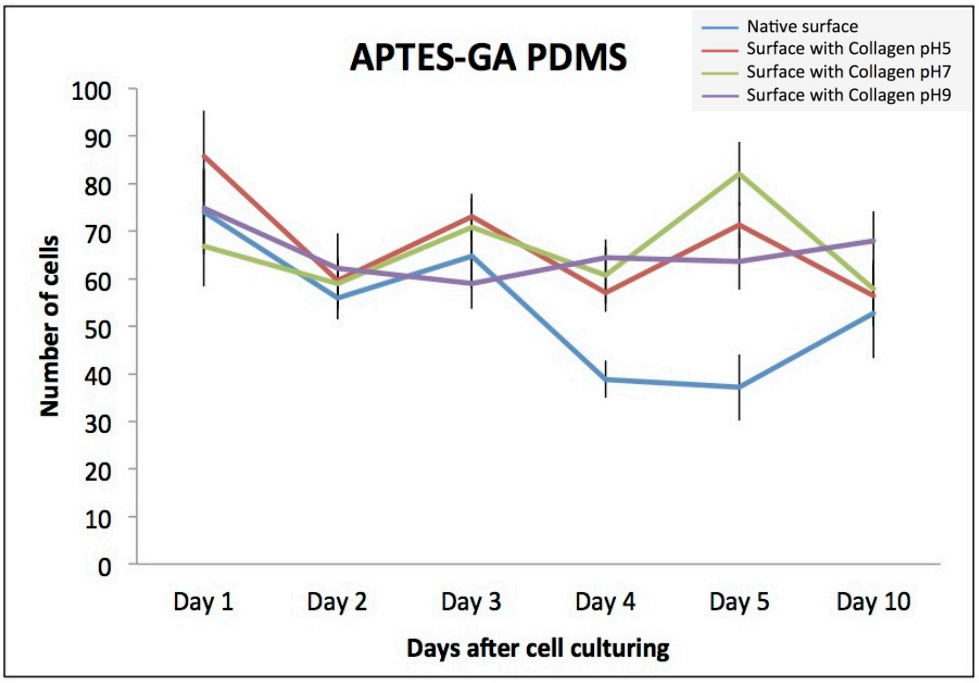

Figure 48: Quantitative analysis of cell growth and proliferation (± SD) on APTES–GA PDMS surface coated collagen (pH 5, 7, 9).

Live/dead cell assays showed that all native surfaces, surface with coll–5 and all APTES–GA–coll coated surfaces are not suited for cell growth and dead cells can be seen on surfaces. It is already known that proteins undergo various conformational changes during adsorption process and cellular interaction is greatly dependent upon this confirmation hence not all the confirmations are beneficial for cell growth [238]. However, the surfaces with collagen at pH 7 and 9, other than gluteraldehyde mediated surfaces were attributed to biocompatible surfaces (Figure 49). Although gluteraldehyde is considered as one of the most common cross linker for collagen meanwhile its toxicity for cell growth has been previously reported [239-241]

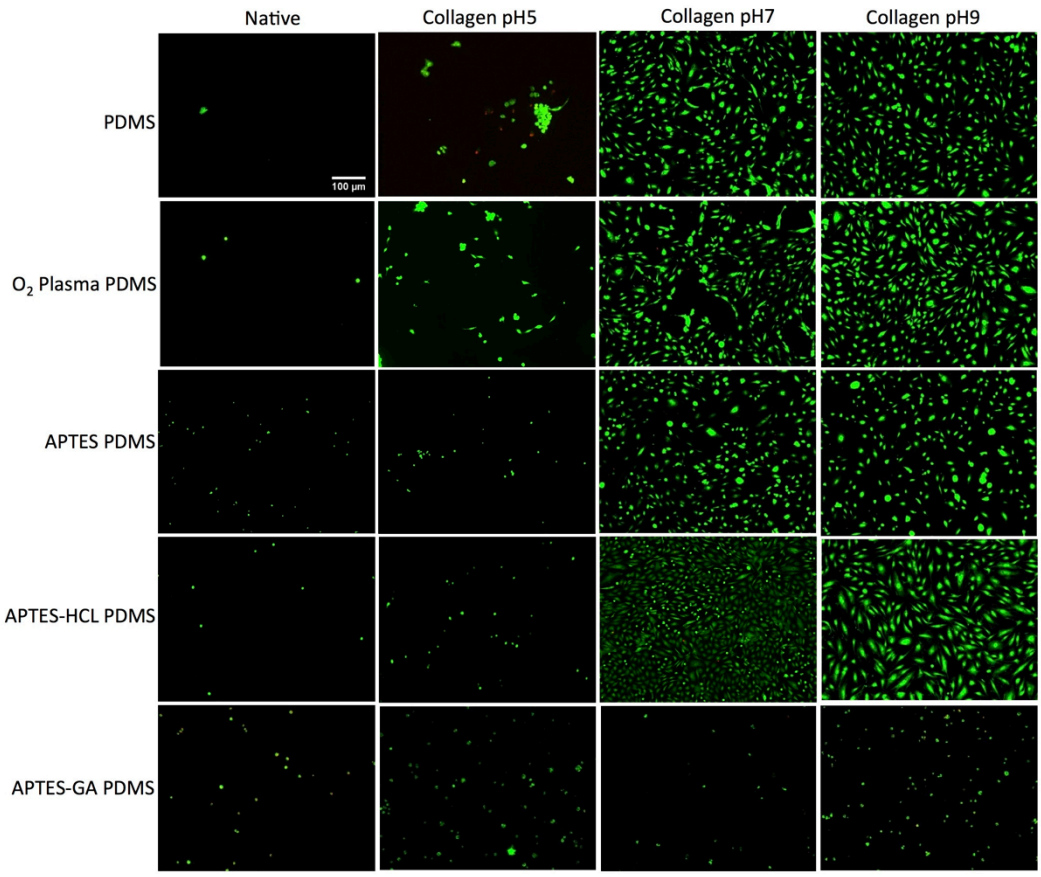

Figure 49: Cell viability on differently treated PDMS surfaces. Where, green spreaded cells represent the live and proliferating cells, red cells represents the dead cells and green round represents the live but not proliferating cells and smashed cytoplasm that attained some calcein (dye) are damaged cells.

3.2.5. AFM measurements inside microfluidic channels:

The microfluidic assays were performed to compare the stability of collagen, which was attached by different linkers on PDMS surfaces. Collagen coated (sec. 2.6), 990–µm–wide, PDMS channels were perfused with sterile PBS for 48 h under various shear stress rates (10–40dyn/cm^2) and finally AFM was used to evaluate the presence or absence of collagen inside the channel (Table 3).

AFM topography inside microfluidic channels showed that in case of coll–5 coatings, APTES–coll–5 and O_2 plasma–coll 5 were stable up to 30 dyn/cm^2 but rms value of APTES collagen coating (rms = 5.9nm ± 0.8nm) was higher than O_2 plasma (rms = 4.2nm ± 1.4nm). APTES–coll–7 was found to be stable upto 40 dyn/cm^2 (rms = 5.8nm ± 1.2nm). Among coll–9 coatings, APTES–coll–9, O_2 plasma–coll–9 and APTES–HCl–coll–9 coatings represented comparable stability at 40 dyn/cm^2 shear stress. Briefly, among all surface functionalizations, APTES–HCl–coll–9 surface exhibited more collagen (rms = 6.8nm ± 2.1nm) after perfusion at 40 dyn/cm^2 due to strong electrostatic interaction between protonated surface and negatively charged collagen. Generally APTES-mediated collagen coatings were observed as more stable under flow conditions. Collagen coatings on APTES–GA treated surfaces and native PDMS surfaces were found to be least stable under shear flow (Figure 50).

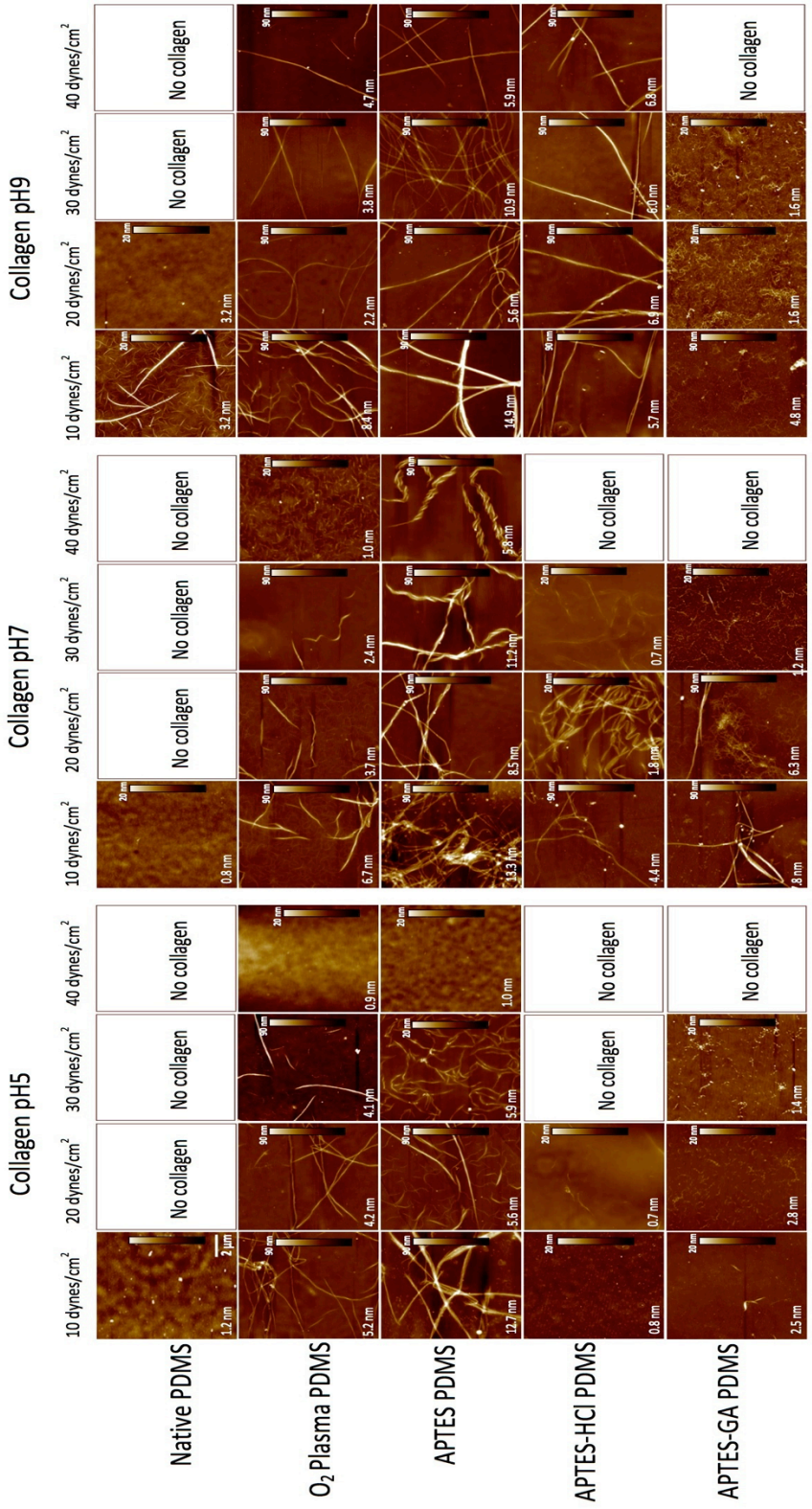

Figure 50: AFM images inside PDMS microfluidic devices (990 μm wide channels) after perfusion at 10–40 dyn/cm^2 shear stress, for 24 h.

3.2.6. Cell growth and attachment under shear stress

To contribute to vascular disease studies, a number of microfluidic models have been designed, which improve the efficiency of shear flow experiments. In current study a two–shear device (device D) was used with six selected biocompatible surface coatings, chosen after cell viability assay, which were (i) O_2 plasma–coll–7 (ii) O_2 plasma–coll–9 (iii) APTES–coll–7 (iv) APTES–coll–9 (v) APTES–HCl–coll–7 (vi) APTES–HCl–coll–9. Native PDMS surface, after hydrophobic recovery, showed no collagen stability in AFM measurements thus not considered for the cell study. After 1 h of initial attachment, all the devices exhibited comparable HUVEVs attachment and growth (Figure 51).

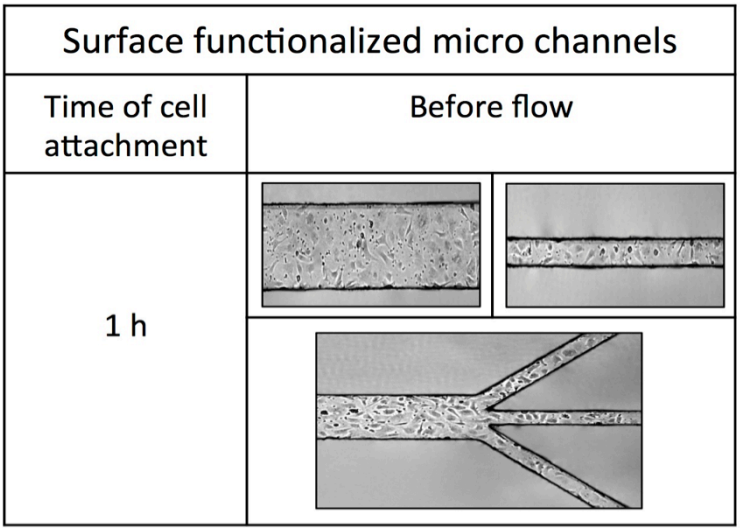

(a)

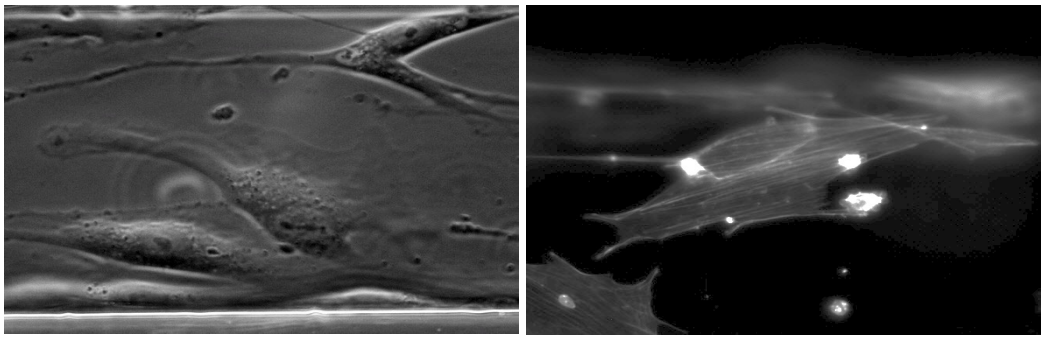

(b) **(c)**

Figure 51: Initial cell attachment after 1 h of incubation inside collagen coated microfluidic channels when no liquid flow is applied, (a) image from various areas of microfluidic channel at 10x magnification, (b) phase contrast image of cell morphology inside microfluidic channel at 40x, (c) Actin filament staining of cells inside microfluidic channel.

These devices were connected to perfuse growth medium and flow rates were adjusted to produce a wide range of shear stress including as well as higher than physiological shear stress; a normal case of cardiovascular diseases [242]. After 48 h

of cell growth at various flow rates, it was observed that the cells–surface bond is stronger in case of all surfaces coated with coll–9 as compared to coll–7. Cells exhibited good growth and proliferation at flow rate of 12 µL/min (20 dyn/cm^2 and 60 dyn/cm^2) in all devices. However, by increasing the flow rate to 18 µL/min (30 dyn/cm^2 and 90 dyn/cm^2) the cellular detachment started in O_2 plasma–coll–7 and APTES–HCl–coll–7 coated devices while in case of APTES–HCl–coll–7 the cell detachment rate was comparatively very slow. The mages of cells at flow rate/ shear stress, up to which cells are growing inside the devices and to the next flow rate/ shear stress, when they start detaching, are given in Figures 52–63. For example, cells in O_2 plasma–coll–7 coated channels are growing normally up to 12 µL/min flow rate (figure 52) therefor images at less flow rate 7µL/min (10 dyn/cm^2 and 30 dyn/cm^2) are not provided but by increasing flow rate to 18 µL/min cells started detaching, this effect of increased shear stress is showed by representative images (figure 53). When the effect of shear stress inside micro channels is discussed, one cannot ignore the fact that in the presence of cells, the actual shear stress can be significantly different and higher than the calculated wall shear stress [243]. Therefore it can be assumed that the cells are tolerating slightly higher shear stress than calculated one and this factor is more influencing in case of narrow channels. When the flow rate was increased to 25 µL/min (40 dyn/cm^2 and 120 dyn/cm^2), the cellular detachment started in APTES–HCl–coll–9 after 48 h of growth and in case of O_2 plasma–coll–9 and very less number of cells can be seen at 32 µL/min flow (50 dyn/cm^2 and 150 dyn/cm^2). Microfluidic devices coated with APTES–coll–9 showed maximum cell–surface bond stability and cells were growing and proliferating at 32 µL/min flow for 48 h. In general, the surfaces exhibited stable collagen coatings in microfluidic channels under shear flow conditions (reference to figure 51) represented better cell growth and proliferation.

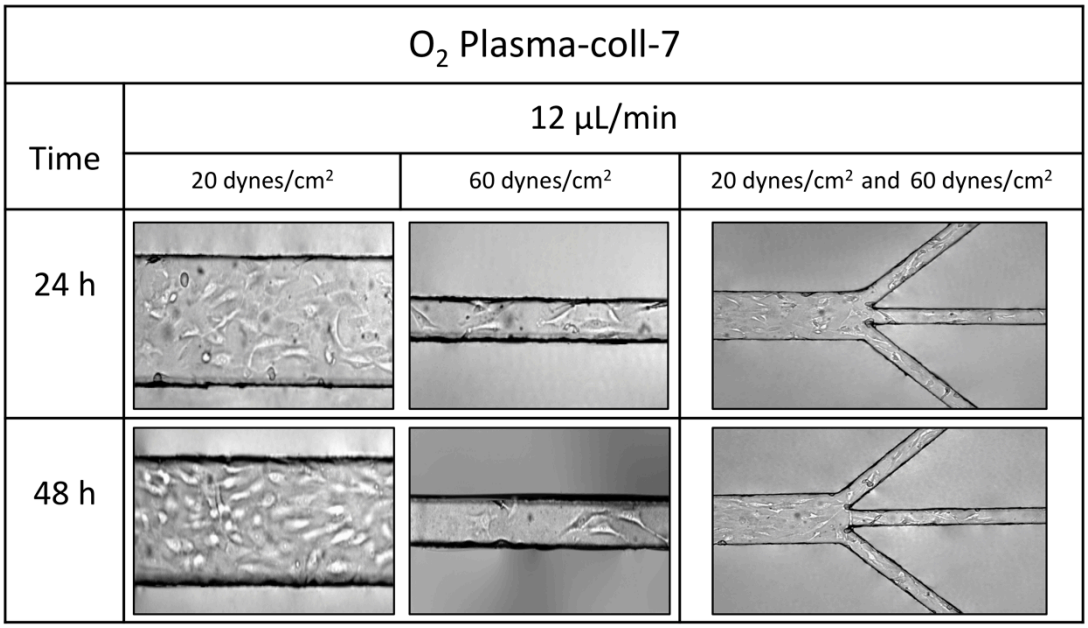

Figure 52: Cell attachment and growth inside O_2 plasma–coll–7 coated channel at 12µL/min flow rate.

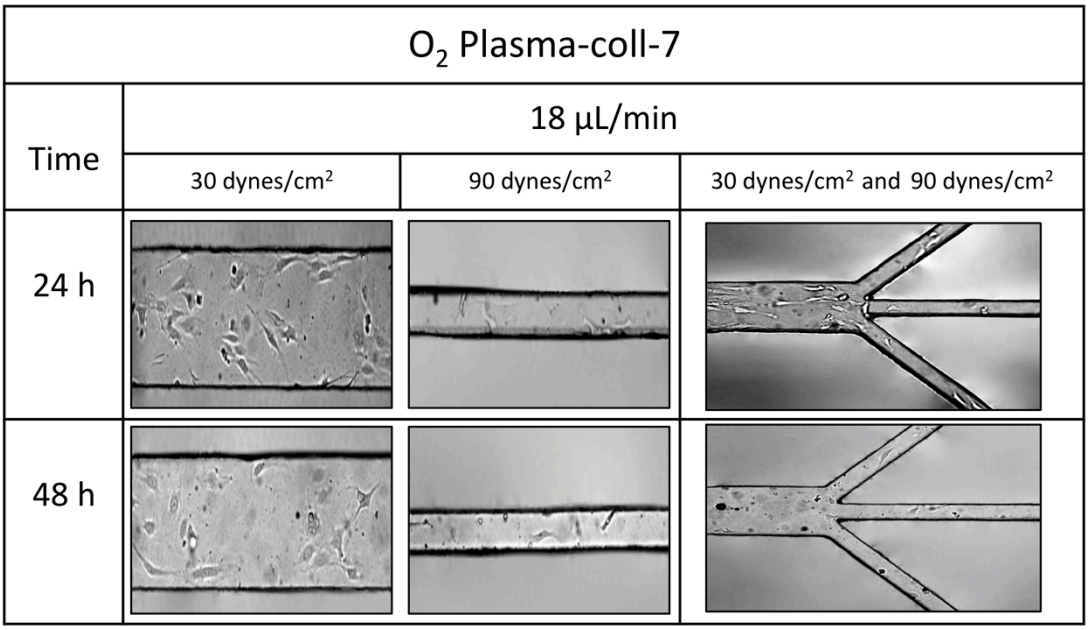

Figure 53: Cell growth inside O_2 plasma–coll–7 coated channel at 18µL/min flow rate where cells start detaching.

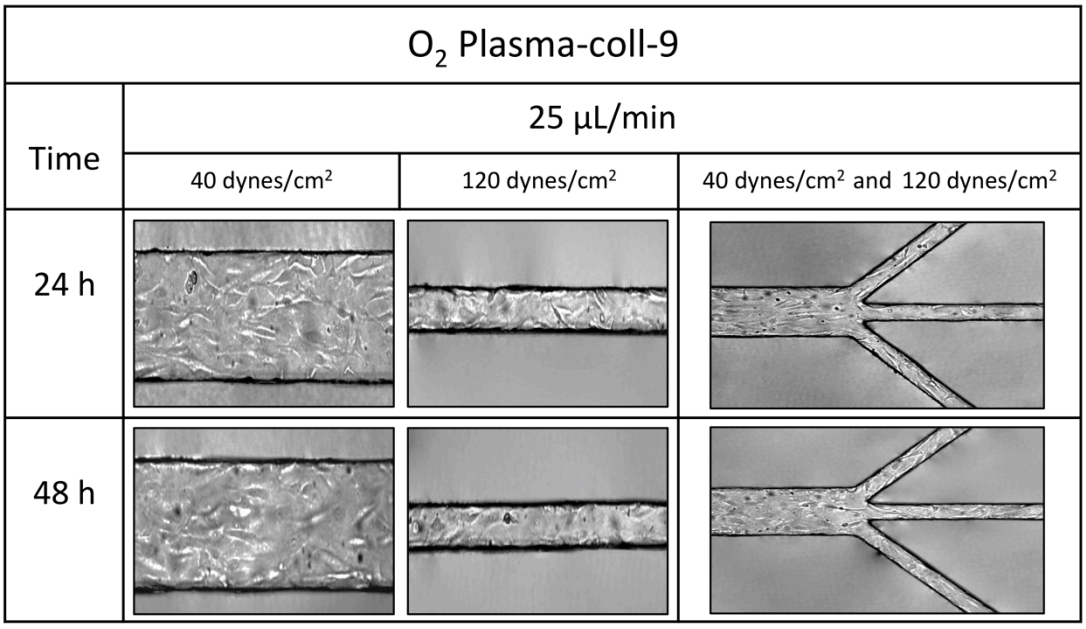

Figure 54: Cell attachment and growth inside O_2 plasma–coll–9 coated channel at 25µL/min flow rate.

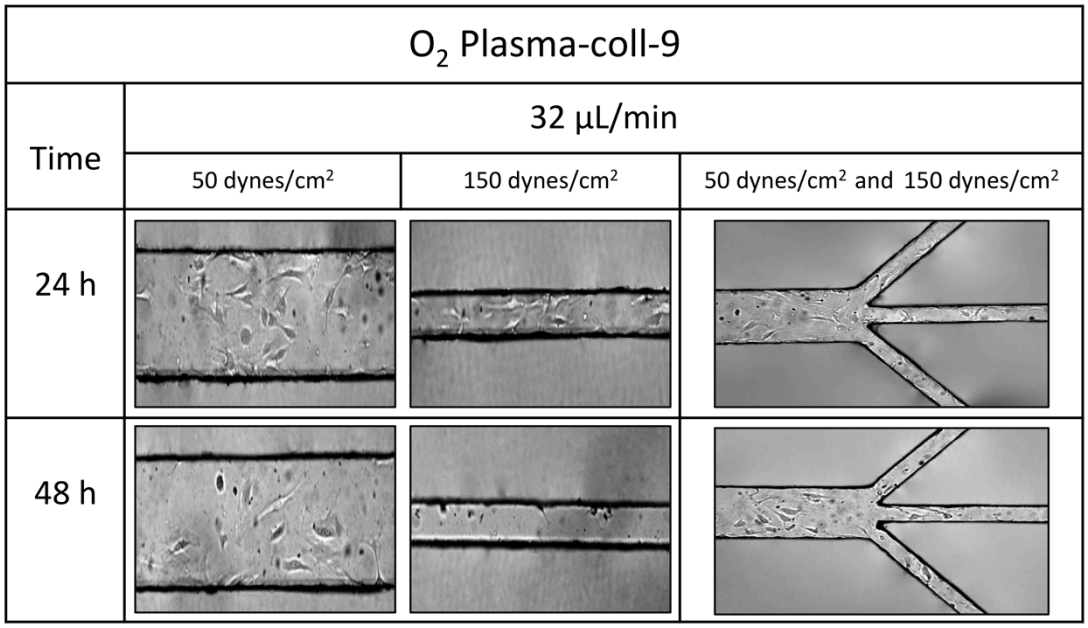

Figure 55: Cell growth inside O_2 plasma–coll–9 coated channel at 25µL/min flow rate where cells start detaching.

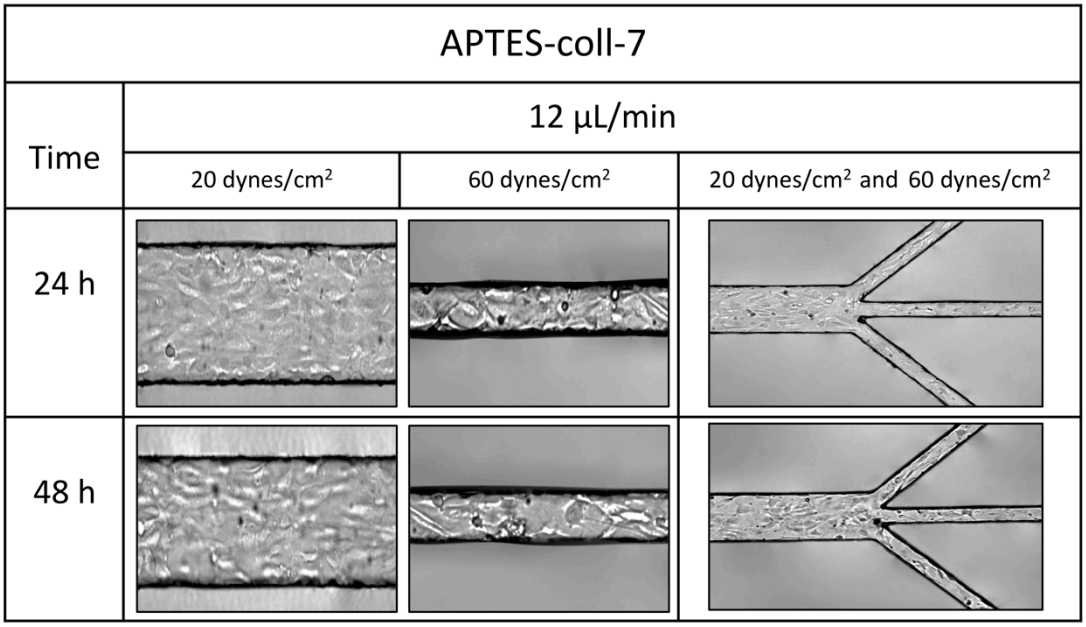

Figure 56: Cell attachment and growth inside APTES–coll–7 coated channel at 12µL/min flow rate.

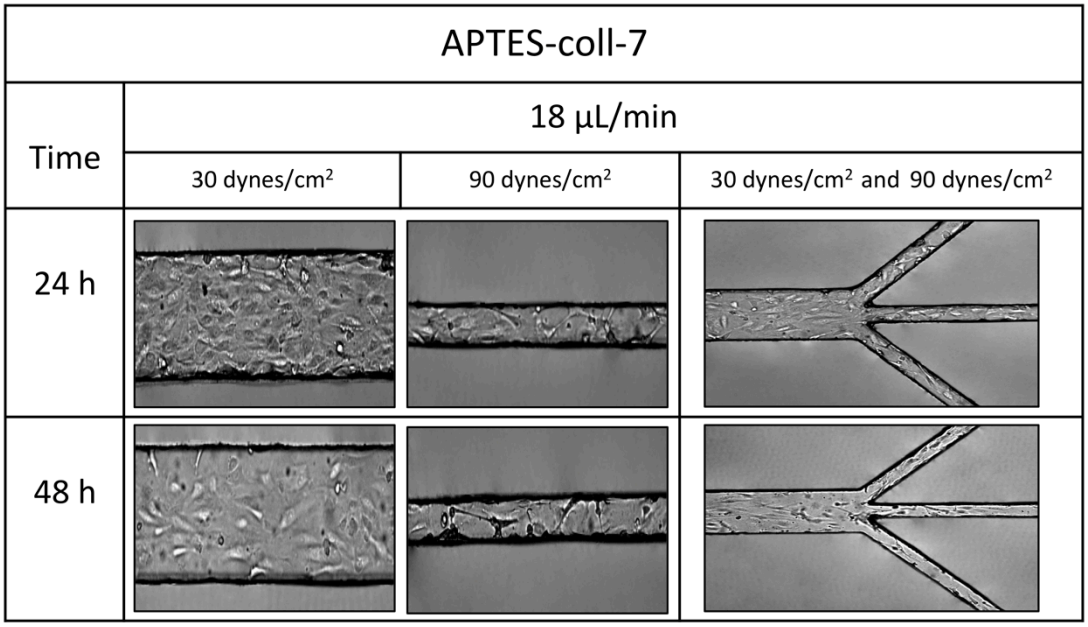

Figure 57: Cell growth inside APTES–coll–7 coated channel at 18µL/min flow rate where cells start detaching.

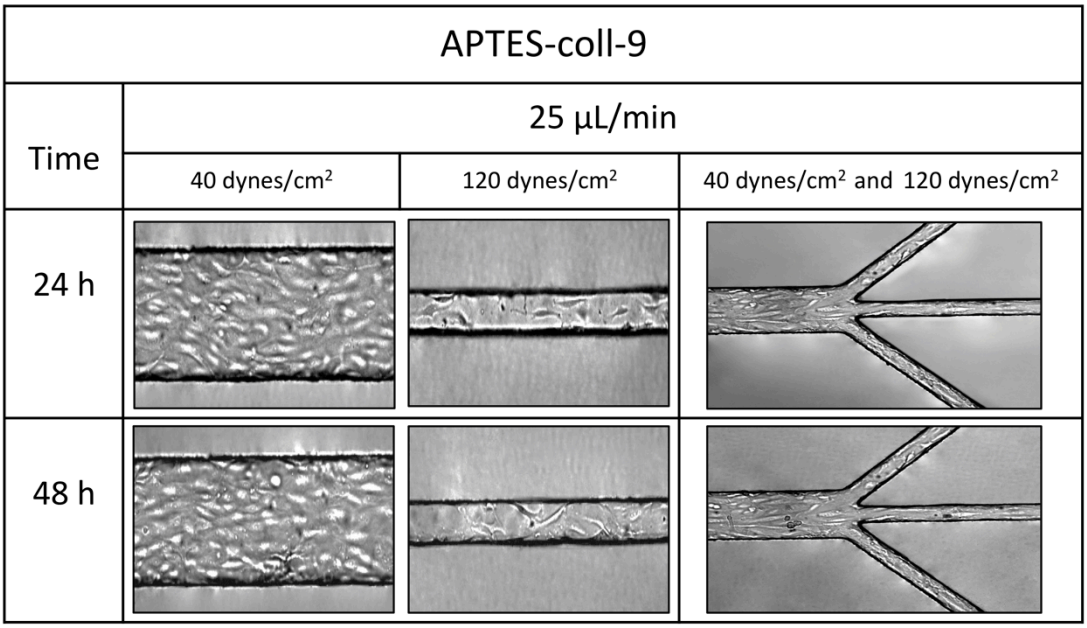

Figure 58: Cell attachment and growth inside APTES–coll–9 coated channel at 25µL/min flow rate.

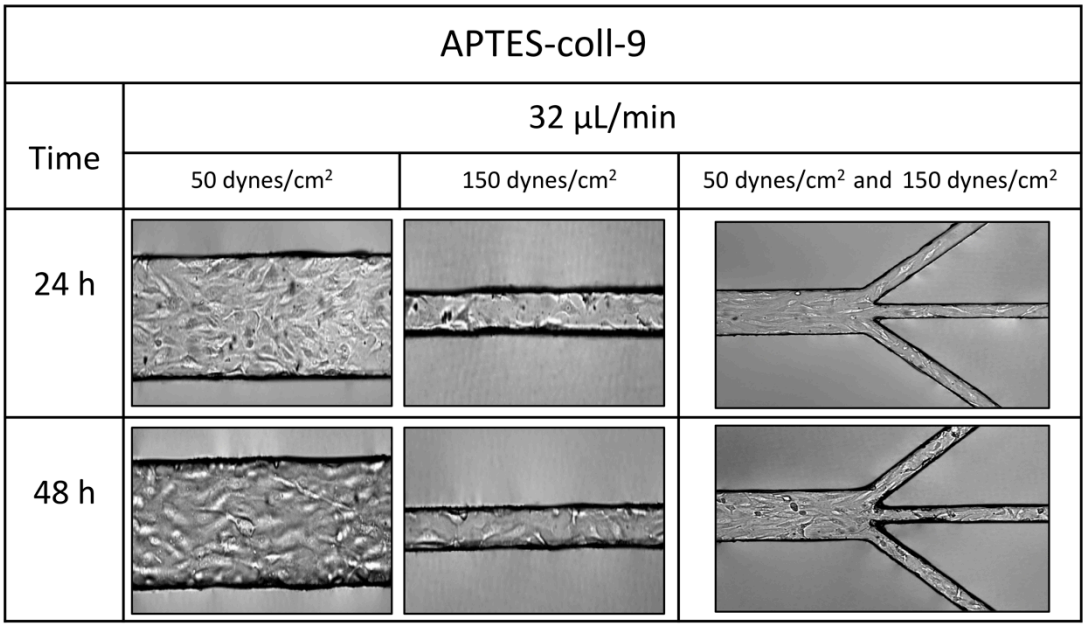

Figure 59: Cell growth inside APTES–coll–9 coated channel at 32µL/min flow rate where cells start detaching.

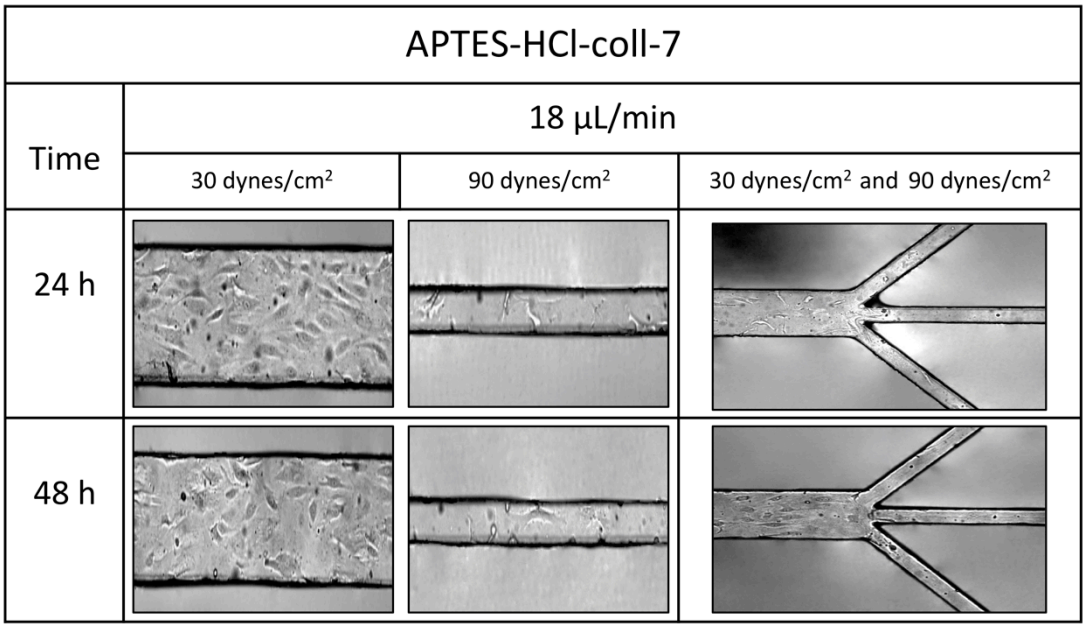

Figure 60: Cell attachment and growth inside APTES–HCl–coll–7 coated channel at 18µL/min flow rate.

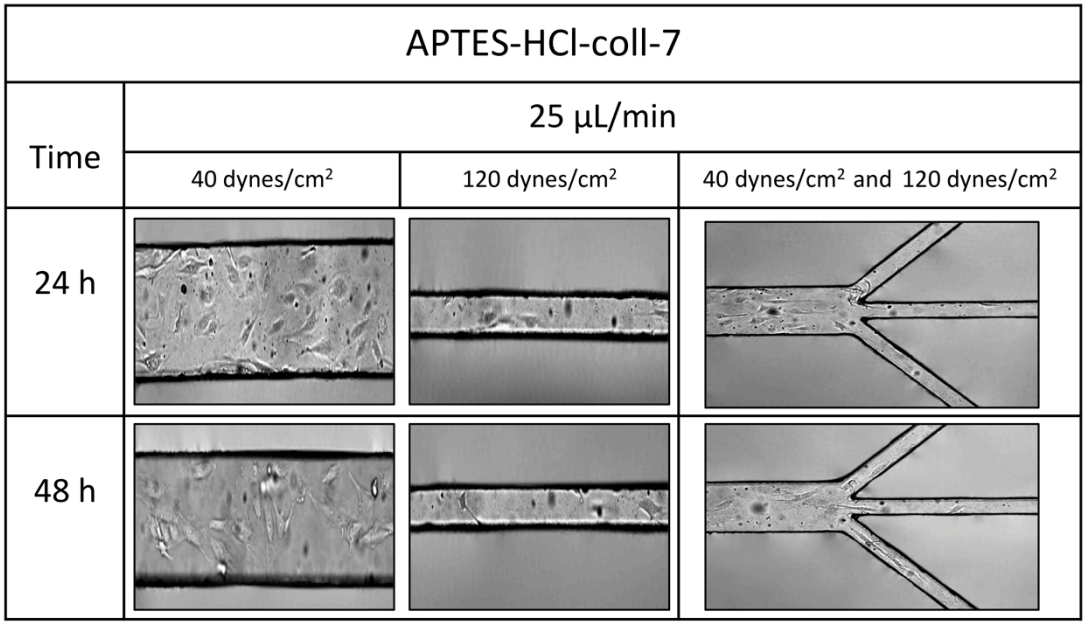

Figure 61: Cell growth inside APTES–HCl–coll–7 coated channel at 25µL/min flow rate where cells start detaching.

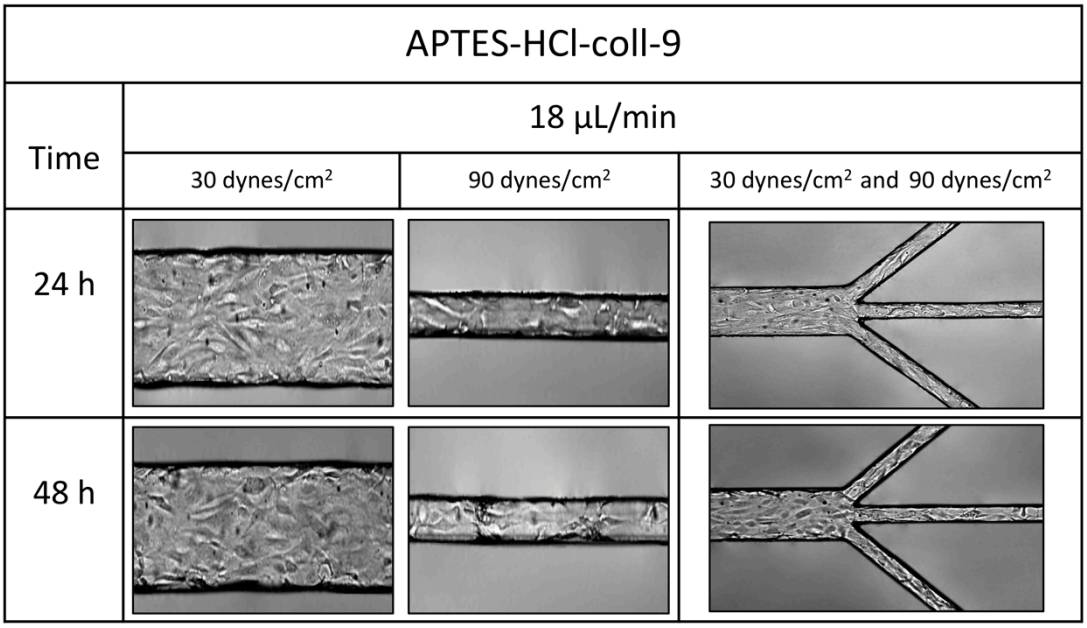

Figure 62: Cell attachment and growth inside APTES–HCl–coll–9 coated channel at 18µL/min flow rate.

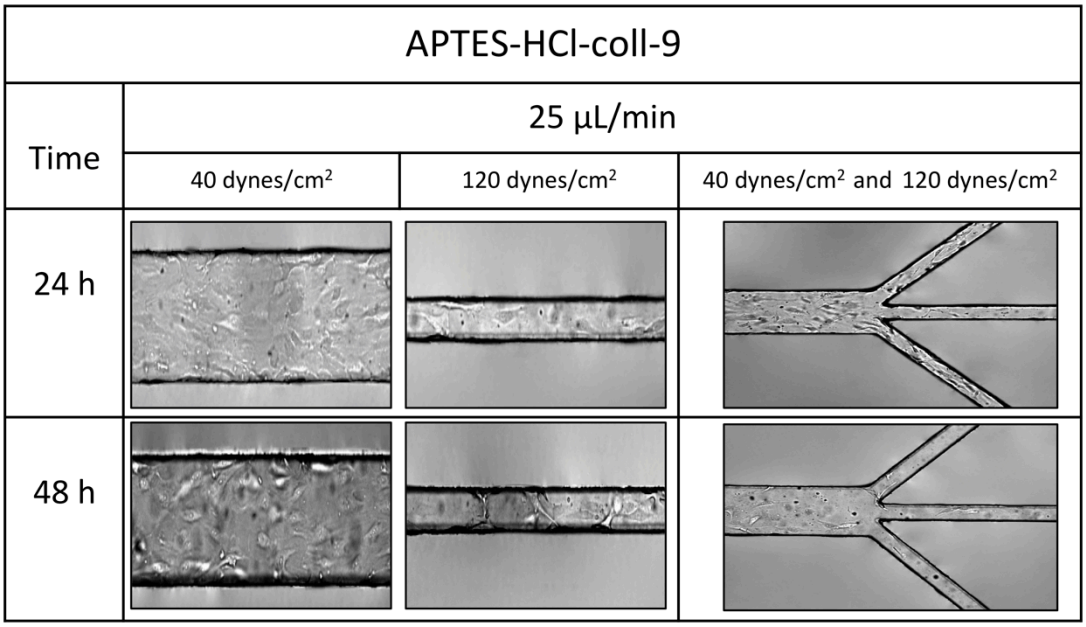

Figure 63: Cell growth inside APTES–HCl–coll–9 coated channel at 25µL/min flow rate where cells start detaching.

Chapter 4. Conclusion

Current work addresses one of the fundamental issues related to microfluidic cell culturing in order to mimic in vitro vascular models. PDMS-based microfluidic devices has become a universal setup for endothelial and other cell growth studies in 3 D microenvironment. And due to the hydrophobic nature of PDMS, it has become quit obvious to modify PDMS surface with ECM protein i.e., collagen and fibronectin to provide cells a natural habitat. Hence vasculature belongs to one of the most dynamic system of our body where internal cell lining is continuously exposed to a shear stress crated by blood flow. Therefore in vitro vascular models based on PDMS microfluidic devices are also aimed to work as a continues dynamic setup where cell growth and related factors can be studied under continues flow. But due to hydrophobic nature of PDMS, instability of ECM protein coatings inside microfluidic channels under flow condition limits the cell growth and proliferation for extended studies.
PDMS surfaces were pre treated with O_2 plasma, APTES, APTES-GA and protonated APTES to develop a strong bond with collagen. Coating efficiency was compared by AFM measurements and cell culturing at high flow rate inside microfluidic devices

Results are concluded as,

1. In the comparative study of various surface functionalization methods, efficacy of APTES–SAMs for stable protein grafting on PDMS surface has been demonstrated. AFM topography showed the presence of collagen inside APTES treated micro channels after subjecting to continues flow of liquid up to 40 dyne/cm^2. Collagen coating inside O_2 plasma treated channels was found to be stable up to the flow rate of 30 dyne/cm^2 while coatings inside APTES-GA treated and native PDMS channels exhibited less stability at high flow rate ($\geq$ 10 dyne/cm^2).

2. Moreover, the present study revealed the influence of pH on collagen fibril formation and stable polymerization on PDMS surfaces. It was observed that collagen polymerized at pH 5 represented more fibril like structure that indicated an incomplete or slow fibrillogenesis process. The rate of fibrillogensis increased by increasing pH of the solution and at pH 7 and 9, collagen exhibited long fiber like structure. Moreover the collagen prepared in PBS/$NaHCO_3$ buffer system at pH 9, exhibits a strong electrostatic interaction with APTES and protonated APTES treated surface that ultimately enhanced cell growth under high shear stress conditions (20-150 dynes/cm^2). Thus, the pH of the solution plays a vital role in the development of in vivo like protein architecture that ultimately provides the cells natural like substrate to grow.

3. Stability of APTES-mediated collagen coating in PDMS microfluidic devices attributed to the enhanced cell growth and proliferation. Evenly distributed collagen on PDMS surface led to an improved cell-substrate bond, which effectively supported the cell adhesion at high flow rate in microfluidic devices. This coating facilitated endothelial cell growth at high shear stress

(150 dynes/cm^2), in narrow channels with 66µm channel width, for 48 h. However the actual shear stress was much higher than applied shear stress as the growing cells inside the channels covers much of the area, which further reduces the channel volume. Therefore by using APTES linkage for protein it is possible to study endothelial growth and functions at or above physiological shear stress.

4. Differently developed coatings were evaluated for cell viability and biocompatibility. Interestingly some of the surfaces were not found to be biocompatible even these surfaces also contained collagen protein. For example, gluteraldehyde is conventionally used chemical to polymerize biomolecules, especially collagen, but GA mediated collagen coating did not support cell growth. Results exposed the cytotoxicity of APTES-GA modified surfaces for endothelial cells hence not considered as biocompatible. Moreover, the surfaces prepared with collagen at pH 5 were not supportive for cell adhesion and proliferation. Its means that as the fibrillogenesis of collagen is slow at pH 5 therefore at fibril state protein did not provide sufficient adhesion sites to the cells to attach and grow. Thus it is very important to polymerize protein on surface in its in vivo like structure and architecture for cell-substrate bond formation.

According to the findings it is demonstrated that the APTES linkage supported a homogeneous distribution and a long–term stability of the collagen fibers on the PDMS surfaces as well as inside the channels. By using this surface functionalization technique, it has become possible to study endothelial behavior at complete magnitude of physiological shear stress (0.7 dyne/cm^2 – 130 dyne/cm^2) in a continues microfluidic system. Establishment of thin layer coating for stable cell growth in narrow channels will be helpful to examine various vascular functions in natural like dimensions.

Moreover, the immobilization of single ECM protein (collagen) with its proper architecture on surface influenced the cell attachment and growth; therefore the synergistic effect of all building blocks of ECM on cell behavior cannot be ignored. The surface modification technique based on APTES can also be applied to other ECM proteins, enabling long term in vitro studies in PDMS micro-channels.

Microfluidic set ups, more related to physiological systems could be more beneficial to develop better organ-on-chip models and enhance our understanding about diseases and their related treatments.

References:

[1] WHO Cardiovascular diseases (CVDs). (https://www.who.int/news-room/fact-sheets/detail/cardiovascular-diseases-(cvds): World Health Organizarion)

[2] Paszkowiak J J and Dardik A 2003 Arterial Wall Shear Stress: Observations from the Bench to the Bedside *Vascular and Endovascular Surgery* 37 47-57

[3] Lee S J, Liu J, Oh S H, Soker S, Atala A and Yoo J J 2008 Development of a composite vascular scaffolding system that withstands physiological vascular conditions *Biomaterials* 29 2891-8

[4] Kim S, Kim W, Lim S and Jeon J S 2017 Vasculature-On-A-Chip for In Vitro Disease Models *Bioengineering (Basel)* 4

[5] Moake J L 2002 Thrombotic microangiopathies *N Engl J Med* 347 589-600

[6] Lipowsky H H 2005 Microvascular rheology and hemodynamics *Microcirculation* 12 5-15

[7] Haga J H, Li Y S and Chien S 2007 Molecular basis of the effects of mechanical stretch on vascular smooth muscle cells *J Biomech* 40 947-60

[8] Meer A v d 2009 Microfluidic Technology in Vascular Research. (Wöhrmann Print Service, Zuthpen, The Netherlands: University of Twente, Enschede, The Netherlands)

[9] Davis G E and Senger D R 2005 Endothelial extracellular matrix: biosynthesis, remodeling, and functions during vascular morphogenesis and neovessel stabilization *Circulation research* 97 1093-107

[10] Rizzo V, Morton C, DePaola N, Schnitzer J E and Davies4 P F 2003 Recruitment of endothelial caveolae into mechanotransduction pathways by flow conditioning in vitro *Am J Physiol Heart Circ Physiol* 285 H1720-H9

[11] RUGGERI Z M 2003 Von Willebrand factor, platelets and endothelial cell interactions *J. Thromb. Haemost.* 1 1335-42

[12] Tsai M, Kita A, Leach J, Rounsevell R, Huang J N, Moake J, Ware R E, Fletcher D A and Lam W A 2012 In vitro modeling of the microvascular occlusion and thrombosis that occur in hematologic diseases using microfluidic technology *J Clin Invest* 122 408-18

[13] Mannino R G, Qiu Y and Lam W A 2018 Endothelial cell culture in microfluidic devices for investigating microvascular processes *Biomicrofluidics* 12 042203

[14] Potter C M, Lundberg M H, Harrington L S, Warboys C M, Warner T D, Berson R E, Moshkov A V, Gorelik J, Weinberg P D and Mitchell J A 2011 Role of shear stress in endothelial cell morphology and expression of cyclooxygenase isoforms *Arterioscler Thromb Vasc Biol* 31 384-91

[15] Fuard D, Tzvetkova-Chevolleau T, Decossas S, Tracqui P and Schiavone P 2008 Optimization of poly-di-methyl-siloxane (PDMS) substrates for studying cellular adhesion and motility *Microelectronic Engineering* 85 1289-93

[16] Zhou J, Khodakov D A, Ellis A V and Voelcker N H 2012 Surface modification for PDMS-based microfluidic devices *Electrophoresis* 33 89-104

[17] Stone H A, Stroock A D and Ajdari A 2004 Engineering Flows in Small Devices *Annual Review of Fluid Mechanics* 36 381-411

[18] Halldorsson S, Lucumi E, Gomez-Sjoberg R and Fleming R M 2015 Advantages and challenges of microfluidic cell culture in polydimethylsiloxane devices *Biosens Bioelectron* 63 218-31
[19] Feynman R P 1960 There's Plenty of Room at the Bottom *Engineering and Science* 23 22-36
[20] Terry S C, Jerman J H and Angell J B 1979 A Gas ChromatographicAir Analyzer Fabricated on a Silicon Wafer *IEEE Transactions on Electron Devices* 26 1880-6
[21] Manz A, N.Graber and H.M.Widmer 1990 Miniaturized total chemical analysis systems- A novel concept for chemical sensing *Sensors and Actuators B: Chemical* 1 244-8
[22] Mark D, Haeberle S, Roth G, von Stetten F and Zengerle R 2010 Microfluidic lab-on-a-chip platforms: requirements, characteristics and applications *Chem Soc Rev* 39 1153-82
[23] Bayraktar T and Pidugu S B 2006 Characterization of liquid flows in microfluidic systems *International Journal of Heat and Mass Transfer* 49 815-24
[24] Chen K and Fan Z H 2016 *Circulating Tumor Cells: Isolation and Analysis,* ed Z H Fan: John Wiley & Sons, Inc)
[25] Stroock A D 2008 *Optical Biosensors: Today and tomorrow* ed F S Ligler and C R Taitt: Elsevier B.V.) p 712
[26] Bragheri F, Martinez Vazquez R and Osellame R 2016 Microfluidics 310-34
[27] Svendsen W E 2015 *Lab-on-a-Chip Devices and Micro-Total Analysis Systems.,* ed J Castillo-León and W E Svendsen: Springer, Cham) pp 17-26
[28] Ramadan Q, Jafarpoorchekab H, Huang C, Silacci P, Carrara S, Koklu G, Ghaye J, Ramsden J, Ruffert C, Vergeres G and Gijs M A 2013 NutriChip: nutrition analysis meets microfluidics *Lab on a chip* 13 196-203
[29] Long C, Finch C, Esch M, Anderson W, Shuler M and Hickman J 2012 Design optimization of liquid-phase flow patterns for microfabricated lung on a chip *Annals of biomedical engineering* 40 1255-67
[30] Zheng W, Jiang B, Wang D, Zhang W, Wang Z and Jiang X 2012 A microfluidic flow-stretch chip for investigating blood vessel biomechanics *Lab on a chip* 12 3441-50
[31] Koo Y, Hawkins B T and Yun Y 2018 Three-dimensional (3D) tetra-culture brain on chip platform for organophosphate toxicity screening *Sci Rep* 8 2841
[32] Huang G Y, Zhou L H, Zhang Q C, Chen Y M, Sun W, Xu F and Lu T J 2011 Microfluidic hydrogels for tissue engineering *Biofabrication* 3 012001
[33] Huang Y, Cai D and Chen P 2011 Micro- and nanotechnologies for study of cell secretion *Anal Chem* 83 4393-406
[34] Yin H and Marshall D 2012 Microfluidics for single cell analysis *Curr Opin Biotechnol* 23 110-9
[35] Skelley A M, Kirak O, Suh H, Jaenisch R and Voldman J 2009 Microfluidic control of cell pairing and fusion *Nat Methods* 6 147-52
[36] Faley S L, Copland M, Wlodkowic D, Kolch W, Seale K T, Wikswo J P and Cooper J M 2009 Microfluidic single cell arrays to interrogate signalling dynamics of individual, patient-derived hematopoietic stem cells *Lab on a chip* 9 2659-64
[37] Kalisky T and Quake S R 2011 Single-cell genomics *Nature Methods* 8 311-4

[38] Toriello N M, Douglas E S, Thaitrong N, Hsiao S C, Francis M B, Bertozzi C R and Mathies R A 2008 Integrated microfluidic bioprocessor for single-cell gene expression analysis *Proc Natl Acad Sci U S A* 105 20173-8
[39] Marcy Y, Ouverney C, Bik E M, Losekann T, Ivanova N, Martin H G, Szeto E, Platt D, Hugenholtz P, Relman D A and Quake S R 2007 Dissecting biological "dark matter" with single-cell genetic analysis of rare and uncultivated TM7 microbes from the human mouth *Proc Natl Acad Sci U S A* 104 11889-94
[40] Liu Q, Wu C, Cai H, Hu N, Zhou J and Wang P 2014 Cell-based biosensors and their application in biomedicine *Chem Rev* 114 6423-61
[41] Yeo L Y, Chang H C, Chan P P and Friend J R 2011 Microfluidic devices for bioapplications *Small* 7 12-48
[42] Chen Q, Wu J, Zhang Y and Lin J M 2012 Qualitative and quantitative analysis of tumor cell metabolism via stable isotope labeling assisted microfluidic chip electrospray ionization mass spectrometry *Anal Chem* 84 1695-701
[43] Gao D, Li H, Wang N and Lin J M 2012 Evaluation of the absorption of methotrexate on cells and its cytotoxicity assay by using an integrated microfluidic device coupled to a mass spectrometer *Anal Chem* 84 9230-7
[44] Regnault C, Dheeman D and Hochstetter A 2018 Microfluidic Devices for Drug Assays *High-Throughput* 7 18
[45] Thorsen T A 2004 Microfluidic Tools for High-Throughput Screening *BioTechniques* 36 197-9
[46] Guo M T, Rotem A, Heyman J A and Weitz D A 2012 Droplet microfluidics for high-throughput biological assays *Lab on a chip* 12 2146-55
[47] Andries D. van der Meer, Kim Vermeul, Andre´ A. Poot, Jan Feijen and Vermes I n 2010 A microfluidic wound-healing assay for quantifying endothelial cell migration *American Journal of Physiology- Heart and Circulatory Physiology* 298 H719-H25
[48] Gray K M and Stroka K M 2017 Vascular endothelial cell mechanosensing: New insights gained from biomimetic microfluidic models *Semin Cell Dev Biol* 71 106-17
[49] Jain R K 2003 Molecular regulation of vessel maturation *Nat Med.* 9 685-93
[50] Chang W G and Niklason L E 2017 A short discourse on vascular tissue engineering *NPJ Regen Med* 2
[51] Kang D, Kim J H, Jeong Y H, Kwak J Y, Yoon S and Jin S 2016 Endothelial monolayers on collagen-coated nanofibrous membranes: cell-cell and cell-ECM interactions *Biofabrication* 8 025008
[52] Wang L, Zhang Z L, Wdzieczak-Bakala J, Pang D W, Liu J and Chen Y 2011 Patterning cells and shear flow conditions: convenient observation of endothelial cell remoulding, enhanced production of angiogenesis factors and drug response *Lab on a chip* 11 4235-40
[53] Wautier J-L and Wautie M-P 2013 Molecular basis of erythrocyte adhesion to endothelial cells in diseases *Clinical Hemorheology and Microcirculation* 53 11-21
[54] Merkel K H H, Ginsberg P L, Parker J C J and Post M J D 1978 Cerebrovascular Disease in Sickle Cell Anemia- A Clinical, Pathological and Radiological Correlation *Stroke* 9 45-52

[55] Munzel T, Sinning C, Post F, Warnholtz A and Schulz E 2008 Pathophysiology, diagnosis and prognostic implications of endothelial dysfunction *Ann Med* 40 180-96
[56] Capulli A K, Tian K, Mehandru N, Bukhta A, Choudhury S F, Suchyta M and Parker K K 2014 Approaching the in vitro clinical trial: engineering organs on chips *Lab on a chip* 14 3181-6
[57] Esch E W, Bahinski A and Huh D 2015 Organs-on-chips at the frontiers of drug discovery *Nat Rev Drug Discov* 14 248-60
[58] Suresh S 2011 Mechanical response of human red blood cells in health and disease: Some structure-property-function relationships *Journal of materials research* 21 1871-7
[59] Miller J S, Stevens K R, Yang M T, Baker B M, Nguyen D H, Cohen D M, Toro E, Chen A A, Galie P A, Yu X, Chaturvedi R, Bhatia S N and Chen C S 2012 Rapid casting of patterned vascular networks for perfusable engineered three-dimensional tissues *Nat Mater* 11 768-74
[60] Bogorad M I, DeStefano J, Karlsson J, Wong A D, Gerecht S and Searson P C 2015 Review: in vitro microvessel models *Lab on a chip* 15 4242-55
[61] Huh D, Leslie D C, Matthews B D, Fraser J P, Jurek S, Hamilton G A, Thorneloe K S, McAlexander M A and Ingber D E 2012 A human disease model of drug toxicity-induced pulmonary edema in a lung-on-a-chip microdevice *Sci Transl Med* 4 159ra47
[62] Gale B, Jafek A, Lambert C, Goenner B, Moghimifam H, Nze U and Kamarapu S 2018 A Review of Current Methods in Microfluidic Device Fabrication and Future Commercialization Prospects *Inventions* 3 60
[63] Quake S R and Scherer A 2000 From Micro- to Nanofabrication with Soft Materials *Science* 290 1536-40
[64] Iliescu C, Taylor H, Avram M, Miao J and Franssila S 2012 A practical guide for the fabrication of microfluidic devices using glass and silicon *Biomicrofluidics* 6 16505-1650516
[65] McDonald J C, Duffy D C, Anderson J R, Chiu D T, Wu H, Schueller O J A and Whitesides G M 2000 Fabrication of microfluidic systems in poly(dimethylsiloxane) *Electrophoresis* 21 27-40
[66] Chiu J J and Chien S 2011 Effects of disturbed flow on vascular endothelium: pathophysiological basis and clinical perspectives *Physiol Rev* 91 327-87
[67] Alexander Muck J, Wang J, Jacobs M, Chen G, Chatrathi M P, Jurka V,´ Z V b, Scott D. Spillman, Gautham Sridharan and Scho1ning M J 2004 Fabrication of Poly(methyl methacrylate) Microfluidic Chips by Atmospheric Molding *Anal. Chem.* 76 2290-7
[68] Tsao C W 2016 Polymer Microfluidics: Simple, Low-Cost Fabrication Process Bridging Academic Lab Research to Commercialized Production *Micromachines (Basel)* 7
[69] Shadpour H, Musyimi H, Chen J and Soper S A 2006 Physiochemical properties of various polymer substrates and their effects on microchip electrophoresis performance *J Chromatogr A* 1111 238-51
[70] Vladkova T G 2013 *Surface Engineering of Polymeric biomaterials* (United Kingdom Smithers Rapra Technology Ltd)
[71] Taylor R J, Falconnet D, Niemisto A, Ramsey S A, Prinz S, Shmulevich I, Galitski T and Hansen C L 2009 Dynamic analysis of MAPK signaling using a high-throughput microfluidic single-cell imaging platform *Proc Natl Acad Sci U S A* 106 3758-63

[72] Lee J N, Jiang X, Ryan D and Whitesides G M 2004 Compatibility of mammalian cells on surfaces of poly(dimethylsiloxane) *Langmuir : the ACS journal of surfaces and colloids* 20 11684-91
[73] Lecault V, Vaninsberghe M, Sekulovic S, Knapp D J, Wohrer S, Bowden W, Viel F, McLaughlin T, Jarandehei A, Miller M, Falconnet D, White A K, Kent D G, Copley M R, Taghipour F, Eaves C J, Humphries R K, Piret J M and Hansen C L 2011 High-throughput analysis of single hematopoietic stem cell proliferation in microfluidic cell culture arrays *Nat Methods* 8 581-6
[74] Tay S, Hughey J J, Lee T K, Lipniacki T, Quake S R and Covert M W 2010 Single-cell NF-kappaB dynamics reveal digital activation and analogue information processing *Nature* 466 267-71
[75] Taniguchi Y, Choi P J, Li G W, Chen H, Babu M, Hearn J, Emili A and Xie X S 2010 Quantifying E. coli proteome and transcriptome with single-molecule sensitivity in single cells *Science* 329 533-8
[76] Wang Z, Volinsky A A and Gallant N D 2014 Crosslinking effect on polydimethylsiloxane elastic modulus measured by custom-built compression instrument *Journal of Applied Polymer Science* 131 n/a-n/a
[77] Neves N M, Palchesko R N, Zhang L, Sun Y and Feinberg A W 2012 Development of Polydimethylsiloxane Substrates with Tunable Elastic Modulus to Study Cell Mechanobiology in Muscle and Nerve *PloS one* 7 e51499
[78] Mata A, Fleischman A J and Roy S 2005 Characterization of polydimethylsiloxane (PDMS) properties for biomedical micro/nanosystems *Biomedical microdevices* 7 281-93
[79] Wells R G 2008 The role of matrix stiffness in regulating cell behavior *Hepatology* 47 1394-400
[80] Engler A J, Sen S, Sweeney H L and Discher D E 2006 Matrix elasticity directs stem cell lineage specification *Cell* 126 677-89
[81] Park J S, Chu J S, Tsou A D, Diop R, Tang Z, Wang A and Li S 2011 The effect of matrix stiffness on the differentiation of mesenchymal stem cells in response to TGF-beta *Biomaterials* 32 3921-30
[82] Wen J H, Vincent L G, Fuhrmann A, Choi Y S, Hribar K C, Taylor-Weiner H, Chen S and Engler A J 2014 Interplay of matrix stiffness and protein tethering in stem cell differentiation *Nat Mater* 13 979-87
[83] Nge P N, Rogers C I and Woolley A T 2013 Advances in microfluidic materials, functions, integration, and applications *Chem Rev* 113 2550-83
[84] Watson J M and Baron M G 1996 The behaviour of water in poly(dimethylsiloxane) *Journal of Membrane Science* 110 47-57
[85] Heo Y S, Cabrera L M, Song J W, Futai N, Tung Y C, Smith G D and Takayama S 2007 Characterization and resolution of evaporation-mediated osmolality shifts that constrain microfluidic cell culture in poly(dimethylsiloxane) devices *Anal Chem* 79 1126-34
[86] Tanyeri M and Tay S 2018 Viable cell culture in PDMS-based microfluidic devices *Methods Cell Biol* 148 3-33
[87] Wei Y, Xu Z, Cachia M A, Nguyen J, Zheng Y, Wang C and Sun Y 2016 Embedded silver PDMS electrodes for single cell electrical impedance spectroscopy *Journal of Micromechanics and Microengineering* 26 095006
[88] Curtis A S, Forrester J V, McInnes C and Lawrie F 1983 Adhesion of cells to polystyrene surfaces *J Cell Biol* 97 1500-6

[89] Barker S L and LaRocca P J 1994 Method of production and control of a commercial tissue culture surface. *Journal of tissue culture methods* 16 151-3
[90] Zhang H and Chiao M 2015 Anti-fouling Coatings of Poly(dimethylsiloxane) Devices for Biological and Biomedical Applications *J Med Biol Eng* 35 143-55
[91] Khalili A A and Ahmad M R 2015 A Review of Cell Adhesion Studies for Biomedical and Biological Applications *Int J Mol Sci* 16 18149-84
[92] Vladkova T G 2010 Surface Engineered Polymeric Biomaterials with Improved Biocontact Properties *International Journal of Polymer Science* 2010 1-22
[93] Katzenberg F 2005 Plasma-bonding of poly(dimethylsiloxane) to glass *e-Polymers* 5 059
[94] Eddings M A, Johnson M A and Gale B K 2008 Determining the optimal PDMS–PDMS bonding technique for microfluidic devices *Journal of Micromechanics and Microengineering* 18 067001
[95] Yang C, Wang W and Li Z 2009 Optimization of Corona-triggered PDMS-PDMS Bonding Method. In: *4th IEEE International Conference on Nano/Micro Engineered and Molecular Systems,* (Shenzhen, China pp 319-22
[96] Makamba H, Kim J H, Lim K, Park N and Hahn J H 2003 Surface modification of poly(dimethylsiloxane) microchannels *Electrophoresis* 24 3607-19
[97] Duffy D C, McDonald J C, Schueller O J A and Whitesides G M 1998 Rapid Prototyping of Microfluidic Systems in Poly(dimethylsiloxane) *Anal. Chem.* 70
[98] Vickers J A, Caulum M M and Henry* C S 2006 Generation of Hydrophilic Poly(dimethylsiloxane) for High-Performance Microchip Electrophoresis *Anal. Chem.* 78 7446-52
[99] Hillborg H and Gedde U W 1998 Hydrophobicity recovery of polydimethylsiloxane after exposure to corona discharges *Polymer* 39 1991-8
[100] Kim J, Chaudhury M K and Owen M J 2000 Hydrophobicity recovery of polydimethylsiloxane after exposure to corona discharges *Journal of Colloid and Interface Science* 226 231-6
[101] Efimenko K, Wallace W E and Genzer J 2002 Surface Modification of Sylgard-184 Poly(dimethyl siloxane) Networks by Ultraviolet and Ultraviolet/Ozone Treatment *Journal of Colloid and Interface Science* 254 306-15
[102] Hillborg H, Tomczak N, Ola`h A,¨inherr H S and Vancso G J 2004 Nanoscale Hydrophobic Recovery- A Chemical Force Microscopy Study of UV:Ozone-Treated Cross-Linked Poly(dimethylsiloxane) *Langmuir : the ACS journal of surfaces and colloids* 20 785-94
[103] Berdichevsky Y, Khandurina J, Guttman A and Lo Y H 2004 UV/ozone modification of poly(dimethylsiloxane) microfluidic channels *Sensors and Actuators B: Chemical* 97 402-8
[104] Fritz J and Owen M 1995 Hydrophobic Recovery of Plasma- Treated Polydimethylsiloxane *Journal of Adhesion* 54 33-45
[105] Bodas D and Khan-Malek C 2007 Hydrophilization and hydrophobic recovery of PDMS by oxygen plasma and chemical treatment—An SEM investigation *Sensors and Actuators B: Chemical* 123 368-73

[106] Eddington D T, Puccinelli J P and Beebe D J 2006 Thermal aging and reduced hydrophobic recovery of polydimethylsiloxane *Sensors and Actuators B: Chemical* 114 170-2
[107] Tan S H, Nguyen N T, Chua Y C and Kang T G 2010 Oxygen plasma treatment for reducing hydrophobicity of a sealed polydimethylsiloxane microchannel *Biomicrofluidics* 4 32204
[108] Larson B J, Gillmor S D, Braun J M, Cruz-Barba L E, Savage D E, Denes F S and Lagally M G 2013 Long-term reduction in poly(dimethylsiloxane) surface hydrophobicity via cold-plasma treatments *Langmuir : the ACS journal of surfaces and colloids* 29 12990-6
[109] Zhao L H, Lee J and Sen P N 2012 Long-term retention of hydrophilic behavior of plasma treated polydimethylsiloxane (PDMS) surfaces stored under water and Luria-Bertani broth *Sensors and Actuators A: Physical* 181 33-42
[110] Lee D and Yang S 2012 Surface modification of PDMS by atmospheric-pressure plasma-enhanced chemical vapor deposition and analysis of long-lasting surface hydrophilicity *Sensors and Actuators B: Chemical* 162 425-34
[111] Doherty E A S, Meagher R J, Albarghouthi M N and Barron A E 2003 Microchannel wall coatings for protein separations by capillary and chip electrophoresis *Electrophoresis* 24 34-54
[112] Boxshall K, Wu M-H, Cui Z, Cui Z, Watts J F and Baker M A 2006 Simple surface treatments to modify protein adsorption and cell attachment properties within a poly(dimethylsiloxane) micro-bioreactor *Surface and Interface Analysis* 38 198-201
[113] Huang B, Wu H, Kim S and Zare R N 2005 Coating of poly(dimethylsiloxane) with n-dodecyl-beta-D-maltoside to minimize nonspecific protein adsorption *Lab on a chip* 5 1005-7
[114] Madadi H and Casals-Terré J 2012 Study the Effects of Different Surfactants on Hydrophilicity of Polydimethylsiloxane (PDMS) 233
[115] Tessmar J K and Gopferich A M 2007 Customized PEG-derived copolymers for tissue-engineering applications *Macromol Biosci* 7 23-39
[116] Nnebe I M, Tilton R D and Schneider J W 2004 Direct force measurement of the stability of poly(ethylene glycol)-polyethylenimine graft films *J Colloid Interface Sci* 276 306-16
[117] Blättler T M, Pasche S p, Textor M and Griesser H J 2006 High Salt Stability and Protein Resistance of Poly(L-lysine)-g-poly(ethylene glycol) Copolymers Covalently Immobilized via Aldehyde Plasma Polymer Interlayers on Inorganic and Polymeric Substrates. *Langmuir : the ACS journal of surfaces and colloids* 2 5760-9
[118] Gorochovceva N, Naderi A, Dedinaite A and Makuška R 2005 Chitosan–N-poly(ethylene glycol) brush copolymers: Synthesis and adsorption on silica surface *European Polymer Journal* 41 2653-62
[119] Huang N-P, Michel R, Voros J, Textor M, Hofer R, Rossi A, Elbert D L, Hubbell e A and Spencer N D 2001 Poly(L-lysine)-g-poly(ethylene glycol) Layers on Metal Oxide Surfaces- Surface-Analytical Characterization and Resistance to Serum and Fibrinogen Adsorption *Langmuir : the ACS journal of surfaces and colloids* 17 489-98
[120] Lee S and¨s J V r 2005 An Aqueous-Based Surface Modification of Poly(dimethylsiloxane) with Poly(ethylene glycol) to Prevent Biofouling. *Langmuir : the ACS journal of surfaces and colloids* 21 11957-62

[121] Egea A M, Trévisiol E and Vieu C 2013 Direct patterning of probe proteins on an antifouling PLL-g-dextran coating for reducing the background signal of fluorescent immunoassays *Biointerphases* 8
[122] Decher G 1997 Fuzzy Nanoassemblies- Toward Layered Polymeric Multicomposites 277 1232-7
[123] Wang A J, Xu J J and Chen H Y 2006 Proteins modification of poly(dimethylsiloxane) microfluidic channels for the enhanced microchip electrophoresis *J Chromatogr A* 1107 257-64
[124] Sivagnanam V, Song B, Vandevyver C and Gijs M A M 2009 On-Chip Immunoassay Using Electrostatic Assembly of Streptavidin-Coated Bead Micropatterns *Anal. Chem.* 81 6509-15
[125] Nakanishi K, Sakiyama T, Kumada Y, Imamura K and Imanaka H 2008 Recent Advances in Controlled Immobilization of Proteins onto the Surface of the Solid Substrate and Its Possible Application to Proteomics *Current Proteomics* 5 161-75
[126] Wong I and Ho C M 2009 Surface molecular property modifications for poly(dimethylsiloxane) (PDMS) based microfluidic devices *Microfluid Nanofluid* 7 291-306
[127] Sui G, Wang J, Lee C-C, Lu W, Lee S P, Leyton J V, Wu A M and Tseng H-R 2006 Solution-Phase Surface Modification in Intact Poly(dimethylsiloxane) Microfluidic Channels *Anal Chem* 78
[128] Schreiber F 2000 Structure and growth of self-assembling monolayers *Progress in Surface Science* 67 151-256
[129] Zhang Z, Feng X, Xu F, Liu X and Liu B F 2010 "Click" chemistry-based surface modification of poly(dimethylsiloxane) for protein separation in a microfluidic chip *Electrophoresis* 31 3129-36
[130] Chuah Y J, Kuddannaya S, Lee M H, Zhang Y and Kang Y 2015 The effects of poly(dimethylsiloxane) surface silanization on the mesenchymal stem cell fate *Biomater Sci* 3 383-90
[131] Pallandre A, de Lambert B, Attia R, Jonas A M and Viovy J L 2006 Surface treatment and characterization: perspectives to electrophoresis and lab-on-chips *Electrophoresis* 27 584-610
[132] Schlapak R, Pammer P, Armitage D, Zhu R, Hinterdorfer P, Vaupel M, ̈hwirth T F and Howorka S 2006 Glass Surfaces Grafted with High-Density Poly(ethylene glycol) as Substrates for DNA Oligonucleotide Microarrays *Langmuir : the ACS journal of surfaces and colloids* 2 277-85
[133] Wu D, Qin J and Lin B 2007 Self-assembled epoxy-modified polymer coating on a poly(dimethylsiloxane) microchip for EOF inhibition and biopolymers separation *Lab on a chip* 7 1490
[134] Gilges M, Kleemiss M H and Schomburg G 1994 Capillary Zone Electrophoresis Separations of Basic and Acidic Proteins Using Poly(vinyl alcohol) Coatings in Fused Silica Capillaries *Anal Chem* 66 2038-46
[135] Li M and Kim D P 2011 Silicate glass coated microchannels through a phase conversion process for glass-like electrokinetic performance *Lab on a chip* 11 1126-31
[136] Hu S, Ren X, Bachman M, Sims C E, Li G P and Allbritton N 2002 Surface Modification of Poly(dimethylsiloxane) Microfluidic Devices by Ultraviolet Polymer Grafting *Anal Chem* 74 4117-23

[137] Hu S, Ren X, Bachman M, Sims C E, Li G P and Allbritton N L 2004 Surface-Directed, Graft Polymerization within Microfluidic Channels *Anal Chem* 76 1867-70
[138] He Q, Liu Z, Xiao P, Liang R, He N and Lu Z 2003 Preparation of Hydrophilic Poly(dimethylsiloxane) Stamps by Plasma-Induced Grafting *Langmuir : the ACS journal of surfaces and colloids* 19 6982-6
[139] Pruden K G and Beaudoin S P 2005 Downstream microwave ammonia plasma treatment of polydimethylsiloxane *Journal of Vacuum Science & Technology A: Vacuum, Surfaces, and Films* 23 208-14
[140] Husseman M, Malmström E E, McNamara M, Mate M, Mecerreyes D, Benoit D G, Hedrick J L, Mansky P, Huang E, Russell T P and Hawker C J 1999 Controlled Synthesis of Polymer Brushes by "Living" Free Radical Polymerization Techniques *Macromolecules* 32 1424-31
[141] Lou X, He P, Okelo G O and He L 2006 Radical polymerization in biosensing *Anal Bioanal Chem* 386 525-31
[142] Xiao D, Le T V and Wirth M J 2004 Surface Modification of the Channels of Poly(dimethylsiloxane) Microfluidic Chips with Polyacrylamide for Fast Electrophoretic Separations of Proteins *Anal Chem* 76 2055-61
[143] Henares T G, Mizutani F and Hisamoto H 2008 Current development in microfluidic immunosensing chip *Anal Chim Acta* 611 17-30
[144] Kim D and Herr A E 2013 Protein immobilization techniques for microfluidic assays *Biomicrofluidics* 7 41501
[145] Israelachvili J N 2011 *Intermolecular and Surface Forces* (USA: Elsevier Inc.)
[146] Rusmini F, Zhong Z and Feijen J 2007 Protein Immobilization Strategies for Protein Biochips *Biomacromolecules* 8 1775-89
[147] Xiang Q, Hu G, Gao Y and Li D 2006 Miniaturized immunoassay microfluidic system with electrokinetic control *Biosens Bioelectron* 21 2006-9
[148] Qin M, Wang L-K and Feng X-Z 2007 Bioactive Surface Modification of Mica and Poly(dimethylsiloxane) with Hydrophobins for Protein Immobilization *Langmuir : the ACS journal of surfaces and colloids* 23 4465-71
[149] Wang R, Yang Y-L, Qin M, Wang L-K, Yu L, Shao B, Qiao M-Q, Wang C and Feng X-Z 2007 Biocompatible Hydrophilic Modifications of Poly(dimethylsiloxane) Using Self-Assembled Hydrophobins *Chem. Mater* 19 3227-31
[150] Spurlin T A, Forry S P, Cooksey G A and Plant A L 2010 Characterization of collagen fibrils films formed on polydimethylsiloxane surfaces for microfluidic applications *Langmuir : the ACS journal of surfaces and colloids* 26 14111-7
[151] Razafiarison T, Silvan U, Meier D and Snedeker J G 2016 Surface-Driven Collagen Self-Assembly Affects Early Osteogenic Stem Cell Signaling *Adv Healthc Mater* 5 1481-92
[152] Zhou H-X 2001 Disparate Ionic-Strength Dependencies of On and Off Rates in Protein–Protein Association *Biopolymers* 59 427-33
[153] Yim E K F, Reano R M, Pang S W, Yee A F, Chen C S and Leong K W 2005 Nanopattern-induced changes in morphology and motility of smooth muscle cells *Biomaterials* 26 5405-13
[154] Chung S H and Min J 2009 Morphological investigations of cells that adhered to the irregular patterned polydimethylsiloxane (PDMS) surface without reagents *Ultramicroscopy* 109 861-7

[155] Zhang W, Choi D S, Nguyen Y H, Chang J and Qin L 2013 Studying cancer stem cell dynamics on PDMS surfaces for microfluidics device design *Sci Rep* 3 2332
[156] Toworfe G K, Composto R J, Adams C S, Shapiro I M and Ducheyne P 2004 Fibronectin adsorption on surface-activated poly(dimethylsiloxane) and its effect on cellular function *Journal of Biomedical Materials Research* 71A 449-61
[157] Juárez-Moreno J A, Ávila-Ortega A, Oliva A I, Avilés F and Cauich-Rodríguez J V 2015 Effect of wettability and surface roughness on the adhesion properties of collagen on PDMS films treated by capacitively coupled oxygen plasma *Applied Surface Science* 349 763-73
[158] Juárez-Moreno J A, Brito-Argáez L G, Ávila-Ortega A, Oliva A I, Avilés F and Cauich-Rodríguez J V 2017 Effect of the type of plasma on the polydimethylsiloxane/collagen composites adhesive properties *International Journal of Adhesion and Adhesives* 77 85-95
[159] Waters L J, Finch C V, Bhuiyan A, Hemming K and Mitchell J C 2017 Effect of plasma surface treatment of poly(dimethylsiloxane) on the permeation of pharmaceutical compounds *J Pharm Anal* 7 338-42
[160] Krenkova J and Foret F 2004 Immobilized microfluidic enzymatic reactors *Electrophoresis* 25 3550-63
[161] Yakovleva J, Davidsson R, Bengtsson M, Laurell T and Emnéus J 2003 Microfluidic enzyme immunosensors with immobilised protein A and G using chemiluminescence detection *Biosensors and Bioelectronics* 19 21-34
[162] Smith C L, Milea J S and Nguyen G H 2005 *Immobilisation of DNA on Chips II,* ed C Wittmann (Germany: Springer-Verlag Berlin Heidelberg) pp 63-90
[163] Seong G H and Crooks R M 2002 Efficient Mixing and Reactions within Microfluidic Channels Using Microbead-Supported Catalysts *J. Am. Chem. Soc.* 124 13360-1
[164] Ramsay G 1998 DNA chip: State of the art *Nat Biotechnol* 16 40-4
[165] Schroeder H, Adler M, Gerigk K, Müller-Chorus B, Götz F and Niemeyer C M 2009 User Configurable Microfluidic Device for Multiplexed Immunoassays Based on DNA-Directed Assembly *Anal Chem* 81 1275-9
[166] Laib S and MacCraith B D 2007 Immobilization of Biomolecules on Cycloolefin Polymer Supports *Anal Chem* 79 6264-70
[167] Wacker R and Niemeyer C M 2004 DDI-microFIA--A readily configurable microarray-fluorescence immunoassay based on DNA-directed immobilization of proteins *Chembiochem* 5 453-9
[168] Shin K S, Lee S W, Han K C, Kim S K, Yang E K, Park J H, Ju B K, Kang J Y and Kim T S 2007 Amplification of fluorescence with packed beads to enhance the sensitivity of miniaturized detection in microfluidic chip *Biosens Bioelectron* 22 2261-7
[169] Larsson A, Karlsson-Parra A and SjOqulst J 1991 Use of Chicken Antibodies in Enzyme Immunoassays to Avoid Interference by Rheumatoid Factors *Clin. Chem.* 37 411-4
[170] Hermanson G T 2008 *Bioconjugate Techniques* (San Diego: Academic Press)
[171] Yu L, Li C M, Zhou Q and Luong J H T 2007 Poly(vinyl alcohol) Functionalized Poly(dimethylsiloxane) Solid Surface for Immunoassay *Bioconjugate Chemistry* 18
[172] Kuddannaya S, Chuah Y J, Lee M H, Menon N V, Kang Y and Zhang Y 2013 Surface chemical modification of poly(dimethylsiloxane) for the enhanced

adhesion and proliferation of mesenchymal stem cells *ACS Appl Mater Interfaces* 5 9777-84
[173] Glass N R, Tjeung R, Chan P, Yeo L Y and Friend J R 2011 Organosilane deposition for microfluidic applications *Biomicrofluidics* 5 36501-365017
[174] Park J J, Luo X, Yi H, Valentine T M, Payne G F, Bentley W E, Ghodssi R and Rubloff G W 2006 Chitosan-mediated in situ biomolecule assembly in completely packaged microfluidic devices *Lab on a chip* 6 1315-21
[175] Delamarche E, Bernard A, Schmid H, Michel B and Biebuyck H 1997 Patterned Delivery of lmmunogFabulins to Surfaces Using Microfluidic Networks *Science* 276 779-81
[176] Thierry B, Kurkuri M, Shi J Y, Lwin L E and Palms D 2010 Herceptin functionalized microfluidic polydimethylsiloxane devices for the capture of human epidermal growth factor receptor 2 positive circulating breast cancer cells *Biomicrofluidics* 4 32205
[177] Keranov I, Vladkova T, Minchev M, Kostadinova A and Altankov G 2008 Preparation, characterization, and cellular interactions of collagen-immobilized PDMS surfaces *Journal of Applied Polymer Science* 110 321-30
[178] Hou S, Yang K, Qin M, Feng X Z, Guan L, Yang Y and Wang C 2008 Patterning of cells on functionalized poly(dimethylsiloxane) surface prepared by hydrophobin and collagen modification *Biosens Bioelectron* 24 918-22
[179] Du Y, Cropek D, R M, Mofrad K, Weinberg E J, Khademhosseini A and Borenstein J 2008 *Microfluidics for Biological Applications,* ed W-C Tian and E Finehout: Springer US)
[180] Lyu Z, Yu Q and Chen H 2016 *Polymeric Biomaterials for Tissue Regeneration,* ed C Gao: Springer, Singapore) pp 103-21
[181] Adams J C and Watt F M 1993 Regulation of development and differentiation by the extracellular matrix *Development* 117 1183-98
[182] Kleinman H K, Luckenbill-Edds L, Cannon F W and Sephel G C 1987 Use of extracellular matrix components for cell culture *Analytical biochemistry* 166 1-13
[183] Jarvelainen H, Sainio A, Koulu M, Wight T N and Penttinen R 2009 Extracellular matrix molecules: potential targets in pharmacotherapy *Pharmacol Rev* 61 198-223
[184] Frantz C, Stewart K M and Weaver V M 2010 The extracellular matrix at a glance *J Cell Sci* 123 4195-200
[185] Hynes R O 2002 Integrins Bidirectional, Allosteric Signaling Machines *Cell* 110 673-87
[186] Ambrose E J 1961 The movements of fibrocytes *Experimental Cell Research* 8 54-73
[187] Curtis A S G 1964 The mechanism of adhesion of cells to glass. A study by Interference Reflection Microscopy *J Cell Biol* 20 199-215
[188] Bershadsky A D, Tint I S, Neyfakh A A and Vasiliev J M 1985 Focal contacts of normal and RSV-transformed quail cells *Experimental Cell Research* 158 433-44
[189] Owen G R, Meredith D, I a G and Richards R 2005 FOCAL ADHESION QUANTIFICATION – A NEW ASSAY OF MATERIAL BIOCOMPATIBILITY? : REVIEW *European Cells and Materials* 9
[190] Keselowsky B G, Collard D M and Garcia A J 2004 Surface chemistry modulates focal adhesion composition and signaling through changes in integrin binding *Biomaterials* 25 5947-54

[191] Miron R J, Bosshardt D D, Hedbom E, Zhang Y, Haenni B, Buser D and Sculean A 2012 Adsorption of enamel matrix proteins to a bovine-derived bone grafting material and its regulation of cell adhesion, proliferation, and differentiation *J Periodontol* 83 936-47
[192] Deng J, Sun M, Wang S, Han L, Mao Z, Li D, Chen H and Gao C 2015 Adsorption of fibronectin on salt-etched polyelectrolyte multilayers and its roles in mediating the adhesion and migration of vascular smooth muscle cells *Macromol Biosci* 15 241-52
[193] Sun M, Deng J, Tang Z, Wu J, Li D, Chen H and Gao C 2014 A correlation study of protein adsorption and cell behaviors on substrates with different densities of PEG chains *Colloids Surf B Biointerfaces* 122 134-42
[194] Keselowsky B G, Collard D M and´a A s J G 2002 Surface chemistry modulates fibronectin conformation and directs integrin binding and specificity to control cell adhesion *J Biomed Mater Res* 66 247-59
[195] Rozario T and DeSimone D W 2010 The extracellular matrix in development and morphogenesis: A dynamic view *Developmental Biology* 341 126-40
[196] Astbury W T and Bell F O 1940 Molecular Structure of the Collagen Fibres *Nature* 145 421-2
[197] Pauling L and Corey R B 1951 The Structure of fibrous proteins of the collagen-gelatin group *Proc. Natl. Acad. Sci* 37 272-81
[198] Rich A and Crick F H C 1955 The Structure of Collagen *Nature* 176 915-6
[199] Cowan P M, McGavin S and North A C T 1955 The Polypeptide Chain Configuration of Collagen *Nature* 176 1062-4
[200] Ishibazawa A, Nagaoka T, Takahashi T, Yamamoto K, Kamiya A, Ando J and Yoshida A 2011 Effects of shear stress on the gene expressions of endothelial nitric oxide synthase, endothelin-1, and thrombomodulin in human retinal microvascular endothelial cells *Invest Ophthalmol Vis Sci* 52 8496-504
[201] Yu W, Qu H, Hu G, Zhang Q, Song K, Guan H, Liu T and Qin J 2014 A microfluidic-based multi-shear device for investigating the effects of low fluid-induced stresses on osteoblasts *PloS one* 9 e89966
[202] Delaine-Smith R M, MacNeil S and Reilly G C 2012 Matrix production and collagen structure are enhanced in two types of osteogenic progenitor cells by a simple fluid shear stress stimulus *European Cells and Materials* 24 162-74
[203] Yang Y, Kulangara K, Sia J, Wang L and Leong K W 2011 Engineering of a microfluidic cell culture platform embedded with nanoscale features *Lab on a chip* 11 1638-46
[204] Polacheck W J, Li R, Uzel S G and Kamm R D 2013 Microfluidic platforms for mechanobiology *Lab on a chip* 13 2252-67
[205] Song J W, Gu W, Futai N, Warner K A, Nor J E and Takayama S 2005 Computer-Controlled Microcirculatory Support System for Endothelial Cell Culture and Shearing *Analytical Chemistry* 77 3993-9
[206] Chau L, Doran M and Cooper-White J 2009 A novel multishear microdevice for studying cell mechanics *Lab on a chip* 9 1897-902
[207] Elliott J T, Woodward J T, Umarji A, Mei Y and Tona A 2007 The effect of surface chemistry on the formation of thin films of native fibrillar collagen *Biomaterials* 28 576-85
[208] Jiang F, Horber H, Howard J and Muller D J 2004 Assembly of collagen into microribbons: effects of pH and electrolytes *J Struct Biol* 148 268-78

[209] He L, Cai S, Wu B, Mu C, Zhang G and Lin W 2012 Trivalent chromium and aluminum affect the thermostability and conformation of collagen very differently *J Inorg Biochem* 117 124-30
[210] Dupont-Gillain ChC, Pamula E, Denis FA, De Cupere VM, Dufrêne YF and PG. R 2004 Controlling the supramolecular organisation of adsorbed collagen layers *J Mater Sci Mater Med.* 15 347-53
[211] Zisman W A 1964 *Contact Angle, Wettability, and Adhesion,* ed F M Fowkes: ACS publications) pp 1-51
[212] Vogler E A 1999 Water and the acute biological response to surfaces. *J Biomater Sci Polym Ed* 10 1015-45
[213] Young T 1805 An Essay on the Cohesion of Fluids *Philosophical Transactions of the Royal Society of London* 95 65-87
[214] Rottenfusser R Retrieved 17.03.2017 ZEISS Microscopy Online Campus | Microscopy Basics. (http://zeiss-campus.magnet.fsu.edu/articles/basics/introduction.html: Zeiss Microscopy)
[215] Murphy D B 2001 *Fundamentals of light microscopy and electronic imaging* (Canada: John Wiley & Sons, Inc., Publications)
[216] Sanderson M J, Smith I, Parker I and Bootman M D 2014 Fluorescence microscopy *Cold Spring Harbor protocols* 2014 pdb top071795
[217] Spring K R and Davidson M W Retrieved 05.03.2019 Introduction to Fluorescence Microscopy. (https://www.microscopyu.com/techniques/fluorescence/introduction-to-fluorescence-microscopy: MicroscopyU)
[218] Binnig G, Quate C F and Gerber C 1986 Atomic force microscope *Phys Rev Lett* 56 930-3
[219] Chang K-C, Chiang Y-W, Yang C-H and Liou J-W 2012 Atomic force microscopy in biology and biomedicine *Tzu Chi Medical Journal* 24 162-9
[220] Payton O, Champneys A R, Homer M E, Picco L and Miles M J 2010 Feedback-induced instability in tapping mode atomic force microscopy: theory and experiment *Proceedings of the Royal Society A: Mathematical, Physical and Engineering Sciences* 467 1801-22
[221] Goldsbury C S, Scheuring S and Kreplak L 2009 Introduction to Atomic Force Microscopy (AFM) in Biology 17.7.1-.7.9
[222] Qiu W 2012 PDMS based waveguides for microfluidics and EOCB. In: *The Department of Mechanical Engineering*: Louisiana State University and Agricultural and Mechanical College)
[223] Xia Y and Whitesides G M 1998 Soft Lithography *Annu. Rev. Mater. Sci.* 28 153-84
[224] Olivier L A, Yen J, Reichert W M and Truskey G A 1999 Short-Term cell:substrate contact dynamics of subconfluent endothelial cells following exposure to laminar flow *Biotechnol Prog* 15 33-42
[225] Wang C, Lu H and Schwartz M A 2012 A novel in vitro flow system for changing flow direction on endothelial cells *J Biomech* 45 1212-8
[226] Provost J and Wallert M A 1998 Hemocytometer Cell Counting Protocol. In: *Investigating the Biochemistry & Cellular Physiology of NHE1,* (http://home.sandiego.edu/~josephprovost/Hemocytometer Cell Counting Protocol.pdf: University of Sandiego)
[227] Sandell L and Sakai D 2011 Mammalian Cell Culture *Current Protocols Essential Laboratory Techniques* 5 4.3.1-4.3.32

[228] Siddique A, Meckel T, Stark R W and Narayan S 2016 Improved cell adhesion under shear stress in PDMS microfluidic devices *Colloids and Surfaces B: Biointerfaces*
[229] Zhang M, Yang J, Ding C, Huang L and Chen L 2018 A novel strategy to fabricate water-soluble collagen using poly(γ-glutamic acid)-derivatives as dual-functional modifier *Reactive and Functional Polymers* 122 131-9
[230] Yadavalli V K, Svintradze D V and Pidaparti R M 2010 Nanoscale measurements of the assembly of collagen to fibrils *Int J Biol Macromol* 46 458-64
[231] Kado S and Kimura K 2001 Direct Observation of Cation Complexation of 18-Crown-6 by Atomic Force Microscopy Using Chemically Modified Tips *Chemistry Letters* 30 630-1
[232] Gaver D P and Kute S M 1998 A theoretical model study of the influence of fluid stresses on a cell adhering to a microchannel wall *Biophysical Journal* 75 721-33
[233] Lee S and¨s J V r 2005 An Aqueous-Based Surface Modification of Poly(dimethylsiloxane) with Poly(ethylene glycol) to Prevent Biofouling *Langmuir : the ACS journal of surfaces and colloids* 21 11957-62
[234] Fre´de´ric A. Denis, Per Hanarp, Duncan S. Sutherland, Julie Gold, Christian Mustin, Paul G. Rouxhet and Dufreˆne Y F 2002 Protein Adsorption on Model Surfaces with Controlled Nanotopography and Chemistry *Langmuir : the ACS journal of surfaces and colloids* 18
[235] Li Y, Asadi A, Monroe M R and Douglas E P 2009 pH effects on collagen fibrillogenesis in vitro: Electrostatic interactions and phosphate binding *Materials Science and Engineering: C* 29 1643-9
[236] Tan G, Ouyang K, Wang H, Zhou L, Wang X, Liu Y, Zhang L and Ning C 2016 Effect of Amino-, Methyl- and Epoxy-Silane Coupling as a Molecular Bridge for Formatting a Biomimetic Hydroxyapatite Coating on Titanium by Electrochemical Deposition *Journal of Materials Science & Technology* 32 956-65
[237] E. Metwalli, D. Haines, O. Becker, S. Conzone and Pantano C G 2006 Surface characterizations of mono-, di-, and tri-aminosilane treated glass substrates *Journal of Colloid and Interface Science* 298 825-31
[238] Scotchford C A 2009 *Cellular Response to Biomaterials,* ed L D Silvio: Woodhead Publishing Limited.) pp 462-78
[239] JE G, CA S and S D 2002 Cytotoxicity of glutaraldehyde crosslinked collagen:poly(vinyl alcohol) films is by the mechanism of apoptosis *J Biomed Mater Res.* 6 121-30
[240] Kiernan J A 2000 Formaldehyde, formalin, paraformaldehyde and glutaraldehyde- What they are and what they do *Microscopy Today* 00-1 8-12
[241] Marinucci L, Lilli C, Guerra M, Belcastro S, Becchetti E, Stabellini G, Calvi E M and Locci P 2003 Biocompatibility of collagen membranes crosslinked with glutaraldehyde or diphenylphosphoryl azide- An in vitro study *Journal of biomedical materials research. Part A* 1;67 504-9
[242] Hasan Erbil Abaci, Drazer G and Gerecht S 2013 Recapitulating the Vascular Microenvironment in Microfluidic Platforms *Nano LIFE* 3 130001-11
[243] Lu H, Koo L Y, Wang W M, Lauffenburger D A, Griffith L G and Jensen K F 2004 Microfluidic Shear Devices for Quantitative Analysis of Cell Adhesion *Anal Chem* 76 5257-64

Acknowledgments

Foremost, I want to express my sincere gratitude to my supervisor Prof. Dr. Robert Stark, who gave me opportunity to work on this challenging and multitasking project in his group. I am very thankful to him for his continues support, his encouraging attitude and helpful behavior during my research work. His understanding nature and immense knowledge had always been a great combination to discuss research problems and explore new methods. His confidence and believe on my research skills always enhanced my motivation to solve the mysteries of this puzzling assignment.
Secondly, I want to thank Dr. Suman Narayan for her guidance and input in my research work. I am so much grateful for the efforts and time she spent on designing my microfluidic devices and fabrication of SU8 master molds. I can never forget the challenging but exciting time we spent together for the establishment of new lab facilities to start the research project.
I want to thank Higher Education Commission Pakistan for providing me PhD research grant in Germany and Deutscher Akademischer Austauschdienst (DAAD) for their help and assistance for my degree in Germany.
I would like to thank Prof. Dr. Robert stark, Prof. Dr. Markus Biesalski, Prof. Dr. Wolfgang Ensinger and Prof. Dr. Christina Trautman for spending their precious time to review my thesis and for being my committee members.
A very heartfelt thanks and regards for Prof. Dr. Ingrid Fleming from VRC Frankfurt, for providing me HUVECs culture and Dr. Tobias Meckel from TU Darmstadt, for providing me FCos-7 cells for studies.
I want to thank Isabelle Pause, for her contribution in my research work by studying HUVECs growth on collagen coated PDMS surfaces during her master thesis.
Then I would like to thank Anahid Amiri and Adriana Guaidia for their assistance during my lab work.
A team is not a group of people who work together. A team is a group of people who always be there to help each other. A big thanks to all of my group members, my colleagues from “Physics of Surface” for providing such a nice environment to work. Everyone’s cooperative attitude made the things easy to manage. Especially Dr. Christian Dietz, despite his busy schedule, he had always been available to discuss problems and to solve them. Marcus Schulze, our IT responsible person, thanks for always be willing to help me not only related to IT but also for research, lab and every other stuff to manage.
I would like to thank Dr. Christian Dietz and Marcus Schulze for teaching and guiding me about Atomic Force Microscopy (AFM) measurments.
Many thanks to Lukas Stühn for being such a nice and helping lab fellow.
The people we surround ourselves with, either raise or lower our standards. They help us to become the best version of ourselves. These are our friends. Very special thanks, to my friends for being so much supportive during my challenging and hard times.
There are no enough words that can acknowledge the efforts of my parents for making me what I am. I want to pay my sincere thanks and regards to my parents for always

inspiring me, my brother and sisters for their throughout support. A very deep gratitude for my parents in law for being so much encouraging for my PhD and career. Especially, my father in law (RIP) who always wanted to see me with a Dr. title.
Finally, the most important gratitude is for my family who always wanted me to smile even in stressful time during work. Thanks to my husband Amad Ur Rehman for not only believing in me but also putting his best efforts to solve my problems. His understanding nature always helps me to cope with my stresses. Very sincere thanks for his support and struggle for helping me to establish a work-family-balance. Thanks, full of love, for my Kids, My son Arsal Rehman and daughter Aaira Rehman, who understand my problems, never complaint and always tried to make me happy.

Curriculum Vitae

Personal data

Name: Asma Siddique
Email address: assma_siddiq@yahoo.com
Address: Darmstadt, Germany

Education

2019	**Ph.D**	**Microfluidics and Biomaterials** *Technical University Darmstadt, Germany*
2005-2007	**M.Phil.**	**Biotechnology** *NIBGE, Faisalabad, Pakistan*
2002-2004	**M.Sc.**	**Chemistry** *University of Agriculture, Faisalabad, Pakistan*
2002	**Graduation**	**Chemistry, Botany, Zoology** *University of Punjab, Lahore, Pakistan*

Academic Projects

PhD Thesis:
Surface modification for enhanced cell adhesion under high shear stress conditions

M.Phil. Thesis:
Genetic diversity among thermophilic cellulytic fungi by using RAPD

M.Sc. Thesis:
Antioxidant activity of Moringa oleifera leaves under accelerated and ambient storage of sunflower oil

Working Experience

2012-Present Researcher
Physics of surfaces, Dept. of Materials Science, TU Darmstadt, Germany
Project: Establishment of microfluidic set up to mimic vascular microenvironment

2008-2011 Research Officer
PCSIR, Labs. Complex, Lahore, Pakistan
Project: Production of biofuel from plant biomass

2007-2008 Research Associate
NIBGE, Faisalabad, Pakistan
Project: Fungal strain improvement for hyperproduction od cellulase

Technical Skills

Microfluidics chip formation, 3D cell studies, Biomaterials, Cell-Surface interaction, Surface chemistry, Protein immobilization techniques, Mammalian cell culturing (HUVECs, Fibroblasts, HeLa etc), Atomic Force Microscopy (AFM) of biomaterials surfaces as well inside microfluidic devices, Fluorescence labeling/imaging of cells and proteins.
DNA isolation, PCR, DNA Fingerprinting, Sequencing, Microbial cell culturing, Fermentation Technology, Mutagenesis
Chromatographic techniques, Spectrometry, Titrimetric & Potentiometric Techniques

Publications

Book chapter Published:

Irfan M., Ghazanfar M., Ur Rehman A., **Siddique A**. (2019) Strategies to Reuse Cellulase: Immobilization of Enzymes (Part II). In: Srivastava M., Srivastava N., Ramteke P., Mishra P. (eds) Approaches to Enhance Industrial Production of Fungal Cellulases. Fungal Biology. Springer, Cham: DOI: 10.1007/978-3-030-14726-6_9

Paper Published:

Asma Siddique, Tobias Meckel, Robert W. Stark, Suman Narayan, (2017), Improved cell adhesion under shear stress in PDMS microfluidic devices, Colloids and Surfaces B: Biointerfaces, 150: 456-464: doi.org/10.1016/j.colsurfb.2016.11.011

Asma Siddique, Ambreen Gul, Muhammad Irfan, Muhammad Nadeem & Quratulain Syed, (2017), Comparison of different pretreatment methods for efficient conversion of bagasse into ethanol, Biofuels, 8:1, 135-141: DOI: 10.1080/17597269.2016.1215066

Asma Siddique, Aftab Bashir, and Farooq Latif. 2012. Exploration of unique relation among industrial fungi by statistical analysis. Songklanakarin J. Sci. Technol. 34 (6), 607-613

Khan, S.A., **Siddique, A**. and Latif, F. (2009). Fibrolytic enzyme production from *Humicola insolens* and its applications in animal feed. Pakistan J. Zool. Suppl. Ser. 9:41-45

Farooq Anwar, **Asma Siddique**, Shahid Iqbal and M. Rafique Asi. (2007). Stabilization of sunflower oil with *Moringa oleifera* leaves under ambient storage. Journal of Food Lipids, 14: 35-49

Siddique, A., F. Anwar, M. Manzoor and A, Fatima. (2005). Antioxidant activity of different solvent extracts of *Moringa oleifera* leaves under accelerated storage of Sunflower oil. Asian Journal of Plant Science, 4(6): 630-635.

Books Published:

Asma Siddique, Farooq Latif and Aftab Bashir. (2012). RAPD Markers and their Application: Genetic diversity among thermophilic cellulolytic fungi and Mutation studies. LAP Lambert Academic Publishing, Germnay.

Sohail Ahmad Khan, **Asma Siddique** and Farooq Latif. (2010) Exogenous Fibrolytic Enzymes in Cattle Feed: An attempt to improve feed efficiency in cattle. LAP Lambert Academic Publishing, Germnay.

CONFERENCES/SUMPOSIUM with oral/poster presentations:

- μFlu'18-NEGF'18, Strasbourg, France, 28 Feb.-02 March 2018
- Lab-on-Chip & Microfluidics 2017, Munich, Germany, 10-11 May 2017.
- EMBL Conference, Microfluidics 2012, EMBL Germany, 23-25 July 2014.
- Microfluidics for Systems Biology and Bioprocess development, DECHEMA, Germany, 21 Feb. 2013.
- EMBL Conference, Microfluidics 2012, EMBL Germany, 25-27 July 2012.
- 5th International Symposium on Biotechnology (ISB09), University of Sindh, Jamshoro, Pakistan, 4-7 October, 2009
- National Bioforum: 24-28 March 2008.
- 6th international and 16th National Chemistry Conference, 6-8 April 2006.